University Of Alberta

Nitrogen Retention in the High Rate Stage of Composting

by

Yi Liang ©

A Thesis Submitted to the Faculty of Graduate Studies and Research
in Partial Fulfillment of the Requirements for the Degree of
Doctor of Philosophy

in

Bioresource and Food Engineering

Department of Agricultural, Food and Nutritional Science
University of Alberta
Edmonton, Alberta
Fall, 2000

National Library
of Canada

Acquisitions and
Bibliographic Services

395 Wellington Street
Ottawa ON K1A 0N4
Canada

Bibliothèque nationale
du Canada

Acquisitions et
services bibliographiques

395, rue Wellington
Ottawa ON K1A 0N4
Canada

Your file Votre référence

Our file Notre référence

The author has granted a non-exclusive licence allowing the National Library of Canada to reproduce, loan, distribute or sell copies of this thesis in microform, paper or electronic formats.

L'auteur a accordé une licence non exclusive permettant à la Bibliothèque nationale du Canada de reproduire, prêter, distribuer ou vendre des copies de cette thèse sous la forme de microfiche/film, de reproduction sur papier ou sur format électronique.

The author retains ownership of the copyright in this thesis. Neither the thesis nor substantial extracts from it may be printed or otherwise reproduced without the author's permission.

L'auteur conserve la propriété du droit d'auteur qui protège cette thèse. Ni la thèse ni des extraits substantiels de celle-ci ne doivent être imprimés ou autrement reproduits sans son autorisation.

0-612-59621-4

Canadä

University of Alberta

Library Release Form

Name of Author: **Yi Liang**

Title of Thesis: **Nitrogen Retention in the High Rate Stage of Composting**

Degree: **Doctor of Philosophy**

Year This Degree Granted: **2000**

Permission is hereby granted to the University of Alberta Library to reproduce single copies of this thesis and to lend or sell such copies for private, scholarly, or scientific research purposes only.

The author reserves all other publication and other rights in association with the copyright in the thesis, and except as herein before provided, neither the thesis nor any substantial portion thereof may be printed or otherwise reproduced in any material form whatever without the author's prior written permission.

1402, 12020-49Ave.
Edmonton, Alberta
Canada T6H 5B5

Date: May 31, 2000

University of Alberta

Faculty of Graduate Studies and Research

The undersigned certify that they have read, and recommend to the Faculty of Graduate Studies and Research for acceptance, a thesis entitled **Nitrogen Retention In The High Rate Stage Of Composting** submitted by **Yi Liang** in partial fulfillment of the requirements of the degree of **Doctor of Philosophy** in **Bioresource and Food Engineering.**

J.J. Leonard
(Supervisor)

John Feddes
J.J. Feddes

W.B. McGill

J.P. Tewari

A.K Lau
(External Examiner)

Dated: May 29, 2000

ABSTRACT

Composting is accepted as an effective treatment method for solid organic wastes. Losses of nitrogen, however, tend to be high during composting of some nitrogen-rich organic materials. This results in reduced nutrient value of the product even though compost is generally used as a soil conditioner. The lowered nitrogen:phosphorus ratio leads to the restriction of land application rates and increases the risk of environmental degradation.

In this study, a mathematical model was developed to simulate substrate decomposition and ammonia volatilization during high rate stage of composting. Substrate was partitioned into several groups based on both the chemical components and different decomposition rates. Ammonia volatilization was related with interstitial carbon dioxide concentration, and calculated based on the analysis of a CO_2-NH_3-H_2O multisolute aqueous system.

pH value is an important factor influencing the fate of nitrogen in the composting materials. The determination of pH value was investigated and a protocol was developed for pH measurement of compost.

A laboratory-scale composting experiment was carried out to investigate the influence of (a) two types of carbon amendments and (b) two chemicals forming buffer solutions on nitrogen loss. The experimental data were used to validate the simulation model and showed that the readily available form of carbon amendment reduced ammonia volatilization remarkably. Amendment with cellulose had only a small influence on ammonia volatilization. The addition of buffering chemicals slightly reduced ammonia volatilization.

The simulation model succeeded in reflecting well-known phenomena of the composting technologies. The simulated temperatures and moisture contents were in the range of 87 % to 102% and 97 to 100% of measured values, respectively. The simulated carbon dioxide evolutions were within 69% to 120% of the experimental data, with an average of 89%. The prediction of the ammonia volatilization from the simulation model ranged from 102% to 190% of the experimental data, with an average of 134%. Further modification of the model is discussed.

ACKNOWLEDGMENTS

To my supervisor, Dr. J.J. Leonard, a special thanks for sharing his knowledge and ideas, for his help and guidance, and for his encouragement to cross the hurdles.

To my committee, Dr. J.J. Feddes and Dr. W.B. McGill (whose knowledge and wisdom lead me through so much darkness), for their valuable advice and suggestions.

To Dr. N.G. Juma, for spending many hours sharing his expertise in simulation modelling.

To Chris Ouellette, Jason Price, David Bosch, and Guoliang Qu, for giving not only the technical support, but also the tremendous help to me as I went about my work.

To Stacey Schaub, for her enthusiasm and energy for both career and life enlightening me.

To Ms. M. Molina-Ayala, Ms. L. Smith and Mr. C.T. Figueiredo for technical assistance.

To the Canada Alberta Environmentally Sustainable Agriculture agreement and Alberta Agriculture, Food and Rural Development for financial support.

Finally, a sincere thanks to my parents, my husband and my sister, for their love and understanding.

TABLE OF CONTENTS

CHAPTER 1 INTRODUCTION **1**

1.1 COMPOSTING AND THE NEED FOR NUTRIENT RETENTION 1
  1.1.1 What is composting *1*
  1.1.2 Nutrient Retention in Composting *2*
1.2 NITROGEN LOSS DURING THE COMPOSTING PROCESSES 3
  1.2.1 Pathways of Nitrogen Losses during Composting *3*
  1.2.2 Volatilization of Ammonia during Composting *4*
1.3 MODELING APPROACHES 14
  1.3.1 Modeling Approaches for Carbon and Nitrogen Decomposition *14*
  1.3.2 Modeling Approaches in Composting *14*
1.4 RESEARCH NEED 16
1.5 AIMS AND SCOPE OF THE RESEARCH 16
1.6 REFERENCES 17

CHAPTER 2 A MATHEMATICAL MODEL OF SUBSTRATE DECOMPOSITION AND AMMONIA VOLATILIZATION IN THE HIGH RATE STAGE OF COMPOSTING **23**

2.1 INTRODUCTION 23
2.2 MODEL DESCRIPTION 25
  2.2.1 Structure *26*
  2.2.2 Model Development *28*
2.3 SIMULATION RESULTS 47
2.4 SENSITIVITY ANALYSIS 52
2.5 DISCUSSION 62
2.6 CONCLUSIONS 63
2.7 NOMENCLATURE 64
2.8 REFERENCES 66

CHAPTER 3 DETERMINATION OF COMPOST PH **70**

3.1 INTRODUCTION 70
3.2 MATERIALS AND METHODS 71
  3.2.1 Compost Materials *71*
  3.2.2 Instrumentation *72*
  3.2.3 Preliminary Considerations *73*
  3.2.4 Test Methods *75*
  3.2.5 Statistical Analyses *77*
3.3 RESULTS AND DISCUSSION 77
  3.3.1 Sampling-Measurement Time *78*
  3.3.2 Dilution-Measurement Time *79*
  3.3.3 Dilution Ratio *82*
  3.3.4 Two- and Three-point Determinations *84*
  3.3.5 Effect of Number of Samples on Accuracy *85*
  3.3.6 Determining the Number of Samples *85*
3.4 CONCLUSIONS 87
3.5 REFERENCES 88

CHAPTER 4 THE INFLUENCE OF CARBON AVAILABILITY AND PH MODIFICATION ON AMMONIA LOSSES IN LABORATORY-SCALE COMPOSTING OF MANURE AND STRAW **89**

4.1 INTRODUCTION 89
4.2 MATERIALS AND METHODS 92
  4.2.1 Vessel System *92*
  4.2.2 Experimental Conditions and Treatments *97*
  4.2.3 Laboratory Analyses *104*
  4.2.4 Statistical Analyses *104*
4.3 RESULTS 105
  4.3.1 Chemical Properties *105*
  4.3.2 Temperature *106*
  4.3.3 Dry Matter Loss *109*
  4.3.4 Nitrogen Content *109*
  4.3.5 pH *109*
  4.3.6 Ammonia Volatilization *110*
  4.3.7 Carbon Dioxide Evolution vs. Ammonia Loss *113*
  4.3.8 Nitrogen Retention *116*
4.4 DISCUSSION 117
  4.4.1 General *117*
  4.4.2 Influence of Aeration on Ammonia Volatilization *118*
  4.4.3 Effect of Carbon Amendments on Ammonia Volatilization *119*
  4.4.4 Effect of Buffering Chemicals on Ammonia Volatilization *123*
  4.4.5 Ammonia Emitted vs. Nitrogen Loss *124*
4.5 LIMITATIONS AND SOURCES OF ERROR 125
4.6 CONCLUSIONS 126
4.7 REFERENCES 126

CHAPTER 5 PERFORMANCE OF A SIMULATION MODEL DESCRIBING AMMONIA VOLATILIZATION DURING COMPOSTING **130**

5.1 INTRODUCTION 130
5.2 MODEL APPLICATION 132
5.3 RESULTS 135
5.4 DISCUSSIONS 156
5.5 CONCLUSIONS 164
5.6 REFERENCES 165

CHAPTER 6 SYNTHESIS **166**

6.1 SUMMARY 166
6.2 CONCLUSIONS 168
6.3 FUTURE CONSIDERATIONS 169
6.4 REFERENCES 170

APPENDIX A **171**

C code of simulation model

LIST OF TABLES

Table 2-1. Parameters of microbial growth kinetics used in simulation 33

Table 2-2. Thermodynamic parameters 36

Table 2-3. Parameter values used in determining Henry's constants for NH_3 and CO_2 in water 41

Table 2-4. Parameter values used in determining dissociation constants for NH_3 and CO_2 in water 43

Table 2-5. Technical parameters for simulation of composter 47

Table 2-6. Simulated ammonia emission at C/N=30 50

Table 2-7. Simulated ammonia emission at moisture content of 70% 50

Table 2-8. Parameter values used in sensitivity analysis 52

Table 3-1. pH measurements within 1 h between collection and measurement and after 24 h 77

Table 3-2. Linear regression relationships between dilution ratio (X) and pH ($\hat{Y}$) 82

Table 3-3. Estimation of pH by two-point determination (20ml and 60ml) 83

Table 3-4. Comparison of pH vlaues calculated from two or three dilution points 83

Table 3-5. Sample size calculated based on desired confidence level and D using estimated population standard deviation (σ) 86

Table 3-6. Sample size calculated based on desired confidence level and D using estimated sample standard deviation (s) 86

Table 4-1. Characteristics of raw materials 98

Table 4-2. Calculation of equivalent amount of KOH that can be accommodated by 47kg of mixture 102

Table 4-3. Experimental treatments. 103

Table 4-4. Initial chemical properties of composting mixtures 105

Table 4-5. Final chemical properties of compost mixtures 106

Table 4-6. Ventilation air received and NH_3 loss during the first 100h (molasses treatment) 112

Table 4-7. Ventilation air received and NH_3 loss during the first 100h (Paper treatment) 112

Table 4-8. Ventilation air received and NH_3 loss during the first 100h (Buffer treatment I) 112

Table 4-9. Ventilation air received and NH_3 loss during the first 100h (Buffer treatment II) 113

Table 4-10. Carbon dioxide and ammonia losses over entire gas measurement time. 114

Table 4-11. Carbon dioxide and ammonia losses, and aeration demand in the first 100h of composting .. 115

Table 4-12. Comparison of nitrogen loss and NH_3-N emitted. 116

Table 4-13. Retention of nitrogen 117

Table 5-1. Initial variables used in the model 134

Table 5-2. Parameters used in the model. 135

Table 5-3. Average temperatures of experimental data and model outputs at 200h (℃) 140

Table 5-4. Cumulative CO2 evolutions (g) of experimental data and model outputs at 200h 141

Table 5-5. Cooling-fan-on time (h) of experimental data and model output 148

Table 5-6. Ammonia emissions (g) of experimental data and model outputs at 200h 155

LIST OF FIGURES

Figure 1-1. Temperature variation with time indicating the phases of microbial activity. A-mesophilic, B-thermophilic, C- cooling , D- curing 2

Figure 1-2. Relative concentration of ammonium and ammonia in solution in a pH range of 4 to 10 6

Figure 2-1. Flow chart of C and N transfers in the simulation model 26

Figure 2-2. Assumed temperature effect on decomposition rate 31

Figure 2-3. Assumed moisture effect on decomposition rate 31

Figure 2-4. Assumed pH effect on decomposition rate 31

Figure 2-5. Immobilization and mineralization coefficients at various microbial C/N ratio 38

Figure 2-6. Predicted composting performance vs. time between two constant aeration rates, 0.06 and 0.04 kg $(kgd.m.\ h)^{-1}$ 48

Figure 2-7. Simulated ammonia emission from composting materials with C/N=30 at two moisture contents and four aeration rates 51

Figure 2-8. Simulated ammonia emission from composting materials with moisture content=70% at three C/N ratios and three aeraion rates 51

Figure 2-9. Sensitivity analysis showing maximum temperature as the selected parameter was altered from -50 to +100% of deault value 56

Figure 2-10. Sensitivity analysis showing maximum biomass C as the selected parameter was altered from -50 to +100% of deault value 57

Figure 2-11. Sensitivity analysis showing cumulative CO_2-C as the selected parameter was altered from -50 to +100% of deault value. 58

Figure 2-12. Sensitivity analysis showing peak NH3-N emission as the selected parameter was altered from -50 to +100% of deault value 59

Figure 2-13. Sensitivity analysis showing cumulative NH_3-N as the selected parameter was altered from -50 to +100% of deault value 60

Figure 2-14. The sensitivity of compost temperature and cumulative NH_3-N emission to ambient temperature 61

Figure 3-1. pH measurements vs. standing time (within 2 hours) 79

Figure 3-2. pH values of mature compost (diluted with up to 2000 ml of DD water) 80

Figure 3-3. pH vlues for three replicates of 10-d compost (diluted with various amounts of DD water) 81

Figure 3-4. RMS error of pH using different sample sizes 85

Figure 4-1. Flow diagram of the composting system 94

Figure 4-2. Gas sampling system 94

Figure 4-3. A titration curve of 0.3744 moles of monobasic phosphate and 0.5856 moles of dibasic phosphate mixed in 5 g of initial mixture 102

Figure 4-4. Average temperatures with paper treatments 108

Figure 4-5. pH values of treatments with various amounts of buffer chemicals (Experiment 4) 110

Figure 4-6. Cumulative ammonia emitted from vessels received various amounts of paper. 111

Figure 4-7. Relationship between NH_3-N emitted and aeration demand 119

Figure 5-1. Flow chart of C and N transfers in the simulation model (adopted from Chapter 2)..............130

Figure 5-2a. Model output and experiemntal data for temperature in paper treatment..............137

Figure 5-2b. Model output and experiemntal data for temperature in buffer I treatment..............138

Figure 5-2b. Model output and experiemntal data for temperature in buffer II treatment..............139

Figure 5-3. Model output and experiemntal data for CO_2 evolution in molasses treatment..............143

Figure 5-4. Model output and experiemntal data for CO_2 evolution in paper treatment..............144

Figure 5-5. Model output and experiemntal data for CO_2 evolution in buffer I treatment..............145

Figure 5-6. Model output and experiemntal data for CO_2 evolution in buffer II treatment..............146

*Figure 5-7. Simulation outputs of ammonia emission from **molasses** experiment. 1A: no molasses; 1B, 1C, 1D: increased molasses..............149*

Figure 5-8. Model output and experiemntal data for NH_3 evolution in molasses treatment..............151

Figure 5-9. Model output and experiemntal data for NH_3 evolution in paper treatment..............152

Figure 5-10. Model output and experiemntal data for NH_3 evolution in buffer I treatment..............153

Figure 5-11. Model output and experiemntal data for NH_3 evolution in buffer II treatment..............154

*Figure 5-12. Comparison of model outputs (line) and experimental data (symbols) for pH from Treatment 4A in **buffer II** experiment..............156*

Figure5-13. Comparison of model outputs, original (thick line) vs. that under modified assumption of partial material participating decomposition after 50 h (thin line)..............161

Chapter 1

Introduction

1.1 COMPOSTING AND THE NEED FOR NUTRIENT RETENTION

1.1.1 What is composting

Composting is a self-heating aerobic process in which the decomposition of organic materials is accelerated by the growth and enzymatic activity of a mixed population of bacteria and fungi (Miller, 1991). Biomass and humus-like substances are formed, and carbon dioxide, ammonia, water and nitrate are produced. Composting reduces the weight and volume of the waste materials while abating odours and destroying pathogens. Composting not only is a widely acceptable means of waste treatment, but also is reliable in recycling the organic matter in the wastes. It is being widely employed for the treatment of sewage sludge, food-processing wastes, forestry industry wastes, municipal solid wastes, and, with a significant application to agricultural wastes, such as animal manure.

The typical time-temperature curve is shown in Figure 1-1. At the start of the composting process, as the indigenous mesophilic organisms multiply, the temperature rises. Simple organic acids are produced in this initial stage. This is called the mesophilic stage. At temperatures over 40°C the activity of the mesophiles falls off and the degradation is taken over by the thermophiles. This stage is characterized by the greatest potential rates of decomposition and is usually termed the thermophilic stage. At this stage, thermotolerant actinomycetes are the most numerous organisms. As the rapidly degradable material is consumed, the rate of heat generation becomes less than the rate of heat loss and the composting mass starts to cool down until it reaches the ambient temperature. This is called the cooling stage. The three stages of the composting cycle take place quickly, usually within days or weeks. The final stage, curing, refers to a low-activity, loosely managed stage and normally requires a period of months. The first three stages are referred to as the high rate stage in the following pages of this thesis.

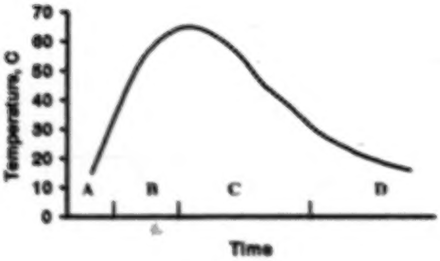

Figure 1-1 Temperature variation with time indicating the phases of microbial activity. A- mesophilic, B- thermophilic, C- cooling , D- curing (adapted from Gray et al., 1971).

1.1.2 Nutrient Retention in Composting

A considerable amount of literature exists concerning the optimization of composting operations to achieve high decomposition rate and a stabilized end product. However, less information is available concerning the fate of nutrients, and capturing these to increase the resource value of decomposable organic materials. Since finished compost is often used as a soil amendment, the nutrients in the compost would be of value from an agricultural standpoint. Of the major nutrients, nitrogen (N) is often the key limiting-factor to crop production in agricultural ecosystems, and has been cited as a crucial factor in increasing food production (Schrader, 1984). Nitrogen is the nutrient most susceptible to loss, especially from the nitrogen-rich organic waste, such as animal manure. Because of nitrogen loss, N:phosphorus (P) ratios are generally lower than crop needs, resulting in build up of excess P in soil. This leads to the restriction of land application rates and increases the risk of environmental degradation (Wright, 1998).

While inorganic forms of nitrogen are the directly available forms used by plant and crop production, they are subject to severe loss by gaseous volatilization and leaching after application, either from fertilizers or fresh organic materials, such as animal manures and sewage sludge (Lauer et al., 1977; Lockyer et al., 1989). The nitrogen organically bound in humic substances of compost is slowly available over a longer period, which reduces the potential pollution problems, such as excessive biological oxygen demands of surface water and odour.

1.2 NITROGEN LOSS DURING THE COMPOSTING PROCESSES

1.2.1 Pathways of Nitrogen Losses during Composting

The nitrogen in fresh organic waste is mainly bound in protein. The transformation of protein nitrogen into inorganic (ammonia, nitrate, nitrite) and organic (microbial biomass, humic substances) N-containing components is caused by different biological processes and spontaneous chemical reactions. The principal processes governing the forms of N species are mineralization (the conversion of organic N to inorganic N), volatilization (release of ammonia nitrogen (NH_3-N) to the atmosphere), nitrification (the conversion of NH_3-N to nitrite followed by nitrate), immobilization (assimilation by the microbial population), and denitrification (the reduction of oxides of nitrogen (NO_x-N) to N_2 gas and/or nitrous oxide followed by release of the gases to the atmosphere) (Black, 1968).

Loss of nitrogenous compounds during aerobic decomposition of organic wastes occurs on the one hand through emission of gases such as NH_3 and NO_x and on the other hand as leachate in the form of bound nitrogen, such as ammonium (NH_4^+) and nitrate (NO_3^-) (Martins and Dewes, 1992). Ammonia volatilization is believed to be the main pathway for nitrogen loss in composting (Hansen et al., 1989; Hong et al., 1997; Kirchmann and Witter, 1989; Witter and Lopez-Real, 1987, 1988). For various organic wastes composted, the loss can amount to more than 50% of the nitrogen initially present (Witter and Lopez-Real, 1987). Nitrogen transformations in the initial stage of composting of nitrogen-rich materials are generally characterized by high rates of ammonification (Bhoyar et al., 1979; Bishop and Godfrey, 1983). It has been determined that nitrification will not proceed at significant rates until volatilization essentially ceases (Bishop and Godfrey, 1983; Edwards and Daniel, 1992), mainly due to the predominance of the high temperature, moisture and high concentration of ammonia.

1.2.2 Volatilization of Ammonia during Composting

High losses of ammonia nitrogen not only reduce the fertilizing value of the end-product and represent a waste of a valuable resource, but also contribute to pollution of the environment. Ammonia is recognized as an important catalyst in the acid rain complex, therefore the ammonia generated from composting operations is as unacceptable as its volatilization following the spreading of slurries and manures on the field (Lopez-Real, 1996).

Van Harreveld (1981), as cited by Witter and Lopez-Real (1988), showed that ammonia was the main component of odour emissions during the composting of horse manure and straw for mushroom production. Pain et al. (1988) also showed strong correlations between odour and ammonia emissions from dairy and pig manure after land application. Release of ammonia into the atmosphere also raises the pH of rainwater, enhances the wet deposition of sulphate, and results in acidification of the soils due to increased sulphate deposition and nitrification of the deposited ammonium in the vicinity of the source of ammonia emissions (Witter and Lopez-Real, 1988).

1.2.2.1 Fundamental Principles of Ammonia Volatilization

Ammonia, a polar molecule, is a gas at normal atmospheric temperatures and pressures. It is also a basic gas which reacts readily with protons, metals, and acidic compounds to form ions, compounds or complexes of varying stability and is thereby protected in solution or solid forms. Ammonia also has a very strong affinity for water and its reactions in water fundamentally determine the rate of volatilization (Freney et al., 1983). The volatilization of ammonia is the result of a series of physico-chemical processes. The various processes that are related to ammonia loss may be represented as:

$$\begin{array}{ccccc} & & & & NH_3 \text{ (gas in surrounding environment)} \\ & & & & \uparrow \\ NH_4^+ \text{ (in solution)} & \leftrightarrow & NH_3 \text{ (in solution)} & \leftrightarrow & NH_3 \text{ (gas in compost matrix)} \end{array}$$

The driving force for ammonia volatilization from a moist solid matrix, (i.e. soil, compost), or a solution is considered to be the difference in NH_3 partial pressure between that in equilibrium with the liquid phase and that in the surrounding environment (Freney et al., 1983).

In the liquid phase, the equilibrium between ammonium and NH_3 can be represented as:

$$NH_3 + H_2O \overset{K_b}{\Leftrightarrow} NH_4^+ + OH^-$$

where: $K_b = \dfrac{[NH_4^+][OH^-]}{[NH_3]}$

It is apparent that the relative concentration of ammonium and NH_3 is controlled by the pH value of the solution, which is defined as the logarithm of the reciprocal of the concentration of H^+ that it contains. Figure 1-2 shows the relative concentration of ammonium and NH_3 at a number of pH values. At pH≤7 the NH_4^+ is almost exclusively present, whereas NH_3 predominates at pH≥9, and has a much larger potential to be volatilized.

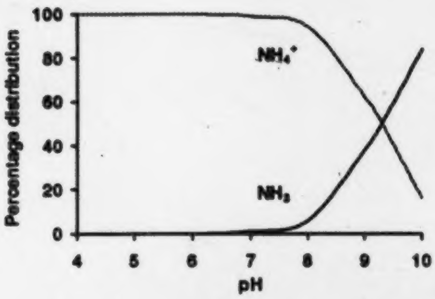

Figure 1-2. Relative concentration of ammonium and ammonia in solution in a pH range of 4 to 10 (adopted from Court et al., 1964, as cited in Freney et al., 1983).

The dissociation constants for aqueous ammonia vary markedly with temperature, which indicates that the equilibrium between ammonium and dissolved NH_3 is also influenced by temperature.

The partition of NH_3 between the liquid and gaseous phases follows Henry's law, which can be expressed as the ratio of the concentration of NH_3 in the liquid phase and the concentration of NH_3 in the gaseous phase. The ratio is constant at a particular temperature, and is commonly termed as Henry's law constant. This constant varies with temperature and, as a consequence, the partition of NH_3 between the two phases also varies markedly with temperature.

Therefore, temperature, ammoniacal nitrogen concentration (the combined amount of nitrogen associated with both ionized and un-ionized forms of ammonia) and pH value are the factors influencing the partial pressure of NH_3 in equilibrium with a solution that is subject to potential ammonia volatilization.

1.2.2.2 Factors Affecting NH_3 Volatilization

In composting, ammonia is produced from either aerobic or anaerobic decomposition of protein and amino acids. Ammonia volatilization has been monitored and measured in a variety of mixtures using different experimental set-ups (Hansen et al., 1989, 1991, 1993; Morisaki et al., 1989; Sikora and Sowers, 1985). The most important factors that influence the emission of NH_3 were found to be C/N ratio, pH value, temperature, aeration, and moisture content. Also, a cover of adsorbent material was thought to be an alternative way of conserving volatilized ammonia in composting (Witter and Lopez-Real, 1988).

C/N ratio

C/N ratio is a variable to characterize the composition of the materials under decomposition. Any substrate with a low carbon-to-nitrogen ratio (C/N) will likely release excess ammonia into the vapor phase (Haug, 1993). Optimum values of C/N ratio have been used as a major process descriptor when studying volatilization of ammonia in composting. A C/N ratio of about 25 to 30 is considered to be the optimum for composting, since living organisms use 25 to 35 units of carbon for every unit of nitrogen during active aerobic growth (Bishop and Godfrey, 1983).

When dealing with the same type of nitrogen-rich source and bulking materials, low C/N ratios result in increased loss of excess nitrogen by ammonia volatilization (Kirchmann and Witter, 1989; Maeda and Matsuda, 1997; Sikora, 1999). The cumulative mass of NH_3-N emitted was over 3 times greater for C/N = 15 than for C/N = 20 using caged egg-layer poultry manure and ground corncobs (Hansen et al., 1989).

However, when more heterogeneous mixtures or different types of organic materials are composted, higher C/N ratio does not necessarily indicate an effective solution for preventing nitrogen loss. The readily available carbon, or microbial availability of carbon, is a more meaningful expression concerning substrate decomposition and nitrogen conservation. Several studies have been done in respect of the availability of carbon to microorganisms (Barrington et al., 1997; Mahimairaja et al., 1994; Mote and Griffis, 1980). A readily available carbon source causes immediate N immobilization when an appreciable amount is added to soils (Okereke and Meints, 1985). Subair (1995) also found that glucose amendment was effective in reducing NH_3 volatilization from incubation of liquid hog manure. When composting a combination of food waste, straw, paper and topsoil, Brink (1995) reported straw to be a good carbon source for nitrogen retention. Losses of nitrogen during the composting of cattle manure and straw have been reduced by increasing the proportion of ground straw to chopped straw whilst maintaining a C/N ratio of 31.6 (Meyer and Sticker, 1983). As these authors pointed out, the higher surface area possibly increased microbial availability of carbon from ground straw, and an improvement of density condition may also have reduced nitrogen loss. This indicates that the simple C/N ratio needs to be modified in order to be used more meaningfully in determining and predicting loss of N. The availability of the energy source in the composting materials determines the amount of nitrogen that can be immobilized.

pH Values

Ammonia and pH are interdependent. Ammonification causes a pH rise that is typically seen during the active period of composting, and pH determines a dynamic equilibrium between NH_3/NH_4^+, which defines the proportion of NH_3 and NH_4^+ within the ammoniacal nitrogen. Since the NH_3 portion of ammoniacal N increases as pH and temperature of compost increase, higher pH values increase the concentration of NH_3 present in the solution and in the compost free air space (FAS), therefore increasing the potential for NH_3 loss.

The hydrolysis of uric acid and urea result in elevated pH levels that facilitate NH_3 volatilization (Reynolds and Wolf, 1987). Various organic chemicals have been used to reduce uric acid hydrolysis or inhibit the urease enzyme in livestock manure (Carlile, 1984; Varel et al., 1997). However, these chemicals have been found to render the manure unsuitable for composting (Kithome et al., 1999).

Various acids have been added to manure slurries to reduce pH (Al-Kanani, 1992). Other chemicals such as superphosphate and gypsum were also effective in reducing ammonia volatilization, apparently due to the decrease in pH of the manure slurries during an incubation study (Termeer and Warman, 1993). Schulte (1997) pointed out that critical parameters for controlling emissions via acidification appear to be the buffering system of the manure and the degree to which mixing must occur for uniform reduction of pH.

The addition of chemicals to litter in poultry houses has been shown to be effective in reducing ammonia concentration in the building, mainly due to the pH decrease and the shifting of the NH_3 /NH_4^+ equilibrium to favor NH_4^+ species in the solution (Moore et al., 1995).

Experimental data from composting (Körner and Stegmann, 1997; Nakasaki et al., 1993; Witter and Lopez-Real, 1988) indicate that the most severe losses of NH_3 occurred when high pH values were measured. By adding calcium chloride to straw-slurry compost, Jacobson (1987) reduced pH by 1.4 units and eliminated ammonia loss. When composting short paper fiber and broiler litter, mixed with additives such as Alum ($Al_2(SO_4)_3$), HiClay® Alumina and sulfuric acid to reduce the initial pH values, NH_3-N losses were found to have an exponential relationship with initial pH values (Ekinci et al., 1998), showing that pH was an important factor to control ammonia.

Temperature / Aeration

Several critical parameters for NH_3 emission are governed by temperature. First, it influences the NH_4^+-NH_3 dissociation constant as well as Henry's constant, which increases the gaseous portion of NH_3 at higher temperatures (Schulte, 1997). Temperature also influences the mass transfer coefficient for NH_3 at the liquid-air boundary (Haslam et al., 1924). As a result, increasing temperatures increase the relative proportion of NH_3 to NH_4^+ present at a given pH, decreases the solubility of NH_3 in water, and increases diffusion of NH_3 through the compost. Therefore, the higher the temperature the greater the potential for NH_3 loss (Freney et al., 1983).

Aeration removes carbon dioxide, heat and water vapor as well as supplying oxygen. Aeration strategy is a control variable used to regulate composting processes to achieve desirable temperatures and O_2 concentration in the compost. In the thermophilic stage of composting, higher aeration significantly increases carbon dioxide concentration in exhaust gas (Suler and Finstein, 1977).

High NH_3 volatilization has been observed when thermophilic temperatures (>40°C) were achieved and have sometimes been associated with higher aeration (Beck et al., 1997; Hansen et al., 1989; Körner and Stegmann, 1998; Maeda and Matsuda, 1997). A lower degree of ammonia emission was found at a moderate aeration rate when testing levels of 57, 73, and 90 $L/m^3/min$ using a dairy manure and rice hull mixture (Hong et al., 1997). However, Maeda and Matsuda (1997) found a linear relationship between ammonia emission as a percentage of initial total nitrogen and the cumulative air supplied to the composting mixture. Käck (1996), as cited by Beck et al. (1997) also reported a positive correlation between ammonia volatilization and aeration rate and indicated that aeration was the most important process parameter for ammonia volatilization during composting. Composting under temperature-demand aeration, which maintains temperature below a ceiling point, usually 55°C, results in higher rates of ammonia loss than that under constant aeration (Nakasaki et al., 1987; Sikora and Sowers, 1985). This may have resulted from vigorous substrate decomposition, mainly of proteinaceous substance and insufficient readily available carbon for microbial biosynthesis. Mineralized nitrogen was released in excess of biological needs and easily evolved as ammonia by ventilation or mixing.

Moisture Content

Moisture content not only is an important control variable for determining compost recipes, but also affects ammonia volatilization during the compost process. Since ammonia is highly soluble in water, especially under low or moderate temperature, higher moisture content may help keep more ammonia in the liquid form than in the gas-filled pore space in compost. Ammonia thus conserved may be immobilized by microbial growth in the following stages.

When water is evaporated, the solution in which the NH_4^+ and NH_3 coexist increases in concentration, thereby increasing the concentration of ammoniacal nitrogen forms and increasing the gradient which drives the emission process. Severe drying of the compost may drive the ammonia out of solution due to increased concentration and result in high partial pressure of gaseous ammonia in the compost environment, increasing the risk of ammonia being diffused or stripped to atmosphere.

Ammonia loss was found to be related to the rate of water loss during a study of temperature control on the composting process, based on the fact that the condensate collected from the cooling of moist, warm off-gas contained approximately 80% NH_3 among the total NH_3 lost (Sikora and Sowers, 1985).

1.2.2.3. Sorption and Fixation of Ammonia

The mechanisms of adsorption of NH_3 on minerals and organic matter range from chemical reactions, whereby the NH_3 is bound very strongly, to physical adsorption, where it is bound very weakly (Freney et al., 1983). Adsorption is related to the surface area of sorbing material so that the sizes and kinds of materials affect the amounts of NH_3 adsorbed.

In an experiment to evaluate adsorption of NH_3 gas on bulking agents followed by desorption, Morisaki et al. (1989) found sawdust and bark to be appropriate materials to decrease the amount of NH_3 gas volatilized from organic matter during composting.

Several researchers have investigated the effectiveness of adsorbent covers on the composting mixture to prevent or reduce ammonia volatilization. Zeolite, clay soil and manure compost were found to be very effective in decreasing nitrogen loss through ammonia volatilization, while woodchips and elemental sulphur (S^0) were less effective (Mahimairaja et al., 1994; Witter and Lopez-Real, 1988). Kithome et al. (1999) also reported that composting poultry manure with zeolite, coir (mesocarp of coconut fruit) and alum ($Al_4(SO_4)_3$) reduced NH_3 losses and produced compost with high NH_4^+ concentrations.

It is noteworthy that a partial recovery of nitrogen has been observed in later stages of composting. This is probably due to the activity of nitrogen-fixing bacteria in mesophilic phases (Bishop and Godfrey, 1983). In an experiment with composting poultry manure and ground corncobs run by Hansen et al. (1991), a comparison was made between nitrogen lost from compost media and nitrogen emitted in the form of ammonia. Significantly more nitrogen was emitted in the form of ammonia (9.4 g/kg) than was shown to be lost from the compost itself (5.4 g/kg), and the reason remained unexplained. This phenomena has not been well investigated and understood.

1.3 MODELING APPROACHES

1.3.1 Modeling Approaches for Carbon and Nitrogen Decomposition

Modeling substrate decomposition and nitrogen mineralization and immobilization has been investigated extensively in soil ecological research. Simulation models have been developed for carbon and nitrogen decomposition of organic matter (Knapp et al., 1983; Reuss and Innis, 1977) and ammonia volatilization from soil organic matter and fertilizer decomposition has been studied extensively (Freney et al., 1983; Jayaweera and Mikkelsen, 1990; Parton et al., 1981). Nitrogen transformation associated with decomposition of organic materials in soil have also been explored by simulation modeling (Juma and Paul, 1981; McGill et al., 1981; Parnas, 1975; Van Veen and Frissel, 1979). A model simulating ammonia volatilization after manure application to soil was developed by Hengnirun et al. (1999) and incorporated the factors influencing volatilization rate.

1.3.2 Modeling Approaches in Composting

Simulation methods have been used to describe composting kinetics. Several models have been developed to help in optimization of the process and engineering design of composting facilities (Haug, 1993). Mass and heat balance equations have been used to describe carbon dioxide evolution rate, reaction temperature, volatile matter conversion, and to determine optimal temperature for substrate decomposition and effective drying (Nakasaki et al., 1987).

A Composting Particle Kinetics (CPK) model developed by Hamelers (1993) examined the kinetics of composting at the particle level, connecting basic microbial kinetics with the structure and composition of the waste. The model effectively calculated gradients of oxygen, biomass, and soluble and polymeric substrate in the boundary layer surrounding individual particles. A sensitivity analysis of the CPK model indicates three periods, each being characterized by a different rate limiting step: a biomass amount limiting period; an oxygen diffusion transport rate limiting period; and a hydrolysis rate limiting period. This model is useful to study the influence of waste structure and the presence of an anaerobic core on the kinetics of the process.

A simple dynamic model based on microbial process kinetics using one substrate term was developed by Stombaugh and Nokes (1996). This model provides a way for demonstrating the complex interactions between microbial biomass growth and other physical parameters for different layers within a composter.

Relatively complicated substrates and different biotic components were employed by Kaiser (1996) in simulating kinetics of organic matter conversion and microbial growth. Consumption of four substrates by a four-component microflora, as well as the specific conditions for the decay of lignin were considered. This model clearly demonstrated the role of each classification of microflora on the decomposition of a typical substrate range.

Most of the composting models place emphasis on mass and heat balances to reveal substrate decomposition and describes the process. However, the fate of nitrogen during composting has not been addressed by modeling approaches, which would be effective in developing a more complete picture of the composting process.

1.4 RESEARCH NEED

As can be seen, ammonia volatilization is a very dynamic, complicated bio-physical and bio-chemical process affected by a variety of factors, which are interrelated among themselves. Results from individual studies provide valuable information of certain specific aspects, but lack internal relationship. Mechanisms by which nitrogen is lost are not fully understood, which makes it difficult to design and manage processes so that the nutrients, especially nitrogen, are conserved in an optimum manner.

Mathematical modeling provides an excellent vehicle for understanding and demonstrating the dynamic, complex interactions that occur in the composting process. The mechanisms of nitrogen transformation in the composting process can be better explored if the information of ammonia volatilization can be incorporated into a mathematical model. It is also important to associate the nitrogen losses with substrate characteristics and its decomposition, and to identify the design parameters and handling strategies that will minimize nitrogen losses and improve the fertilization value of compost product.

1.5 AIMS AND SCOPE OF THE RESEARCH

The overall objectives of this project are (1) to develop a mathematical model of the composting process that accurately describes nitrogen transformation and the factors controlling the fate of nitrogen, and (2) to verify this model under controlled conditions using a laboratory-scale composting system.

This introduction is followed by five chapters. The development of a mathematical model of substrate decomposition and ammonia volatilization in the high rate stage of composting is discussed in Chapter 2. During the development of the model, it was recognized that an accurate representation of pH measurement was important to investigate the ammonia volatilization. Therefore, a thorough investigation of determination of compost pH was carried out and is detailed in Chapter 3. Chapter 4 describes an experiment carried out using a laboratory-scale manure-and-straw composting system for model validation. The validation of the mathematical model is presented in Chapter 5. Finally, Chapter 6 provides the general conclusions that can be drawn from this work and addresses further research needs.

1.6 REFERENCE

Al-Kanani, T., E. Akochi, A.F. MacKenzie, I. Alli and S. Barrington. 1992. Organic and inorganic amendments to reduce ammonia losses from liquid hog manure. J. Environ. Qual. 21: 709-715.

Barrington, S.F., D. Choinière, M. Trigui, S. Wasay and W. Knight. 1997. Effect of C source on bedding and compost N volatilization. In: J.A. Voermans and G.J. Monteny (eds), Proceedings of the international symposium. Ammonia and odour control from animal production facilities. pp. 579-584. Vinkeloord, The Netherlands.

Beck, J., Kăck, M., Hentschel, A., Csehi, K., Jungbluth, T. 1997. Ammonia emission from composting animal wastes in reactors and windrows. In: J.A. Voermans and G.J. Monteny (eds), Proceedings of the international symposium. Ammonia and odour control from animal production facilities. pp. 381-388. Vinkeloord, The Netherlands.

Bhoyar, R.V., M.S. Olaniya, and A.D. Bhide. 1979. Effect of temperature on mineralization of nitrogen during aerobic composting. Indian J. Environ. Health 21:23-34.

Bishop, P.L. and C. Godfrey. 1983. Nitrogen transformations during sludge composting. Biocycle 24: 34-39.

Black, C.A. 1968. Soil-plant relationships. John Wiley & Sons, Inc. NY.

Brink, N. 1995. Composting of food waste with straw and other carbon sources for nitrogen catching. Acta. Agric. Scand. Sect. B, Soil and Plant Sci. 45: 118-123.

Carlile, F.S. 1984. Ammonia in poultry houses: A literature review. World's Poultry Sci. J. 40: 99-113.

Court, M.N., R.C. Stephen and J.S. Waid. 1964. Toxicity as a cause of the inefficiency of urea as a fertilizer. J. Soil Sci. 15: 42-48.

Edwards, D.R. and T.C. Daniel. 1992. Environmental impacts of on-farm poultry waste disposal – a review. Bioresource Technol., 41: 9-33.

Ekinci, K., H.M. Keener and D.L. Elwell. 1998. Composting short paper fiber with broiler litter and additives – Alum, HiClay® Alumina and sulfuric acid: I. Effect of initial pH and carbon/nitrogen ratio on ammonia emission. ASAE Paper No. 984137. ASAE, St. Joseph, MI.

Freney, J.R., J.R. Simpson and O.T. Denmead. 1983. Volatilization of ammonia. In: J.R. Freney and J.R. Simpson (eds.). Gaseous loss of nitrogen from plant-soil systems. Martinus Nijhoff/Dr W. Junk Publishers.

Gray, K.R., K. Sherman and A.J. Biddlestone. 1971. A review of composting – Part 1. Process Biochemistry 6: 32-36.

Hamelers, H.V.M. 1993. A theoretical model of composting kinetics. In: H.A.J. Hoitink and H.M. Keener (eds.). Science and engineering of composting: Design, environmental, microbiological and utilization aspects. Renaissance Publications, Worthington, OH. pp. 36-58.

Hansen, R.C., H.M. Keener, C.Marugg, W.A.Dick and H.A.J.Hoitink. 1993. Composting of Poultry Manure. In: H.A.J. Hoitink and H.M. Keener (eds.). Science and engineering of composting: Design, environmental, microbiological and utilization aspects. pp.131-153.

Hansen, R.C, C. Marugg, H.M. Keener, W.A. Dick and H.A.J. Hoitink. 1991. Nitrogen transformations during poultry manure composting. ASAE Paper. No. 91-4014. ASAE, St. Joseph, MI. 15p.

Hansen, R.C., H. M. Keener and H. A. J. Hoitink. 1989. Poultry manure composting: Design guidelines for ammonia. ASAE Paper No. 89-4075. ASAE, St. Joseph, MI. 11p.

Haslam, R.T., R.L. Hershey and R.H. Keen. 1924. Effect of gas velocity and temperature on rate of absorption. Industrial and Engineering Chemistry 16: 1224-1231.

Haug, R T. 1993. The Practical Handbook of Compost Engineering. CRC Press, Inc, 2000 Corporate Blvd., N.W. Boca Raton, FL.

Hengnirun, S., S. Barrington, S.O. Prasher and D. Lyew. 1999. Development and verification of a model simulating ammonia volatilization from soil and manure. J. Environ. Qual. 28: 108-114.

Hong, J., K. Park and B. Shon. 1997. Influence of aeration rate on ammonia emission in high rate composting of dairy manure and rice hulls mixtures. ASAE Paper No. 97-4114. ASAE, St. Joseph, MI. 8p.

Jacobsen, S. T. 1987. Ammonia volatilization during composting of straw and slurry. In: E. Welte and I. Szabolcs. (eds.) 4th International CIEC Symp. Agricultural waste management and environmental protection. pp. 283-291.

Jayaweera, G.R. and D.S. Mikkelsen. 1990. Ammonia volatilization from flooded soil systems: a computer model. I. Theoretical aspects. Soil Sci. Soc. Am. J. 54: 1447-1455.

Juma, N.G. and E.A. Paul. 1981. Use of tracers and computer simulation techniques to assess mineralization and immobilization of soil nitrogen. In: M.J. Frissel, and J.A Van Veen (eds.). Simulation of nitrogen behavior of soil-plant systems. Pudoc, Wageningen, The Netherlands. pp. 145-154.

Käck, M. 1996. Ammoniakemissionen bei der Kompostierung separierter Feststoffe aus Flüssigmist in belüfteten Rottereaktoren. Diss., Hohenheim, Forschungsbericht Agrartechnik, MEG-Nr. 285.

Kaiser, J. 1996. Modeling composting as a microbial ecosystem: a simulation approach. Ecological Modeling. 91: 25-37.

Kirchmann, H. and E. Witter. 1989. Ammonia volatilization during aerobic and anaerobic manure decomposition. Plant and Soil. 115: 35-41.

Kithome, M., J.W. Paul and A.A. Bomke. 1999. Reducing nitrogen losses during simulated composting of poultry manure using adsorbents or chemical amendments. J. Environ. Qual. 28:194-201.

Knapp, E.B., L.F. Elliott and G.S. Campbell. 1983. Carbon, nitrogen and microbial biomass interrelationships during the decomposition model. Soil Biol. Biochem. 15(4): 455-461.

Körner I., Stegmann R., 1998. Influence of biowaste composition and composting parameters on the nitrogen dynamics during composting and nitrogen contents in compost. In: Szmidt R.A.K. (ed.). Acta Horticulturae: Proceedings on the international symposium on composting and use of composted materials for horticulture, Auchincruive, UK. Vol. 469, ISHS, Drukkerij Van Damme, Beke, Brugge, Belgium, pp. 97-110.

Lauer, D.A., D.R. Bouldin and S.D. Klausner. 1977. Ammonia volatilization from dairy manure spread on the soil surface. J. Environ. Qual. 5: 134-141.

Lockyer, D.R., B.F. Pain and J.V. Klarenbeek. 1989. Ammonia emissions from cattle, pig and poultry wastes applied to pasture. Environ. Pollut. 56: 19-30.

Lopez-Real, J.M. 1996. Composting of agricultural wastes. In: S.M. De Bertoldi, P. Sequi, B. Lemmes and T. Papi (eds). The science of composting. Black Academic and Professional

Maeda, T. and Matsuda, J. 1997. Ammonia emission from composting livestock manure. In: J.A. Voermans and G.J. Monteny (eds.). Proceedings of the international symposium. Ammonia and odour control from animal production facilities. pp. 145-153. Vinkeloord, The Netherlands.

Mahimairaja, S., N.S. Bolan, M.J. Hedley and A.N. Macgregor. 1994. Losses and transformation of nitrogen during composting of poultry manure with different amendments: an incubation experiment. Bioresource Technol. 47: 265-273.

Martins, O. and T. Dewes. 1992. Loss of nitrogenous compounds during composting of animal wastes. Bioresource Technol. 42: 103-111.

McGill, W.B., H.W. Hunt, R.G. Woodmansee and J.O. Reuss. 1981. Phoenix, a model of the dynamics of carbon and nitrogen in grassland soils. In: F.E. Clark and T. Rosswall (eds.). Terrestrial nitrogen cycles. Ecol. Bull. (Stockholm) 33: 49-115.

Meyer, M. and H. Sticher. 1983. The significance of straw content for the retention of nitrogen during the composting of cattle manure. Z. Pflanzenernaehr. Bodenk, 146: 199-206.

Miller, F.C. 1991. Composting as a process based on the control of ecologically selective factors. In: F.B. Metting (ed.) Soil Ecology: Applications in agricultural and environmental management, pp. 514-544. Marcel Dekker Inc., NY.

Moore, P.A., Jr., T.C. Daniel, D.R. Edwards, and D.M. Miller. 1995. Effect of chemical amendments on ammonia volatilization from poultry litter. J. Environ. Qual., 24: 293-300.

Morisaki, N, C.G. Phae, K. Nakasaki, M. Shoda and H. Kubota. 1989. Nitrogen transformation during thermophilic composting. J. of Ferment. Bioeng. 67(1): 57-61.

Mote, C.R. and C.L. Griffis. 1980. Variation in the composting process for different organic carbon sources. Agric. Wastes. 2: 215-223.

Nakasaki, K., H. Yaguchi, Y. Sasaki and H. Kubota. 1993. Effects of pH control on composting of garbage. Waste Manage. Res. 11: 117-125.

Nakasaki, K., J. Kato, T. Akiyama and H. Kubota. 1987. A new composting model and assessment of optimum operation for effective drying of composting material. J. Ferment. Technol. 65(4): 441-447.

Okereke, G.U. and V.W. Meints. 1985. Immediate immobilization of labeled NH_4^+ sulfate and urea nitrogen in soils. Soil Sci., 140:105-109.

Pain, B.F., Y.J. Rees and D.R. Lockyer. 1988. Odour and ammonia emissions following the application of pig or cattle slurry to land. In: V.C. Nielsen, J.H. Voorburg and P.L'Hermite (eds). Volatile emissions from livestock farming and sewage operations. pp. 2-11. Elsevier applied science, NY.

Parnas, H. 1975. Model for decomposition of organic material by microorganisms. Soil Biol. Biochem. 7: 161-169.

Parton, W.J., W.D. Grould, F.J. Adamsen, S. Torbit and R.G. Woodmansee. 1981. NH_3 volatilization model. In: M.J. Frissel and J.A. Van Veen (eds.). Simulation of nitrogen behaviour of soil-plant systems. Pudoc, Wageningen, The Netherlands. pp. 233-244.

Reuss J.O. and G.S. Innis. 1977. A grassland nitrogen flow simulation model. Ecology. 58: 379-388.

Reynolds, C.M. and D.C. Wolf. 1987. Influence of urease activity and soil properties on ammonia volatilization from urea. Soil Sci. 143: 418-425.

Schrader, L.E. 1984. Functions and transformations of nitrogen in higher plants. In: Hauck, R.D. (ed.) Nitrogen in crop production. Am. Soc. Agron., Madison, Wisconsin, pp 55-66.

Schulte, D.D. 1997. Critical parameters for emission. In: J.A. Voermans and G.J. Monteny (eds), Proceedings of the international symposium. Ammonia and odour control from animal production facilities. pp. 24 Vinkeloord, The Netherlands.

Sikora, L.J. 1999. MSW compost reduces nitrogen volatilization during dairy manure composting. Compost Sci. and Util. 7(4): 34-41.

Sikora, L.J. and M.A. Sowers. 1985. Effect of temperature control on the composting process. J. Environ. Qual. 14: 434-439.

Subair, S. 1995. Reducing ammonia volatilization from liquid hog manure by using organic amendments. MSc. Thesis. McGill University, Montreal, QC.

Suler, D.J. and M.S. Finstein. 1977. Effect of temperature, aeration, and moisture on CO_2 formation in bench-scale, continuously thermophilic composting of solid waste. Appl. and Environ. Microbiol. 33(2): 345-350.

Stombaugh, D.P. and S.E. Nokes. 1996. Development of a biological based aerobic composting simulation model. Transaction of ASAE. 39(1): 239-250.

Termeer, W.C. and P.R. Warman. 1993. Use of mineral amendments to reduce ammonia losses from dairy-cattle and chicken-manure slurries. Bioresource Technol. 44: 217-222.

Van Harreveld, A.P. 1981. Rapportage geurverspreidingsonderzoek bij het compost bedrijf van de Cooperative Nederlandse Champignons-kwekersvereniging B.V. te Ottersum. IMAG rapport 30.

Van Veen, J.A. and M.J. Frissel. 1979. Mathematical modeling of nitrogen transformations in soil. In: J.K.R. Gasser (ed.). Modeling Nitrogen from Farm Wastes. Applied Science Publishers, London. pp. 133-157.

Varel, V.H. J.A. Nienaber and B.H. Byrnes. 1997. Urease inhibitors reduce ammonia emissions from cattle manure. In: J.A. Voermans and G.J. Monteny (eds.). Proceedings of the international symposium. Ammonia and odour control from animal production facilities. pp. 721-728. Vinkeloord, The Netherlands.

Willson, G.B. and J.W. Hummel. 1975. Conservation of nitrogen in dairy manure composting. In: Managing livestock wastes, ASAE Publication, PROC-275. ASAE, St. Joseph, MI. 490- 491 and 496.

Witter, E. and J. Lopez-Real. 1988. Nitrogen losses during the composting of sewage sludge, and the effectiveness of clay soil, zeolite, and compost in adsorbing the volatilized ammonia. Biol. Wastes 23:279-294.

Witter, E. and J. Lopez-Real. 1987. The potential of sewage sludge and composting in a nitrogen recycling strategy for agriculture. Biological Agriculture and Horticulture 5: 1-23.

Wright, R.J. 1998. Executive summary. In: Wright, R.J., W.D. Kemper, P.D. Millner, J.F. Power and R.F. Korcak (eds.). Agricultural uses of municipal, animal, and industrial byproducts. Conservation Research Report No. 44. USDA-ARS. Beltsville, MA, pp. 9-44.

Chapter 2

A Mathematical Model of Substrate Decomposition and Ammonia Volatilization in the High Rate Stage of Composting

2.1 INTRODUCTION

Composting is an effective way to convert organic waste into a waste product and provide a natural amendment or soil conditioner to agricultural land. Composting for resource recovery, however, also requires conservation of nutrients during composting. Nitrogen losses reported in literature range from a slight gain in nitrogen to nearly 70% loss (Witter and Lopez-Real, 1987).

Loss of nitrogenous compounds during aerobic decomposition of organic wastes occur on the one hand through emission of gases such as ammonia (NH_3) and oxides of nitrogen (NO_x) and on the other hand as leachate in the form of bound nitrogen, NH_4^+ and NO_3^- (Martins and Dewes, 1992). Ammonia volatilization is believed to be the main pathway for nitrogen loss (Hansen et al., 1989; Hong et al., 1997; Kirchmann and Witter, 1989; Witter and Lopez-Real, 1987, 1988). High ammonia (NH_3) volatilization has been observed when thermophilic temperatures (>40°C) were achieved and have sometimes been associated with higher aeration (Beck et al., 1997; Hansen et al., 1989; Körner and Stegmann, 1998; Maeda and Matsuda, 1997). Factors affecting nitrogen losses and transformations during high temperature composting of sludge-straw mixtures were investigated by Witter (1986). He found that the high temperatures, alkaline pH values, and forced aeration of the compost pile, which are often associated with the composting process, encourage rapid volatilization of NH_3. However, whether NH_3 loss is temperature-dependent or ventilation-dependent, or how these are linked, is unknown. How N loss is associated with substrate characteristics and its decomposition is also in need of investigation.

Simulation methods have been used to describe composting kinetics. Several models have been used to help in optimization of the process and engineering design of composting facilities. Mass and heat balance equations have been used to describe carbon dioxide evolution rate, reaction temperature, volatile matter conversion, and to determine optimal temperature for substrate decomposition and effective drying (Nakasaki et al., 1987). A Composting Particle Kinetics (CPK) model built by Hamelers (1993) examined the kinetics of composting at the particle level, connecting basic microbial kinetics with the structure and composition of the substrate. The model effectively calculated gradients of oxygen, biomass, and soluble and polymeric substrate in the boundary layer surrounding individual particles. Both single substrate (Stombaugh and Nokes, 1996) and relatively complicated substrate and biotic components (Kaiser, 1996) have been employed in simulating kinetics of organic matter conversion and microbial growth. Most of the composting models emphasize mass and heat balances to reveal substrate decomposition and describes the process. However, the fate of nitrogen during composting has not been addressed by modeling approach, which will be effective in developing a more complete picture of the composting process.

Ammonia volatilization from soil organic matter and fertilizer decomposition has been studied extensively (Freney et al., 1983; Jayaweera and Mikkelsen, 1990; Parton et al., 1981). Decomposition of organic materials and nitrogen (N) transformation in soil have also been explored by simulation modeling (Juma and Paul, 1981; McGill et al., 1981;

Parnas, 1975; Van Veen and Frissel, 1979). These works made it possible to integrate the concept of nitrogen transformation, especially ammonia volatilization, and the substrate decomposition. The mechanisms of nitrogen (N) transformation in the composting process can be explored by modeling methods to understand the rate-controlling factors of nitrogen loss and to examine strategies to enhance N retention during composting.

The objectives of this study were (1) to develop a model to simulate substrate decomposition and nitrogen volatilization in the high rate stage of composting with the aim of predicting the physical, chemical, and biological processes of composting, and (2) to identify the design parameters and management strategies that will minimize N losses. This will bring together the more important factors and develop a clear and integrated picture which can be used to evaluate cause-and-effect relations in resource recovery (especially N retention and C availability) in composting processes in further work.

2.2 MODEL DESCRIPTION

In developing the model, the predominant mechanism for N loss was assumed to be gaseous N losses, especially ammonia volatilization. The model was first developed using Stella II software (High Performance Systems, Hanover, NH) and run on an IBM compatible microcomputer. It was then translated to C language to provide enhanced ability for numerical calculation. Euler's method was chosen to solve ordinary differential equations and the simulation time step was 0.01 hour.

The model was built initially based on the simple mathematical model of Stombaugh and Nokes (1996). Work has been extended to incorporate the factors influencing ammonia volatilization.

2.2.1 Structure

The model requires the input of masses of volatile substances, non-volatile substances, water content, etc., in kg per unit weight of dry matter. Therefore, the quantitative variables in the model have units of kg / kg d. m.. Flows between variables in each time step were in kg· (kg d.m.· hr)$^{-1}$. A simplified flow chart of the simulation model is presented in Figure 2-1.

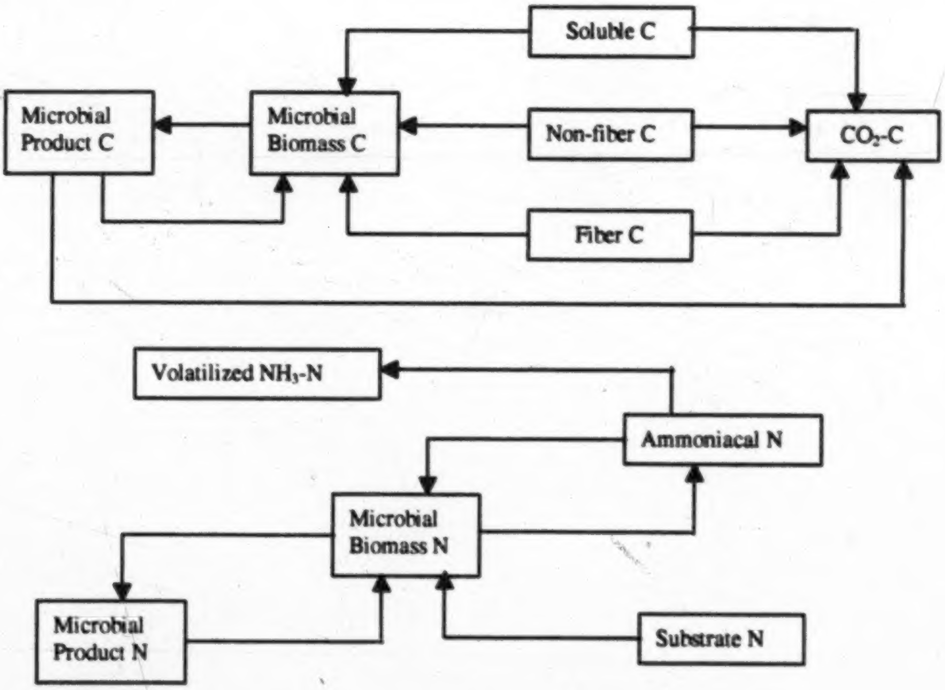
Soluble C
Microbial Product C
Microbial Biomass C
Non-fiber C
CO$_2$-C
Fiber C
Volatilized NH$_3$-N
Ammoniacal N
Microbial Biomass N
Microbial Product N
Substrate N

Figure 2-1. Flow chart of C and N transfers in the simulation model.

C sources under investigation were substrate C, microbial biomass C, microbial product C, and respired CO$_2$-C. The N sources were distinguished as substrate N, microbial biomass N, microbial product N, ammoniacal N in compost solution, and volatilized NH$_3$-N. Due to the objective of relating substrate decomposition to nitrogen transformation, the use of single, non-partitioned substrate was rejected because this could give only a rough representation of the transformation mechanisms. Subdivision of substrates allows better simulation of the decomposition behavior of actual mixtures. In this model complex C substrates were represented by three components: Soluble C, Non-fiber C and Fiber C. Nitrogen was treated as a single variable and was assumed to be associated with and decomposed at the same rate as non-fiber C. The partitioning of C substrate was based on both the chemical components and different decomposition rates of compost raw materials. Additional variables were oxygen (O_2) content, water (H_2O) content and temperature.

Several distinct groups of decomposers are involved in the composting process. These include bacteria, actinomycetes and fungi, etc. However, a lumped microbial biomass component was treated in this model due to the limitation of available experimental data. The microbial biomass has a variable C/N ratio that is allowed to change within a specified range. The microbial products represent microbial metabolic products and organic materials consisting of dead organisms. The initial value of product C was set to zero due to lack of better information from composting experiments or literature.

The variable of ammoniacal nitrogen in solution represents ammonium ion and molecular ammonia associated with the compost solution. Nitrification was assumed to be negligible during high-rate decomposition (Bishop and Godfrey, 1983; Edwards and Daniel, 1992) and was not taken into consideration in this model.

Temperature was defined as a state variable to simulate temperature changes due to heat content changes of the mixture. Water content was also defined as a state variable to account for water generation by bio-reaction and water removal by evaporation. Any water loss due to possible leachate was not accounted. Moisture content was calculated on a wet basis. Variation of temperature, moisture and pH were incorporated into the equations describing microbial biomass growth.

2.2.2 Model Development

2.2.2.1 Microbial Growth and Substrate Decomposition

The description of microbial growth was based on the assumption that all the required nutrients are present in excess. The growth of the biomass on substrate C was described using Michaelis-Menten or Monod-type kinetics. Oxygen was treated as a rate-limiting factor similar to substrates. Reduction factors for temperature, moisture content and pH were incorporated to correct for sub-optimal environmental conditions. Independent action of the three factors was assumed, and was realized by multiplication. Other environmental conditions were assumed to be not rate-limiting. Different values of maximum specific growth rate of organisms ($\mu_{max,i}$) on the three different C substrates, and saturation constants ($K_{s,i}$) were used to represent substrate availability and degradability. The transfer of biomass C to biomass product C was described using first-order reactions, i.e., the amount of biomass C that died per unit time was proportional to its mass. The first-order reaction rate (δ, h^{-1}) was set at 0.025 h^{-1}. The growth of biomass C on microbial product C was also described as a first-order reaction with the rate constant (k_p, h^{-1}) of 0.002 h^{-1}. The calculation of microbial net growth was described by:

$$dX_c/dt = \sum_i \mu_i X_c - \delta \cdot X_c + k_p \cdot P_x \qquad (1)$$

and $$\mu_i = \mu_{max,i} \frac{C_i}{(K_{s,i} + C_i)} \frac{C_{O2}}{(K_{O_2} + C_{O2})} k_{temp} k_{H_2O}\, k_{pH} \qquad (2)$$

where

X_c = concentration of microbial biomass C ($kg_C \cdot kg^{-1}$ d.m.)

t = time (hr)

μ_i = specific growth rate of organisms on each C substrate (h^{-1})

$\mu_{max,i}$ = maximum growth rate of organisms on each C substrate (h^{-1})

δ = microbial death rate (h^{-1})

k_p = first-order rate constant for conversion of microbial products to new biomass (h^{-1})

P_x = concentration of microbial product C ($kg_C \cdot kg^{-1}$ d.m.)

C_i = substrate C content, each as Soluble C, Non-fiber C or Fiber C ($kg_C \cdot kg^{-1}$ d.m.)

$K_{s,i}$ = saturation constant of organisms for each substrate C ($kg \cdot kg^{-1}$ d.m.)

C_{O2} = O_2 content in compost matrix (kg $O_2 \cdot kg^{-1}$ d.m.)

K_{O2} = saturation constant of O_2 content (kg $O_2 \cdot kg^{-1}$ d.m.)

k_{temp} = temperature coefficient (Figure 2-2)

= T/ 30 $0 < T < 30°C$

= 1.0 $30°C < T < 55°C$

= 3.75 - T/ 20 $55°C < T < 75°C$

T = temperature of compost mixture (°C)

k_{H2O} = moisture coefficient (Figure 2-3)

= 0 $0 < m < 0.2$

= (m/0.2) - 1.0 $0.2 < m < 0.4$

= 1.0 $0.4 < m$

m = moisture content ($kg \cdot kg^{-1}$) (wet basis)

k_{pH} = pH coefficient (Figure 2-4)

$= 0 \qquad pH < 4$ or $pH > 12$

$= pH/2 - 2.5 \qquad 4 < pH < 7$

$= 1 \qquad 7 < pH < 9$

$= -pH/3 + 4 \qquad 9 < pH < 12$

$= 0 \qquad 12 < pH < 14$

Temperature and moisture factors are shown in Figures 2-2, 2-3 (Stombaugh and Nokes, 1996) respectively, and pH factor is shown in Figure 2-4. The value for k_{temp} represents a community-level response of several microbial populations. Moisture content of more than 40% is treated as not limiting for microbial growth and k_{H2O} was set at 1.0 in this range. Negative effect due to excessive moisture that leads to reduced free air space and possible anaerobic conditions is not considered in this model. The factor of k_{pH} relates relative rate of decomposition to pH. pH effect is more pronounced for protein degradation than glucose degradation with a narrower optimum range for protein (Nakasaki et al., 1993). For simplicity, the same assumptions regarding k_{pH} were used here.

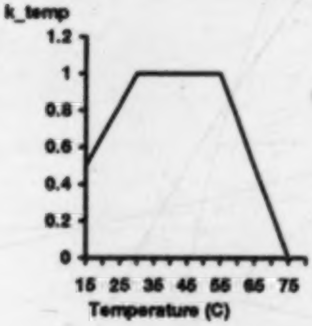

Figure 2-2. Assumed temperature effect on decomposition rate

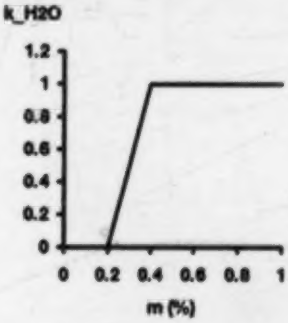

Figure 2-3. Assumed moisture effect on decomposition rate

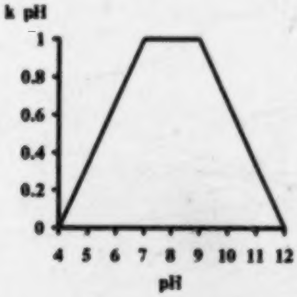

Figure 2-4. Assumed pH effect on decomposition rate

The rate of substrate C decomposition (dC_i/dt, kg· kg^{-1} d.m· h^{-1}) was determined based on the summation of energy required for cell synthesis and respiration maintenance.

$$\frac{dC_i}{dt} = \frac{1}{Y_{X/C_i}}(\mu_i X_c) + \beta_i X_c \tag{3}$$

$$\beta_i = \beta_{max,i} \frac{C_i}{(K_{s,i} + C_i)} \frac{C_{O2}}{(K_{O_2} + C_{O2})} k_{temp} k_{H_2O} k_{pH_i} \tag{4}$$

where:

Y_{X/C_i} – yield coefficients representing efficiency of substrate C utilization (kg cell C produced per kg substrate C consumed)

β_i – microbial maintenance coefficients (h^{-1})

$\beta_{max,i}$ – maximum microbial maintenance coefficients (h^{-1})

The above parameters were estimated and modified based on literature (Stombaugh and Nokes, 1996; Kaiser, 1996) and are shown in Table 2-1.

The change rate of microbial product C is:

$$\frac{dP_X}{dt} = \delta \cdot X_c - \frac{1}{Y_{X/P}} \cdot k_P \cdot P_x \tag{5}$$

where:

$Y_{X/P}$ – yield coefficient representing utilization efficiency of microbial product as substrate (kg cell C produced per kg substrate C oxidized)

Oxidized C (dC_{CO2}/dt, $kg_C \cdot kg^{-1}$ d.m$\cdot$ h^{-1}) can be calculated as CO_2-C as follows:

$$\frac{dC_{CO_2}}{dt} = (\frac{1}{Y_{X/C_i}} - 1) \cdot \sum_i \mu_i X_c + \sum_i \beta_i X_c + (\frac{1}{Y_{X/P}} - 1) \cdot k_P \cdot P_X \tag{6}$$

2.2.2.2 *Thermodynamics*

The change in heat content (kJ$\cdot$ (kg d.m.$\cdot$h)$^{-1}$) is given by:

$$\frac{dQ}{dt} = \frac{dQ_{bio}}{dt} - \frac{dQ_{cond}}{dt} - \left(\frac{dQ_{out}}{dt} - \frac{dQ_{in}}{dt}\right) \tag{7}$$

where:

Q = heat content of compost mixture (kJ· kg^{-1} d.m.)

dQ_{bio}/dt = bio-reaction heat production (kJ· kg^{-1} d.m.· h^{-1})

dQ_{cond}/dt = heat flow via conduction (kJ· kg^{-1} d.m.· h^{-1})

dQ_{out}/dt = heat flow via exhaust air (kJ· kg^{-1} d.m.· h^{-1})

dQ_{in}/dt = heat flow via intake air (kJ· kg^{-1} d.m.· h^{-1})

Table 2-1. Parameters of microbial growth kinetics used in simulation

Parameter	Units	Default value
$\mu_{max.1}$ (for Soluble C)	h^{-1}	0.50
$\mu_{max.2}$ (for Protein C)	h^{-1}	0.50
$\mu_{max.3}$ (for Fiber C)	h^{-1}	0.03
$\delta^{\dagger}$	h^{-1}	0.025
K_p	h^{-1}	0.002
$\beta_{max.1}$	kg$_C$· (kg$_X^{-1}$ h^{-1})	0.08
$\beta_{max.2}$	kg$_C$· (kg$_X^{-1}$ h^{-1})	0.08
$\beta_{max.3}$	kg$_C$· (kg$_X^{-1}$ h^{-1})	0.006
$Y_{X/SC}$	kg$_X$· kg$_C^{-1}$	0.35
$Y_{X/PC}$	kg$_X$· kg$_C^{-1}$	0.35
$Y_{X/FC}$	kg$_X$· kg$_C^{-1}$	0.3
$Y_{X/P}$	kg$_X$· kg$_C^{-1}$	0.35
$Y_{W/S}$	kg$_{H2O}$· kg$_S^{-1}$	0.56
$Y_{O2/S}$	kg$_{O2}$· kg$_S^{-1}$	1.370
$Y_{H/S}^{\dagger}$	kJ· kg$_S^{-1}$	19,100
$K_{S,1}$	kg· kg^{-1} d.m.	0.025
$K_{S,2}$	kg· kg^{-1} d.m.	0.170
$K_{S,3}$	kg· kg^{-1} d.m.	0.40
$K_{O2}^{\dagger}$	kg· kg^{-1} d.m.	0.00003

† Stombaugh (1995)

$$\frac{dQ_{bio}}{dt} = Y_{H/S}\left(\frac{dC_{CO_2}}{dt} / f_c\right) \tag{8}$$

$$\frac{dQ_{cond}}{dt} = UA(T - T_{ambient}) / D_{init} \tag{9}$$

$$\frac{dQ_{out}}{dt} = h_{out} \cdot F_{out} \tag{10}$$

$$\frac{dQ_{in}}{dt} = h_{in} \cdot F_{in} \tag{11}$$

where:

$Y_{H/S}$ = yield coefficient (kJ of heat produced per kg substrate oxidized)

f_c = carbon fraction in volatile substrate (kg$_C$· kg^{-1} volatile substrate)

U = overall heat transfer coefficient of the composter wall (kJ· (m^2· °C· h)$^{-1}$)

A = surface area of heat conduction (m^2)

$T_{ambient}$ = temperature of ambient air (°C)

D_{init} = initial dry matter (kg)

h = specific enthalpies of air (kJ· kg^{-1}dry air)

F_{out}, F_{in} = flow rate of exhaust and intake air (kg$_{da}$· kg^{-1} d.m.· h^{-1})

Assuming equal dry mass flow rates of exhaust air and intake air through the compost mixture, the difference in specific enthalpy, between inlet and outlet, was calculated as the difference of the sums of latent heat and sensible heat for 1 kg of dry air as follows:

$$
\begin{aligned}
\frac{dQ_{out}}{dt}-\frac{dQ_{in}}{dt} &= F\cdot\left(h_{out}-h_{in}\right)\\
&= F\cdot\left(\Delta h_s+\Delta h_l\right)\\
&= F\times\left|\left(c_w\left(w_{out}T \quad w_{in}T_{ambient}\right)+c_a \quad 1.0 \quad \left(T \quad T_{ambient}\right)\right)+h_{fg} \quad \left(w_{sat}(T) \quad w_{in}\right)\right| \qquad (12)
\end{aligned}
$$

where:

Δh_s = sensible heat change (kJ· kg^{-1}dry air)

Δh_l = latent heat change (kJ· kg^{-1}dry air)

c_w = specific heat of water (kJ· (kg water · °C)$^{-1}$)

c_a = specific heat of dry air (kJ· (kg d.a.· °C)$^{-1}$)

h_{fg} = latent heat of vaporization of water (kJ· kg^{-1} H_2O)

w_{out} = humidity ratio of exhaust air at temperature of compost (kgH_2O· kg_{da}^{-1})

w_{in} = humidity ratio of intake air at ambient temperature (kgH_2O· kg_{da}^{-1})

It was assumed that the exhaust air was at the process temperature and saturated at that temperature if the moisture content of the mixture was greater than 18%. A sub-model was developed to calculate humidity ratios of inlet air and exhaust air in the model. The latent heat of vaporization varies depending on temperature level. Thermodynamic parameters are presented in Table 2-2.

The process temperature (T, °C) was calculated from the change of heat content as:

$$\frac{dT}{dt} = \frac{dQ}{dt} / G_{mass} \tag{13}$$

where:

G_{mass} = thermal mass of compost mixture (kJ· kg^{-1} d.m.· $(°C)^{-1}$)

The heat capacities of air and container were neglected in this model. The components of composting matter include volatile substrate, non-volatile substance and water so that:

$$G_{mass} = c_w \cdot W + c_{nvs} \cdot nvs + c_s \cdot S \tag{14}$$

where:

c_{nvs}, c_s = specific heat of components (kJ· (kg nvs or kg vs· $°C)^{-1}$)

nvs = non-volatile substance content (kg nvs· kg^{-1} d.m.)

S = volatile substance content (kg vs· kg^{-1} d.m.)

W = water content (kg H_2O· kg^{-1} d.m.)

Table 2-2. Thermodynamic parameters

Parameter	Description	Default
$c_s^{\dagger}$	Specific heat of substrate	1.480 kJ· (kg °C)$^{-1}$
$c_{nvs}^{\dagger}$	Specific heat of non-volatile substance	0.840 kJ· (kg °C)$^{-1}$
$c_w^{\dagger}$	Specific heat of water	4.180 kJ· (kg °C)$^{-1}$
c_a	Specific heat of dry air	1.006 kJ· (kg °C)$^{-1}$
ρ	Specific air density	1.286 kg_{da}· m^{-3} air
$h_{fg}^{\ddagger}$	latent heat of evaporation	2455~2359 kJ· kg^{-1} H_2O (20-60°C)

†Stombaugh (1995)

‡having lower values at higher temperatures

Oxygen content (C_{O2}, kg· kg^{-1} d.m.) was used as one factor limiting the specific growth rate of microorganisms. The rate of change in the O_2 content was derived as:

$$\frac{dC_{O_2}}{dt} = Y_{O_2/S}\left(\frac{dC_{CO_2}}{dt} / f_c\right) + \frac{\left(O_{2_{in}} - O_2\right)}{\rho} F \tag{15}$$

where:

$Y_{O2/S}$ = yield coefficient (kg O_2 consumed· kg^{-1} substrate oxidized)

O_{2in} = oxygen concentration of intake air (kg O_2· m^{-3} air)

O_2 = oxygen concentration in compost and exhaust air (kg O_2· m^{-3} air)

ρ = specific air density, (kg_{da}· m^{-3} air)

The effects of moisture on decomposition were included in the moisture coefficient k_{H2O} as another limiting factor of microbial growth. The moisture content (m, %) and the rate of change in the water content (W, kg· kg^{-1} d.m.) can be calculated by:

$$m = \frac{W}{S + nvs + W} \tag{16}$$

$$\frac{dW}{dt} = Y_{W/S}\left(\frac{dC_{CO_2}}{dt} / f_c\right) - \left(w_{in} - w_{out}\right) \cdot F \tag{17}$$

where:

$Y_{W/S}$ = yield coefficient (kg water produced· per kg substrate oxidized)

2.2.2.3 Nitrogen Decomposition

Nitrogenous material decomposition (dN_i/dt, kg· kg^{-1}d.m.· h^{-1}) was assumed to be proportional to the non-fiber C decomposition and was calculated by dividing the C consumption rate by the C/N ratio of the non-fiber substrate:

$$\frac{dN}{dt} = \frac{dC_{Nf}}{dt} / CN_S \qquad (18)$$

where

C_{Nf} = Non-fiber C content

CN_S = C/N ratio of non-fiber substrate

The C/N ratio of non-fiber substrate was set at four since this material was considered to be similar to protein and would have a similar decomposition rate.

2.2.2.4 Nitrogen Immobilization-Mineralization

Immobilization describes the rate at which inorganic N (mineral N) is transferred to microbial biomass N. The immobilization of inorganic N by microbes depends on the concentration of ammoniacal N and the microbial C/N ratio. Ammonification occurs concurrently with immobilization. Microorganisms release excess N accumulated during consumption of a N-rich carbon source as ammonia. Based on the work of McGill et al. (1981), immobilization and ammonification were calculated as:

$$U_I = k_{cu} \frac{V_{max} \cdot N_{ib}}{K_m + N_{ib}} X \qquad (19)$$

$$U_a = k_a \cdot k_{ca} \cdot X \qquad (20)$$

where:

U_I – immobilization rate, $kgN \cdot kg^{-1}$ d.m. h^{-1}

U_a – ammonification rate, $kgN \cdot kg^{-1}$ d.m. h^{-1}

k_{cu} – effect of microbial C/N ratio on immobilization

k_{ca} – effect of microbial C/N ratio on ammonification

V_{max}, K_m – constants of Michaelis-Menten kinetics

N_{ib} – the concentration of inorganic N in the compost solution ($kgN \cdot kg^{-1} H_2O$)

k_a – first-order rate constant of ammonification (h^{-1})

The assumed variation of k_{cu} and k_{ca} with C/N ratio is illustrated in Figure 2-5.

The net mineralization rate (U_m, kgN kg^{-1} d.m. h^{-1}) can be described as:

$$U_m = U_a - U_I \qquad (21)$$

A positive value of U_m represents mineralization, while a negative value implies immobilization. The calculation of mineralization and immobilization independently results in a fluctuating C/N ratio of the microbial biomass.

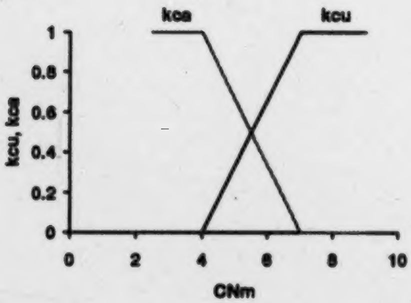

Figure 2-5. Immobilization and mineralization coefficients at various microbial C/N ratios.

The rate of change in microbial N concentration (N_m) was derived as:

$$\frac{dN_m}{dt} = -U_m - \frac{dN}{dt} + k_p P_N \qquad (22)$$

where:

N_m = microbial N concentration, $kg_N\ kg^{-1}$ d.m.

P_N = microbial product N concentration, $kg_N\ kg^{-1}$ d.m.

2.2.2.5 Multisolute Aqueous System of NH_3-CO_2-H_2O

The volatilization of ammonia was assumed to be controlled by physico-chemical processes. The various processes which are related to ammonia loss may be represented as:

$$\begin{array}{ccccc} & & & & NH_3 \text{ (gas in surrounding environment)} \\ & & & & \uparrow \\ NH_4^+ \text{ (in solution)} & \leftrightarrow & NH_3 \text{ (in solution)} & \leftrightarrow & NH_3 \text{ (gas in compost matrix)} \end{array} \qquad (23)$$

Several factors directly influence the process of NH_3 volatilization, such as ammoniacal N concentration, pH, temperature, moisture content, and aeration rate. The driving force for NH_3 volatilization in aerobic composting is considered to be the aeration supply through the compost matrix. The partial pressure gradient of ammonia (P_{NH3}) between the compost free air space (FAS) and the surrounding ambient air determines the ammonia volatilization rate. The P_{NH3} in the compost FAS is dependent on the NH_3 concentration, pH and temperature. The NH_3 concentration is affected by drying, which increases the concentration and therefore, the P_{NH3} gradient.

During composting processes, the decomposition of acidic metabolic substances, such as organic acids generated in association with glucose degradation, will result in pH reduction, while decomposition of alkaline metabolic substances, such as NH_3 produced by the degradation of protein, will increase pH. Experimental data (Freney et al., 1983; Körner and Stegmann, 1997; Nakasaki et al., 1993) indicate that the most severe losses of NH_3 occurred when high pH values were measured. Since the NH_3 portion of ammoniacal N increases as pH and temperature of compost increase, higher pH values increase the concentration of NH_3 present in the solution and FAS, therefore increasing the potential for NH_3 loss. Since the concentration of ammoniacal N depends on the quantity of ammoniacal N and water in the substrate, wetting and drying also play significant roles in determining the rate of NH_3 volatilization.

Carbon dioxide is released in large amounts as a result of organic matter decomposition in composting. Carbon dioxide concentration is influenced by microbial activity and air exchange rate. The compost solution can be treated as a multisolute NH_3-CO_2-H_2O system, with NH_3 and CO_2 as weak electrolytes. A molecular thermodynamic approach for calculating equilibrium gas-liquid compositions of dilute solutions was established, assuming that dissociation species of carbon and nitrogen are the major ions in compost solution. This approach is based on several studies of multisolute aqueous solutions of volatile weak electrolytes (Edwards, 1978; Edwards et al., 1975; Nakamura et al., 1976).

At a given temperature and pressure, weak electrolyte distributes itself between gas and liquid phases. At low concentration, the phase equilibrium is determined by Henry's constant (**H**) and concentration of molecular solute. The gas-liquid equilibrium of NH_3 is commonly applied in the simulation of ammonia loss from soil layers (Avnimelech and Laher, 1977; English et al., 1980; Parton et al., 1981). During the high rate stage in composting processes, gas-liquid equilibrium may not be reached in each simulation time step (0.01 hour). Half of the concentration of ammonia in the liquid phase was applied in this model to calculate ammonia concentration in the gaseous phase based on a normal equilibrium assumption. The two-phase equilibria of NH_3 and CO_2 can be written as:

$$NH_3^{aq} \Leftrightarrow NH_3^{g} \qquad (24)$$

$$CO_2^{aq} \Leftrightarrow CO_2^{g} \qquad (25)$$

The phase equilibrium is accounted for by:

$$P_a = 0.5 \cdot H_a \cdot a_a \qquad (26)$$

where:

P_a = partial pressure of molecular solute (NH_3 or CO_2) in FAS (atm)

H_a = Henry's constant (kg·atm·(mole·K)$^{-1}$)

a_a = activity as molality in solution (mole · kg^{-1} of solvent)

Henry's constant, which is a function of temperature, is the characteristic describing the interaction of a given solute and solvent. The partition of NH_3 between the two phases varies markedly with temperature. Following the approach of Edwards et al. (1975), a semi-empirical equation was used to calculate Henry's constants of NH_3 and CO_2:

$$\ln H = B_1 / T + B_2 \cdot \ln T + B_3 \cdot T + B_4 \qquad (27)$$

The values of the B parameters used are given in Table 2-3.

Table 2-3. Parameter values used in determining Henry's constants for NH_3 and CO_2 in water*

H, kg-atm·(mole-K)$^{-1}$; T, K

Electrolyte	B_1	B_2	B_3	B_4
NH_3	-7579.948	-13.588	0.008597	96.2187
CO_2	-17060.71	-68.316	0.065989	430.1788

* Data of Edwards et al., 1975.

In the liquid phase, weak electrolyte exists in different forms: molecular (undissociated) form and ionic (dissociated) form. The chemical equilibria can be described as:

$$NH_3 + H_2O \Leftrightarrow NH_4^+ + OH^- \tag{28a}$$

$$CO_2 + H_2O \Leftrightarrow H^+ + HCO_3^- \tag{28b}$$

$$HCO_3^- \Leftrightarrow H^+ + CO_3^{2-} \tag{28c}$$

The associated species of anhydrous carbamate (NH_2COO^-) was described as:

$$NH_3 + HCO_3^- \Leftrightarrow NH_2COO^- + H_2O \tag{28d}$$

The dissociation equilibrium of water is required to interrelate the concentrations of hydrogen ion and hydroxyl ion.

$$H_2O \Leftrightarrow H^+ + OH^- \tag{28e}$$

The above equations (28a~28e) give rise to five equilibria relationships as follows:

(I) $$K_1 = \frac{a_{NH4+}a_{OH-}}{a_{NH3}a_{H2O}}$$

(II) $$K_2 = \frac{a_{H+}a_{HCO3-}}{a_{CO2}a_{H2O}}$$

(III) $$K_3 = \frac{a_{H+}a_{CO3--}}{a_{HCO3-}}$$

(IV) $$K_4 = \frac{a_{NH2COO-}a_{H2O}}{a_{NH3}a_{HCO3-}}$$

(V) $$K_5 = \frac{a_{H+}a_{OH-}}{a_{H2O}}$$

where:

a = activity of either cation, anion or molecule

Again, following the approach of Edwards et al. (1975), a semi-empirical equation was used to describe them as follows:

$$\ln K = C_1 / T + C_2 \cdot \ln T + C_3 \cdot T + C_4 \tag{29}$$

Values of the C parameters used in this study are given in Table 2-4.

Table 2-4. Parameter values used to determine dissociation constants of NH_3 and CO_2 in water*

K, mole·kg^{-1}; T, K

Electrolyte	C_1	C_2	C_3	C_4
NH_3	-5914.082	-15.06399	-0.01100801	97.97152
CO_2	-7726.010	-14.50613	-0.0279842	102.2755
HCO_3^-	-9137.258	-18.11192	-0.02245619	116.7371
NH_2COO^-	604.1164	-4.017263	0.00503095	20.15214
H_2O	-13445.90	-22.47730	0.0	140.932

* Data of Edwards et al., 1975.

Equation (28a) can be written as a combination of Equations (30) and (28e) as follows.

$$NH_3 + H^+ \underset{Ka}{\Leftrightarrow} NH_4^+ \tag{30}$$

where $K_a = \frac{a_{NH_3} a_{H^+}}{a_{NH_4^+}}$

K_a = acid dissociation constant for ammonia

It is apparent that the two representations of the equilibrium are the same and that the dissociation parameters, K_1, K_a and K_5, are related as:

$$K_a = \frac{K_5}{K_1}$$

The acid dissociation constant for ammonia was studied by several researchers (Groot Koerkamp and Ezling, 1996; Hashimoto and Ludington, 1971) and different values were found. For example, at temperature of 20°C, the K_a value is around 3.8E-10 mol/L for infinitely diluted solutions, which is the theoretical value commonly used. Hashimoto and Ludington (1971) found that in concentrated chicken manure slurries the constant K_a has a value of 0.81E-10 mol/L whereas Groot Koerkamp and Ezling (1996) found a value of 2.24E-9 mol/L for poultry litter, which has limited free liquid.

It is obvious that the higher this value is used, the higher concentration of unionized ammonia will be present in the mixture. The theoretical value, which falls between the other two values obtained, was applied in this model, on one hand for the reason of the readily available calculation at different temperatures, on the other hand due to the uncertainty of this constant.

Activities are given for any molecular or ionic species k, except water, as follows:

$$a_k = m_k \cdot \gamma_k \tag{31}$$

where:

m_k = apparent concentration as molality (mole / kg of solvent)

γ_k = molal activity coefficient

Activity coefficients γ_i describe physical interactions between solute species in the liquid phase. The effect of liquid phase composition on the activity coefficient of the solute was expressed as (Edwards et al., 1975):

$$\ln \gamma_i = -A_\varphi z_i^2 \left[\frac{\sqrt{I}}{1 + 1.2 \times \sqrt{I}} + \frac{2}{1.2} \ln(1 + 1.2 \times \sqrt{I}) \right] +$$

$$2 \times \sum_{j \neq w} m_j \left\{ \beta_{ij}^{(0)} + \frac{\beta_{ij}^{(1)}}{2I} [1 - (1 + 2\sqrt{I}) \exp(-2\sqrt{I})]\right\}$$

$$-\frac{z_i^2}{4I^2} \sum_{j \neq w} \sum_{k \neq w} m_j m_k \beta_{jk}^{(1)} \{1 - (1 + 2\sqrt{I} + 2I) \exp(-2\sqrt{I}) \} \tag{32}$$

where

A_ϕ = 2.303A_r/3, with A_r as Debye-Hückel parameter

I = ionic strength of solution

$$I = \frac{1}{2} \sum_j z_j^2 m_j$$

$\beta^{(0)}$, $\beta^{(1)}$ = interaction parameters

The activity of water is determined as (Edwards, 1978):

$$\ln a_w = M_w\left\{ \frac{2A_\phi I^{1.5}}{1+1.2\sqrt{I}} - \sum_{i\neq w}\sum_{j\neq w} m_i m_j\left[\beta_{ij}^{(0)} + \beta_{ij}^{(1)}\exp(-2\sqrt{I})\right]\right\}$$

$$-M_w \sum_{i\neq w} m_i \qquad (33)$$

pH is defined as a function of the hydrogen ion activity as:

$$pH = -\log_{10} a_{H+} \qquad (34)$$

Two mass balances exist in the liquid phase:

(VI) $m_N = m_{NH3} + m_{NH4+} + m_{NH2COO-}$

(VII) $m_C = m_{CO2} + m_{HCO3-} + m_{CO3--} + m_{NH2COO-}$

where:

m_N = stoichiometric (bulk) concentration of nitrogen as molality (mole/kg of water)

m_C = stoichiometric (bulk) concentration of carbon as molality (mole/kg of water)

Also, electroneutrality implies that:

(VIII) $m_{NH4+} + m_{H+} = m_{HCO3-} + m_{CO3--} + m_{NH2COO-} + m_{OH-}$

In the NH_3-CO_2-H_2O system, eight species were considered to be present in the compost solution: NH_3 (molecular), NH_4^+, CO_2 (molecular), HCO_3^-, CO_3^{2-}, NH_2COO^-, H^+, and OH^-. Since the amount of nitrogen released into compost solution during the decomposition process is always smaller than the ammonia molar solubility in water, bulk concentration of nitrogen (m_N) was treated as a known variable. It was obtained by converting the ammoniacal N ($kg_N \cdot m^{-3}$ compost) to molality in solution (moles per kg of water). Bulk concentration of carbon (m_C) is unknown because carbon dioxide evolved was more than that which can be dissolved in solution.

Thus there are eight pairs of unknowns (m_i and γ_i for each of these species) plus a_w and m_C as two other unknowns. This implies that a system of eighteen equations is required to determine the unknowns. In addition to the above equations (I) to (VIII), Equation (31) is used to determine eight activity coefficients, one for each species except water. Equation (32) is used for the activity of water. Finally, the relationship between molecular CO_2 concentration in solution and CO_2 partial pressure in FAS was used, with CO_2 partial pressure as a known variable, obtained by subtracting calculated volumetric O_2 concentration from O_2 proportion in air (21%). The eighteen non-linear algebraic equations need to be solved simultaneously in accordance with the carbon dioxide partial pressure and total nitrogen species in the liquid phase in each time step.

In this model, a Newton-Raphson iteration technique was used to achieve a simultaneous solution of the relevant equations using an initial estimate of the concentration of each individual species, namely CO_2, HCO_3^-, NH_3, NH_4^+, $CO_3^{=}$, NH_2COO^-, and activities of H^+, and OH^-. The result is the distribution of the species at each time step. Ammonia in FAS can be determined according to composition in the liquid phase and used for further volatilization calculations.

2.2.2.6. *Volatilization of Ammonia*

The cumulative NH_3 volatilized per unit of compost mass was simply defined via a first-order reaction:

$$U_v = F * [NH_3^g] / \rho \qquad (35)$$

where:

F = Aeration flow rate (kg air· (kg d.m.h)$^{-1}$)

U_v = NH_3 volatilization rate (kg· (kg d.m.h)$^{-1}$)

2.3 SIMULATION RESULTS

Some preliminary runs of the simulation model were made to demonstrate the performance of the model by comparing simulation results with well-known composting phenomena. A laboratory scale composter with a diameter of 0.25 m and compost depth of 0.25 m was simulated. Some technical parameters are shown in Table 2-5.

The influence of several factors influencing ammonia emission was studied. Aeration rate was varied from 0.02 to 0.08 kg d.a. (kg dry matter h)$^{-1}$. Initial moisture content was varied from 60% to 70%. C/N ratio of the compost mixture was varied from 20 to 40.

Table 2-5. Technical parameters for simulation of composter

Parameter	Default value
$T_{ambient}$, T_{intake}	20°C
Volume (m^3)	0.0123
Surface aera (m^2)	0.294
U	4 kJ·(m^2-h-°C)$^{-1}$

2.3.1 Predicted Rates versus Time

Figures 2-6a through 2-6c illustrate predicted rates of composting versus time for two different air flow rates. Moisture content was chosen as 70% and C/N ratio was 30.

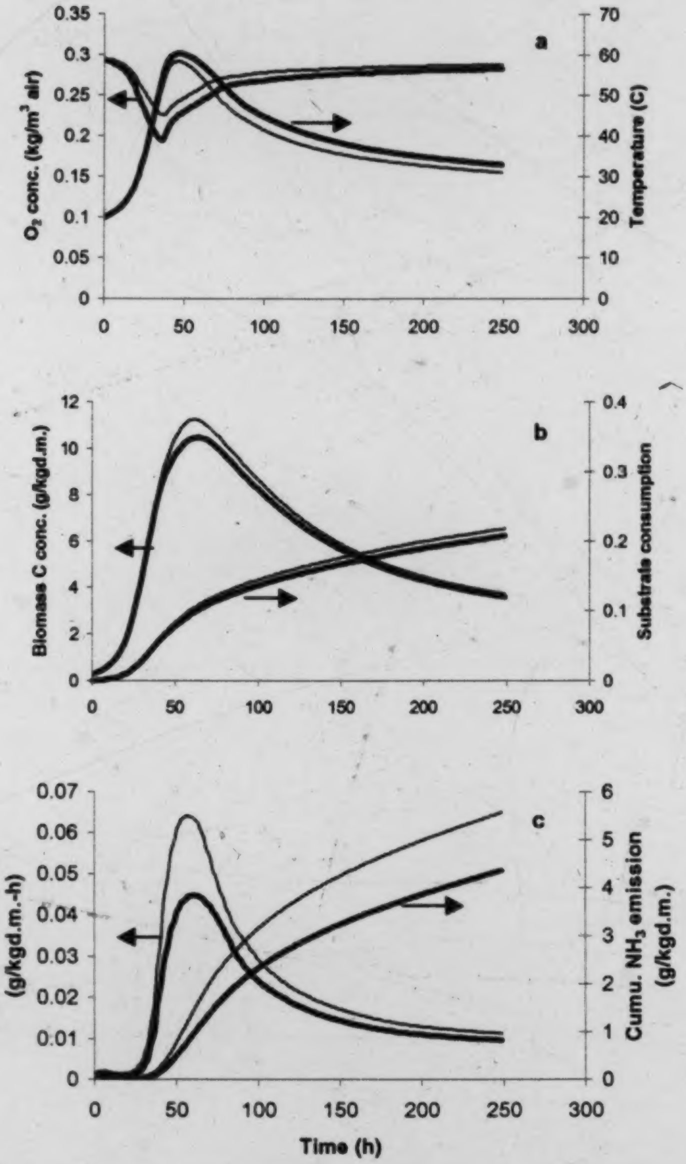

Figure 2-6 Predicted composting performance vs. time between two constant aeration rates 0.06kg (kgd.m. h)$^{-1}$ (thin lines) and 0.04kg (kgd.m. h)$^{-1}$ (thick lines)

Higher aeration resulted in slightly lower composting temperatures (Figure 2-6a). The simulation was terminated at 250 hours and the average temperature at flow rates of 0.04 kg $(kgd.m.h)^{-1}$ and 0.06 kg $(kgd.m.h)^{-1}$ are 40.4°C and 38.0°C, respectively. The reduced oxygen concentrations and high temperature (Figure 2-6a) slightly inhibited microbial biomass growth (Figure 2-6b). The flow rate of 0.06 kg $(kgd.m.h)^{-1}$ resulted in a higher maximum biomass amount but similar substrate consumption. This indicates that either aeration rate was not limiting factors of substrate decomposition. The specific rates of ammonia emission (Figure 2-6c) followed a similar pattern with a higher peak emission rate at 0.06 kg $(kgd.m.h)^{-1}$. Cumulative ammonia emission (Figure 2-6c) reached 4.3 g/kgd.m. (at 0.04 kg $(kgd.m.h)^{-1}$) and 5.5 g/kgd.m. (at 0.06 kg $(kgd.m.h)^{-1}$) of NH_3-N respectively.

2.3.2 Effect of Aeration and Moisture Content on Ammonia Emission

Aeration rate, C/N ratio and moisture content of a mixture influence the total ammonia emission during composting. Ammonia emission at moisture contents of 60% and 70% and C/N ratio = 30 are summarized for a range of aeration rates in Table 2-6 and Figure 2-7. Ammonia emission increased markedly with the rise of air supply. This is related to higher gas exchange and faster decomposition. Ammonia emissions were higher at 60% moisture content than 70%, due to higher ammoniacal nitrogen concentration in the compost solution resulting from the drier conditions. A mixture with a moisture content of 60% and a ventilation rate of 0.08 kg· $(kgd.m.\cdot h)^{-1}$ volatilized 47.3% of initial nitrogen as ammonia during 200 hours of simulation.

Table 2-6. Simulated ammonia emission at C/N=30

Moisture	Aeration rate kg* (kg d.m. h) $^{-1}$	0.02	0.04	0.06	0.08
70%	Total emission g NH_3-N *kg^{-1} d.m.	2.5	4.3	5.5	5.7
	Relative emission % of initial N_{tot}	16%	27.2%	34.8%	36.0%
60%	Total emission g NH_3-N *kg^{-1} d.m.	4.5	6.7	7.3	7.5
	Relative emission % of initial N_{tot}	28.5%	42.3%	45.8%	47.3%

2.3.3 Effect of C/N Ratio on Ammonia Emission

Simulated ammonia volatilization was sensitive to the C/N as seen in Table 2-7 and Figure 2-8 at a moisture content of 70%. Ammonia emission increased significantly as the C/N ratio decreased regardless of aeration rates. A C/N ratio of 20 and flow rate of 0.08 kg d.a. (kgd.m.h)$^{-1}$ resulted in a cumulative ammonia loss of 45.3% of initial total nitrogen in contrast to a C/N ratio of 40 and flow rate of 0.04 kg d.a. (kgd.m.h)$^{-1}$, which resulted in a simulated emission of only 18.8%.

Table 2-7. Simulated ammonia emission at moisture content of 70%

C/N ratio	Aeration rate kg* (kg d.m. h)$^{-1}$	0.04	0.06	0.08
40	Total emission g NH_3-N *kg^{-1} d.m.	2.2	2.8	3.2
	Relative emission % of initial N_{tot}	18.8%	23.6%	26.8%
30	Total emission g NH_3-N *kg^{-1} d.m.	4.3	5.5	5.7
	Relative emission % of initial N_{tot}	27.2%	34.8%	36.0%
20	Total emission g NH_3-N *kg^{-1} d.m.	7.9	9.7	10.8
	Relative emission % of initial N_{tot}	33.3%	40.8%	45.3%

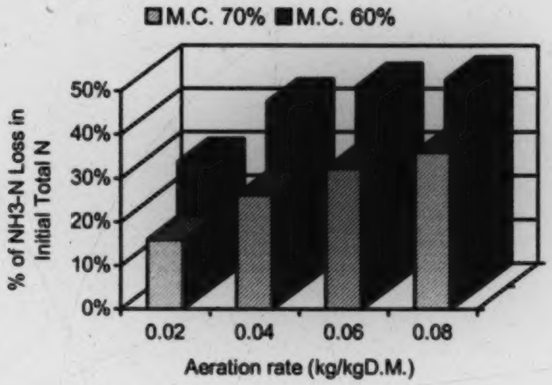

Figure 2-7. Simulated ammonia emission from composting materials with C/N=30 at two moisture contents and four aeration rates.

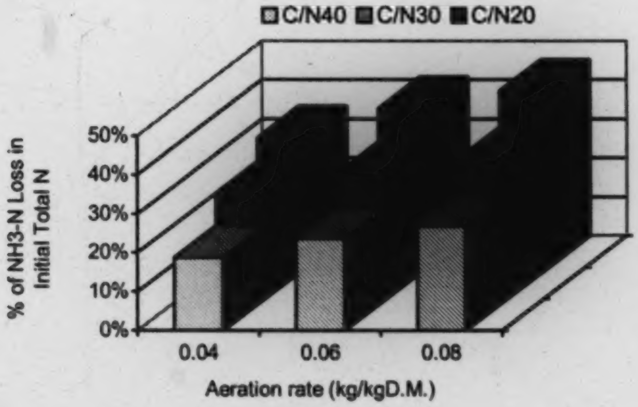

Figure 2-8. Simulated ammonia emission from composting materials with moisture content=70% at three C/N ratios and three aeration rates.

2.4 SENSITIVITY ANALYSIS

A sensitivity analysis was performed to evaluate the relative importance of some model parameters. The laboratory scale composter described in Section 2.3 was used. The parameters examined were maximum specific growth rate $\mu_{max,i}$, half velocity constants for substrates ($K_{s,i}$) and oxygen (K_{O2}), microbial death rate (δ), first-order rate constant for conversion of microbial product C to biomass C (k_P), initial microbial biomass C concentration ($X_{c,initial}$), overall heat transfer coefficient (U) and the ambient temperature (T_{amb}). These parameters were selected for sensitivity analysis because of their significant roles in the model.

The parameters were varied individually and all other parameters were set at their default values. Each parameter was increased by 100% of its default value and then decreased to 50% of its default value over a 10 d simulation period. The parameter values used are shown in Table 2-8.

Table 2-8. Parameter values used in sensitivity analysis

Parameter		-50%	Default	+100%
$\mu_{max,1}$	h^{-1}	0.25	0.50	1.0
$\mu_{max,2}$	h^{-1}	0.25	0.50	1.0
$\mu_{max,3}$	h^{-1}	0.015	0.03	0.06
$K_{s,1}$	$kg_c \cdot kg^{-1} d.m.$	0.0125	0.025	0.05
$K_{s,2}$	$kg_c \cdot kg^{-1} d.m.$	0.085	0.17	0.34
$K_{s,3}$	$kg_c \cdot kg^{-1} d.m.$	0.2	0.4	0.8
K_{O2}	$kg \cdot kg^{-1} d.m.$	0.000015	0.00003	0.00006
δ	h^{-1}	0.0125	0.025	0.05
k_p	h^{-1}	0.001	0.002	0.004
$X_{c,init}$	$kg_c \cdot kg^{-1} d.m.$	1.4E-4	2.8E-4	5.6E-4
U	$kJ \cdot (°C \cdot m^2 \cdot h)^{-1}$	2	4	8
T_{amb}*	°C	15	20	25

* T_{amb} was tested by increasing and decreasing its default value by 5°C

The output values examined were the maximum temperature (T_{max}, °C) and maximum biomass C concentration ($X_{c,max}$, $kg_c \cdot kg^{-1}d.m.$) at any time, cumulative CO_2-C evolution ($kgC \cdot kg^{-1}d.m.$), peak NH_3-N emission rate ($kgN \cdot (kgd.m. \cdot h)^{-1}$) and cumulative NH_3-N emission over the period of 250 h. Results from the analysis are shown in Figures 2-9 through 2-13. For example, as $\mu_{max,2}$ varied from 0.25 to 1.0 h^{-1}, $X_{c,max}$ increased from 8.3 to 12.8 $kg_C \cdot kg^{-1}d.m.$, and peak NH_3-N emission rate increased from 0.035 to 0.086 $kgN \cdot (kgd.m. \cdot h)^{-1}$.

The sensitivity analysis revealed some interaction between temperature, moisture, microbial growth and carbon dioxide and ammonia emissions. Among the kinetic parameter group, $\mu_{max,2}$ was one of the most sensitive parameters. The change of $\mu_{max,2}$ and $K_{s,2}$ influenced the rate of microbial growth. As $\mu_{max,2}$ increased or $K_{s,2}$ decreased, fairly large increases in $X_{c,max}$ occurred (Figures 2-10a, b). With these increases in $X_{c,max}$, corresponding increases in T_{max} (Figures 2-9a, b) occurred. As a consequence, earlier (data not shown) and higher peak ammonia emissions occurred, leading to larger amounts of total ammonia emissions. Therefore, both maximum temperature and ammonia emission rate are sensitive to $\mu_{max,2}$. However, the increase of $\mu_{max,3}$ didn't cause much change to $X_{c,max}$ and T_{max}, because the decomposition of non-fiber C takes place in a later stage. But the increased decomposition in a later stage significantly increased the compost temperature (data not shown) after the peak period, and consequently increased the cumulative carbon dioxide evolution in the later stage (Figure 2-11a). The peak ammonia emission rate was not changed but the cumulative ammonia emission was increased slightly, from 5.6 to 6.3 $kgN \cdot (kgd.m. \cdot h)^{-1}$ (Figure 2-13a), primarily due to the increased compost temperature at the cooling stage. Therefore, the total CO_2 evolution and total NH_3 emission are sensitive to $\mu_{max,3}$.

As a result of the co-decomposition of the three sub-group substrates, the sensitivity to any one parameter is not considerable. For example, the 50% decease of $\mu_{max,2}$ from its default value resulted in only 20% decrease of cumulative ammonia emission. Also, the changes in $\mu_{max,1}$ didn't influence the output values to any great extent. This is primarily due to the relatively low levels of soluble C substrate assigned in the model, compared with the significance of the other two C substrates.

Among the other parameters, microbial death rate (δ) and overall heat transfer coefficient (U) are the most sensitive ones. The changes resulting from varying these two parameters are more profound than those resulting from the microbial growth kinetic parameters. The decrease of δ by 50% from its default value resulted in a 49% increase of $X_{c,max}$, and a corresponding 52% increase of cumulative carbon dioxide evolution. Cumulative ammonia emission increased less significantly (12%), mainly due to the unaffected T_{max}.

Ammonia emission is sensitive to overall heat transfer coefficient (U). The poorer insulation represented by a higher U had no effect on microbial growth and cumulative carbon dioxide evolution, but resulted in decreasing T_{max} from 58.4 to 52.9°C. The decrease in T_{max} resulted in a decrease in peak ammonia emission rate (30%) and cumulative ammonia emission (29%). The increased overall heat transfer coefficient (U) increased the proportion of heat loss by conduction through the composter wall, which in turn decreased the proportion of heat lost by ventilation. More ammonia was conserved due to the resulting lower temperature.

Changes in $X_{c,initial}$ had little effect on any output values examined (Figures 2-9c through 2-13c). Changes in k_P had little effect on maximum compost temperature and maximum biomass C (Figures 2-9a, 2-10a). However, the increase of k_P resulted in a slight increase of carbon dioxide evolution and ammonia emission (Figures 2-11a, 2-13a). This is also due to a slightly elevated compost temperature during the cooling stage when the value of the microbial product C variable became more significant as more microbial biomass decayed.

Changes in T_{amb} had little effect on the output values examined except for cumulative ammonia emission (Figure 2-13c). Even though the maximum temperature from T_{amb} of 25°C was only 1°C higher than that from T_{amb} of 15°C, the temperature profile from T_{amb} of 25°C is generally 3~4°C higher than the temperature profile from T_{amb} of 15°C (Figure 2-14a). The lower ambient temperature resulted in lower cumulative ammonia emission (Figure 2-14b). Carbon dioxide evolution was not negatively influenced by the low ambient temperature (Figure 2-11c).

The sensitivity of ammonia gas-liquid equilibrium was also examined. The assumption of half equilibrium had a great influence on ammonia volatilization. Peak ammonia emission rate is approximately 70% higher at a full equilibrium than half equilibrium (Figure 2-12c), which is used in this study. Cumulative ammonia is approximately 30% higher at a full equilibrium than half equilibrium (Figure 2-13c). Therefore, the ammonia emission is sensitive to the assumption of ammonia gas-liquid equilibrium used in the model.

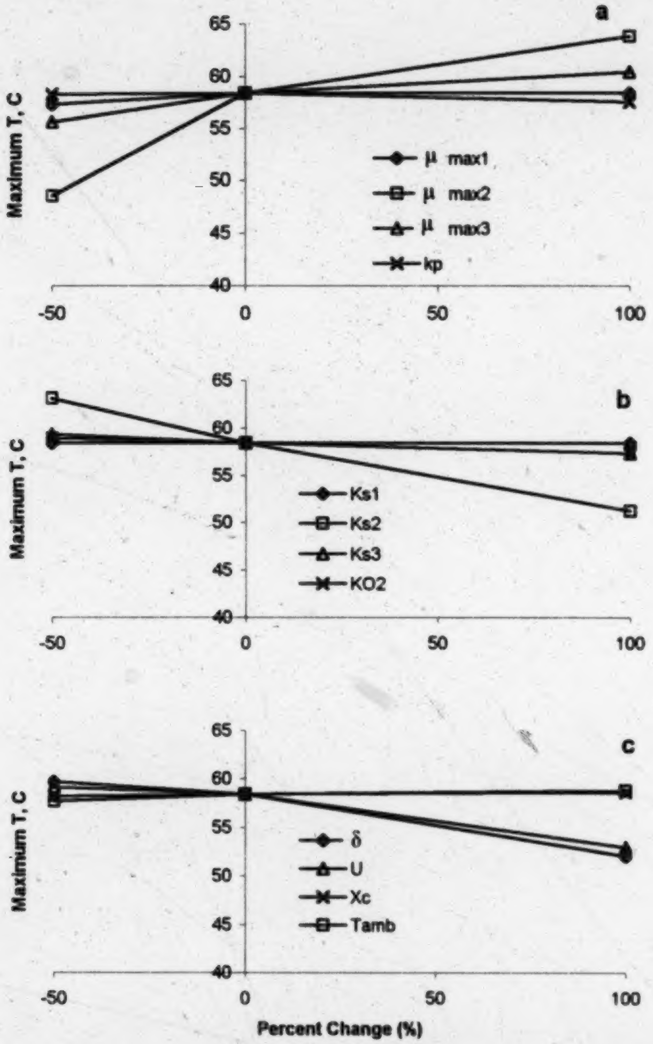

Figure 2-9. Sensitivity analysis showing maximum temperature as the selected parameter was altered from -50% to +100% of its default value. (a) Parameter μ_{max1}, μ_{max2}, μ_{max3}, k_p. (b) Parameter K_{s1}, K_{s2}, K_{s3}, K_{O2}. (c) Parameter δ, U, X_C, T_{amb}

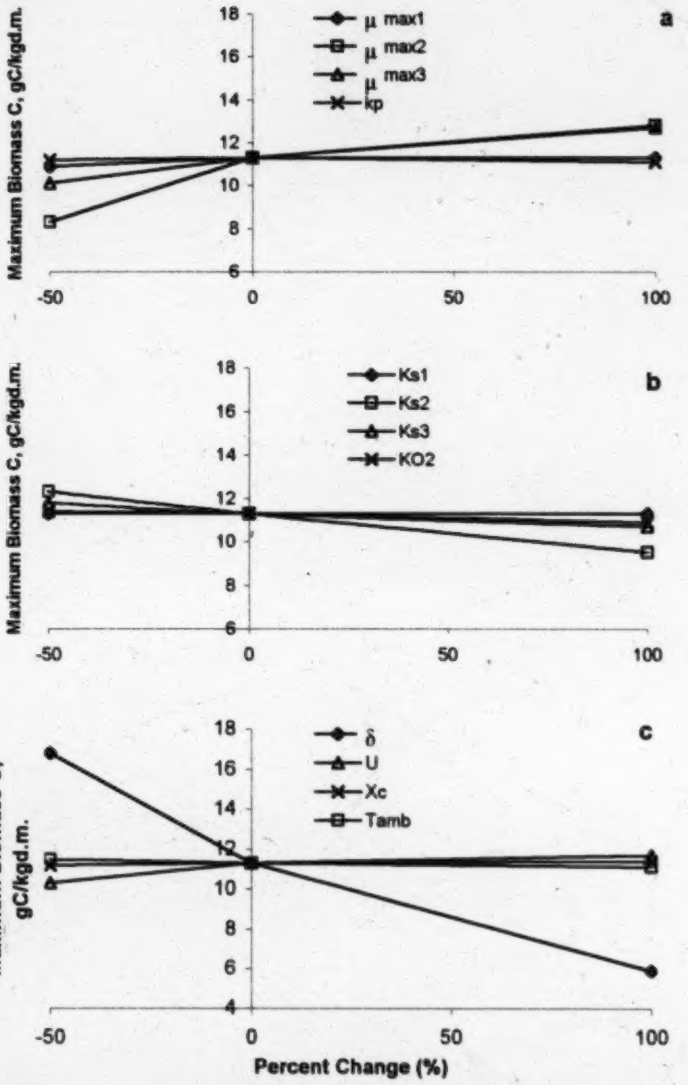

Figure 2-10. Sensitivity analysis showing maximum biomass C as the selected parameter was altered from -50% to +100% of its default value. (a) Parameter μ_{max1}, μ_{max2}, μ_{max3}, k_p. (b) Parameter K_{s1}, K_{s2}, K_{s3}, K_{O2}. (c) Parameter δ, U, X_C, T_{amb}

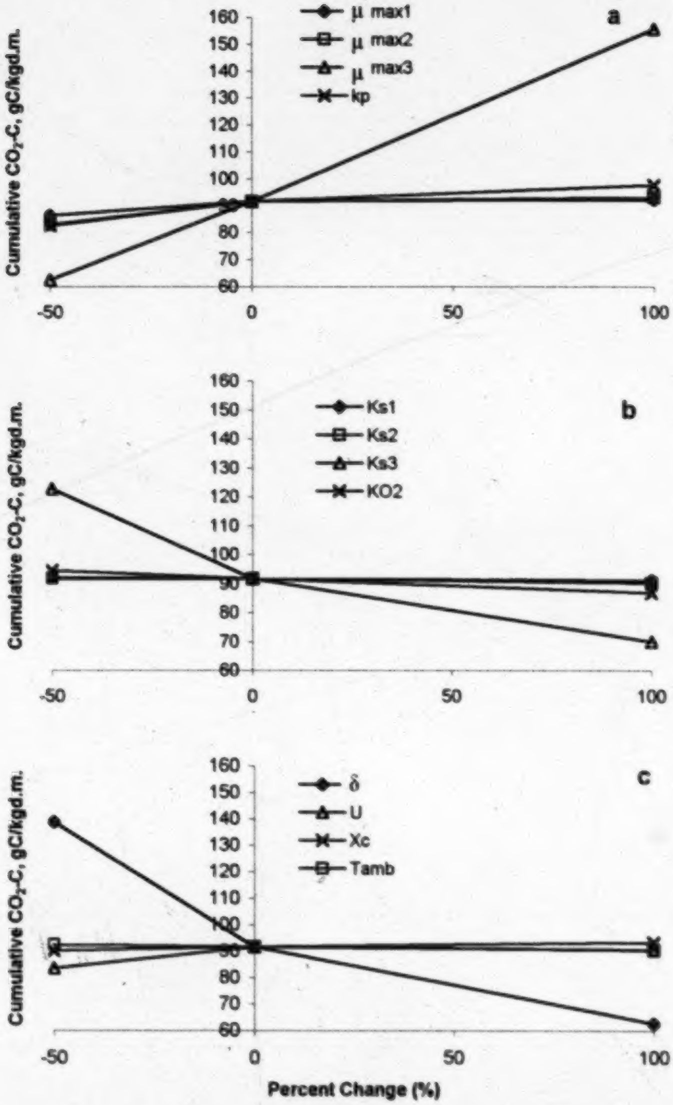

Figure 2-11. Sensitivity analysis showing cumulative CO_2-C as the selected parameter wa altered from -50% to +100% of its default value. (a) Parameter μ_{max1}, μ_{max2}, μ (b) Parameter K_{s1}, K_{s2}, K_{s3}, K_{O2}. (c) Parameter δ, U, X_C, T_{amb}

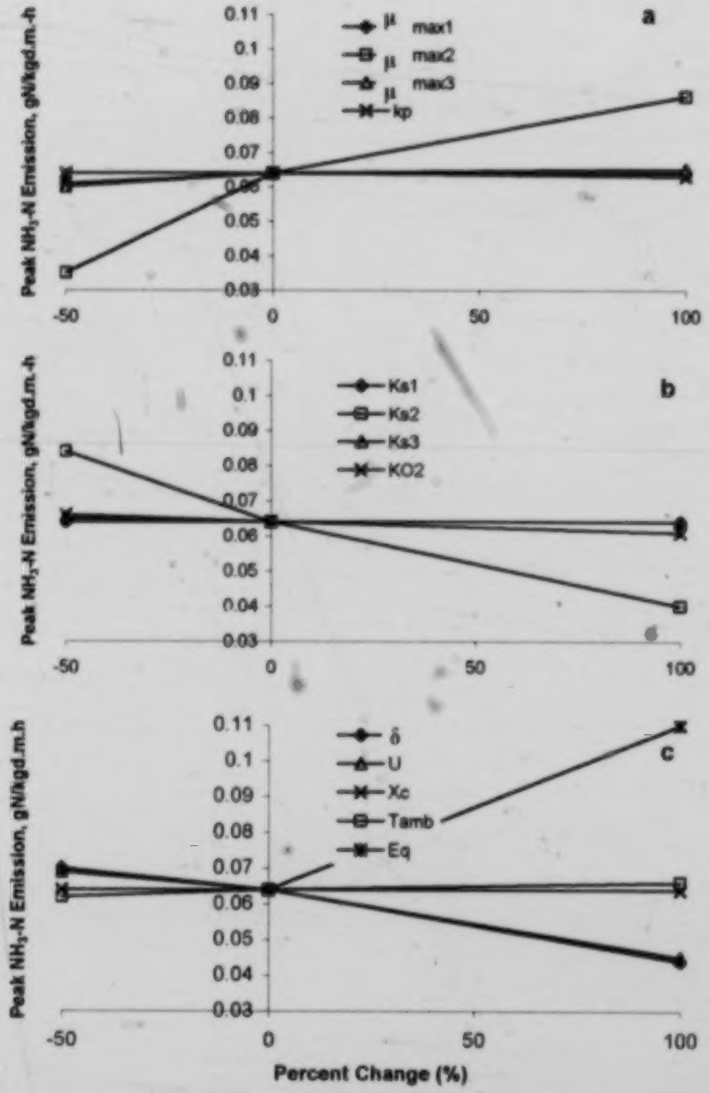

Figure 2-12. Sensitivity analysis showing peak NH_3-N emission as the selected parameter was altered from -50% to +100% of its default value. (a) Parameter μ_{max1}, μ_{max2}, μ_{max3}, k_P. (b) Parameter K_{s1}, K_{s2}, K_{s3}, K_{O2}. (c) Parameter δ, U, X_C, T_{amb}, Equilibrium

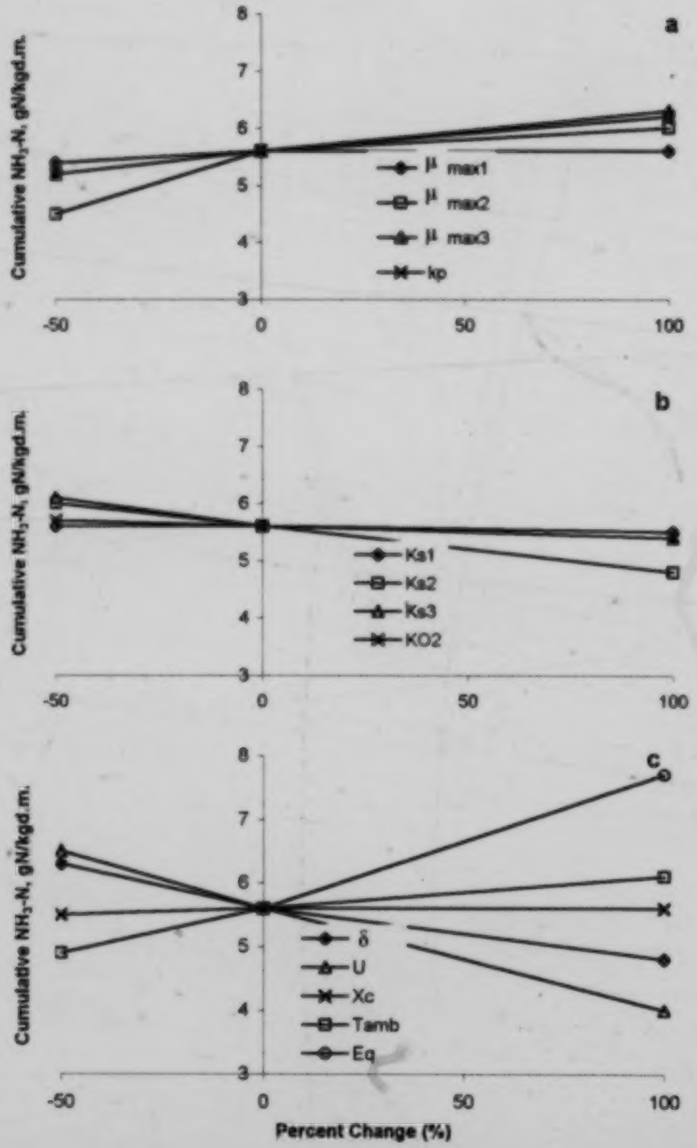

Figure 2-13. Sensitivity analysis showing cumulative NH_3-N emission as the selected parameter was altered from -50% to +100% of its default value. (a) Parameter μ_{max1}, μ_{max2}, μ_{max3}, k_P. (b) Parameter K_{s1}, K_{s2}, K_{s3}, K_{O2}. (c) Parameter δ, U, X_C, $T_{amb,}$ Equilibrium

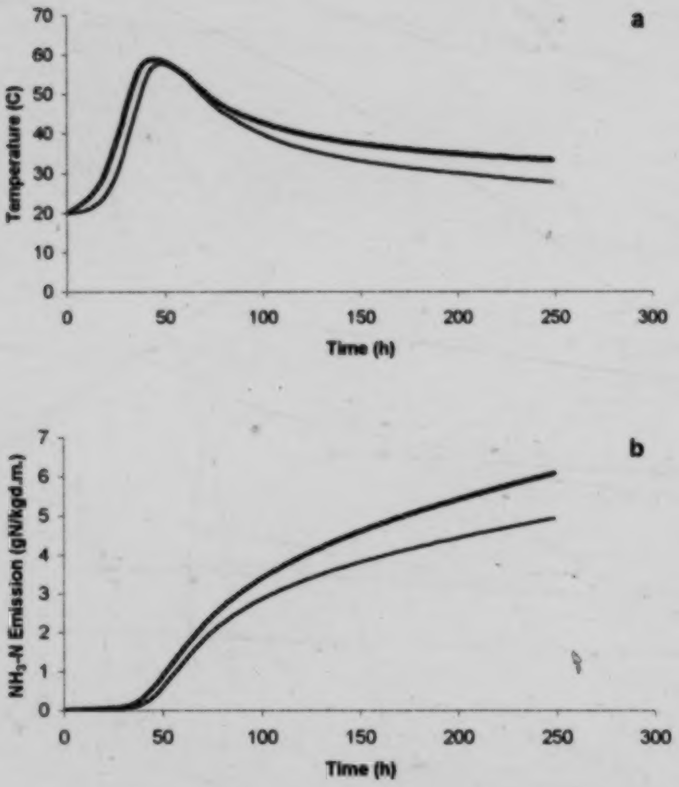

Figure 2-14. The sensitivity of compost temperature and cumulative NH_3-N emission to ambient temperature, T_{amb}=25C (thick line) and T_{amb}=15C (thin line).

2.5 DISCUSSION

The simulation model gave a good prediction of temperature profile as well as of microbial growth and oxygen consumption. The simulation results for the decomposition rate agree with experimental observation qualitatively (Liang et al., 1996).

Preliminary application of the model indicated that simulated ammonia emission decreased with increased C:N ratio, increased with aeration rates and decreased with increased moisture content. These results are in agreement with the findings of other researchers. For instance, Bishop and Godfrey (1983) and Janzen et al. (1997) have reported that lower initial C:N ratio results in higher ammonia volatilization and lower N recovery. Also, Beck et al. (1997) reported that lower aeration rate caused lower cumulative ammonia emission. One possible reason could be due to slower gas exchange rates resulting in less ammonia being stripped out. Another explanation is that decreased ventilation would increase CO_2 partial pressure, which influences pH of solution as well as the equilibrium of $NH_4^+ \leftrightarrow NH_3$ (aqueous) and favors the existence of NH_4^+. This would result in lower NH_3 partial pressure and reduced ammonia loss. When moisture is in the range that oxygen diffusion is not inhibited, relatively higher moisture content will also be beneficial to keep ammonia in the liquid phase since concentration of ammoniacal N depends on both the quantity of ammoniacal N and water in solution.

The cumulative ammonia emission calculated by the model accounted for 16% to 47% of initial total nitrogen as NH_3-N loss. Hansen et al. (1991) measured cumulative N disappearance of 26.2% at 6.79 days with an experiment at C/N=17.3 and moisture content of 60%. Beck et al. (1997) also reported a relative emission of 9.5% of ammonia nitrogen loss at C/N ratio of 19 and aeration of 40 litre·(kg d.m.· h)$^{-1}$.

Thus, overall, the simulation results from the model gave an overestimate of ammonia emission compared with measurements shown in literature. This could be due to the inaccurate description of the immobilization and mineralization processes or improper calculation partly based on the assumption of equilibrium between ammonia gaseous phase and liquid phase. The selected parameter values can also influence the simulation results of ammonia emissions. As shown in the sensitivity analysis, adjustments of parameter values, i.e increases of microbial death rate (δ), heat transfer coefficient (U) or decrease of maximum growth rate on non-fiber C substrate (μ_{max2}), could possibly decrease the prediction of ammonia emission. Morisaki et al. (1989) also calculated ammonia loss based on an equilibrium relation and compared their calculations with measured values. They found that only 5.4% of calculated NH_3 were actually volatilized. The possible explanation suggested by these authors was that the dissolved NH_3 exists mostly in the intracellular water phase rather than in free water in the composting material.

2.6 CONCLUSIONS

A mathematical simulation model for substrate decomposition and nitrogen transformation in composting process was developed. Substrates were subdivided into three groups for simulation of decomposition. Nitrogen transfer processes were assumed to be controlled by the growth and decay of microbial biomass. This lead to a relatively large number of parameters that had to be estimated in order to obtain a reasonable prediction.

Ammonia volatilization was related with interstitial carbon dioxide concentration, which itself was influenced by both microbial activity and air exchange rate. This interrelationship was represented by a CO_2-NH_3-H_2O multisolute aqueous system. This model demonstrated that ammonia volatilization was associated with substrate composition, temperature, aeration, pH and moisture content.

The model succeeded in reflecting well-known phenomena of the composting technologies. Preliminary results of simulations using the model are in general agreement with expected trends and experimental data from literature in this area. However, the proportion of initial N that the model predicts will be lost as NH_3 (16~47%) is high in comparison with published experimental values.

Sensitivity analysis showed that the output from the model is sensitive to the parameter values such as microbial death rate (δ), heat transfer coefficient (U) and maximum growth rate on non-fiber C substrate (μ_{max2}). Further work is needed to define these.

A thorough test is required to evaluate the range of situations to which the existing models can be applied successfully. Further experiments will be required to obtain insight and permit subsequent revision of the model to reduce discrepancies.

2.7 NOMENCLATURE

β_i :microbial maintenance coefficient, h^{-1}

β_{max} :maximal microbial maintenance coefficient, h^{-1}

δ :microbial death rate, h^{-1}.

γ_k :molal activity coefficient.

μ_i :specific growth rate of organisms on different substrate, h^{-1}.

μ_{max} :maximal growth rate, h^{-1}.

ρ :air density, $kg \cdot m^{-3}$.

A :surface area of heat conduction, m^2.
a_a :activity as molality in solution, mole·kg $^{-1}$of solvent.
C_i :C substrate content, kg·kg^{-1} d.m.
C_{Nf} :Non-fiber C content.
C_{O2} :oxygen content, kg·kg^{-1} d.m.
CN_m :microbial C/N ratio, kg C·kg^{-1} N.
CN_S :C/N ratio of non-fiber substrate, kg C·kg^{-1} N.
c_M :microbial carbon, kg·kg^{-3}d.m.
c_a :specific heat of dry air, kJ·(°C-kg dry air)$^{-1}$.
c_{nvs} :specific heat of Non-volatile substance, kJ·(°C-kg nvs)$^{-1}$.
c_v :specific heat of volatile substance, kJ·(°C-kg vs)$^{-1}$.
c_w :specific heat of water, kJ·(°C-kg water)$^{-1}$
D_{init} :initial dry matter, kg
f_c :carbon fraction in volatile substance.
F :air flow rate, kg·(h·kg d.m.)$^{-1}$compost.
G_{mass} :thermal mass of compost mixture, kJ·°C^{-1}.
H_a :Henry's law constant, ratio of concentration in vapor to concentration in liquid
h :specific enthalpies of air, kJ·kg^{-1}
h_{fg} :latent heat of vaporization of water, kJ·kg^{-1} water
k_{cu} :effect of microbial C/N ratio on immobilization
k_{ca} :effect of microbial C/N ratio on ammonification
k_a :first-order rate constant of ammonification
k_p :first order rate constant, h^{-1}
k_{H2O} :moisture-dependent coefficient
k_{temp} :temperature coefficient
k_{pH} :pH coefficient
K_a :acid dissociation constant for ammonia
K_{O2} :oxygen saturation constant, kg O$_2$·m^{-3} air
$K_{S,i}$:substrate saturation constant, kg·kg^{-1}d.m.

m :moisture content, wet basis, kg $\cdot$kg^{-1} d.m.

m_k :appenrent concentration as molality, mole $\cdot$ kg^{-1} of solvent.

N :nitrogen concentration, kg$\cdot$kg^{-1} d.m.

N_{ib} :the concentration of inorganic N in the compost solution

N_m :microbial nitrogen(concentration), kg$\cdot$kg^{-3}d.m.

nvs :non-volatile substance content, dry basis, kg$\cdot$kg^{-1} d.m.

O_2 :oxygen concentration in the air, kg $O_2\cdot m^{-3}$ air.

P_x :microbial product C concentration, kg$\cdot$kg^{-1} d.m.

S :substrate(concentration), kg.

T :temperature of compost mixture, °C.

$T_{ambient}$:temperature - ambient, °C.

T_{intake} :temperature - intake air, °C.

U :overall heat transfer coefficient of vessel wall, kJ$\cdot$(m^2-hr-°C)$^{-1}$.

U_I :change of immobilization rate, kgN$\cdot$kg^{-1} d.m. h^{-1}

U_A :change of ammonification rate, kgN$\cdot$kg^{-1} d.m. h^{-1}

W :water content, kg water$\cdot$m^{-3}.

w :humidity ratio, kg water$\cdot$kg^{-1} dry air.

X_c :concentration of biomass C, kg.

$Y_{H/S}$:yield coefficient, kJ heat$\cdot$kg^{-1} substrate.

$Y_{O2/S}$:yield coefficient, kg oxygen$\cdot$kg^{-1} substrate.

$Y_{W/S}$:yield coefficient, kg water$\cdot$kg^{-1} substrate.

$Y_{X/S}$:yield coefficient, kg biomass$\cdot$kg^{-1} substrate.

2.8 REFERENCES

ASAE standard. 1994. Cooperative Standards Program. St. Joseph, MI.

Avnimelech, Y. and M. Laher. 1977. Ammonia volatilization from soils: equilibrium considerations. Soil Sci. Soc. Am. J., 41: 1080-1084.

Bach, P.D., M. Shoda and H. Kubota. 1985. Composting reaction rate of sewage sludge in an autothermal packed bed reactor. J. Ferment. Technol. 63: 271-278.

Beck, J., M. Käck, A. Hentschel, K. Csehi, T. Jungbluth. 1997. Ammonia emissions from composting animal wastes in reactors and windrows. In: J.A. Voermans and G.J. Monteny (eds,). Ammonia and odour control from animal production facilities. Proceedings of the international symposium. Vinkeloord, The Netherlands.

Bishop, P.L. and C. Godfrey. 1983. Nitrogen transformations during sludge composting. Biocycle. 24: 34-39.

Edwards, D.R. and T.C. Daniel. 1992. Environmental impacts of on-farm poultry waste disposal – a review. Bioresource Technol. 41: 9-33.

Edwards, T.J. 1998. Vapor-liquid equilibria in multicomponent aqueous solutions of volatile weak electrolytes. AIChE J., 24: 966-976.

Edwards, T.J., J. Newman, J.M. Prausnitz. 1975. Thermodynamics of aqueous solutions containing volatile weak electrolytes. AIChE J., 21: 248-259.

English, C.J., J.R. Miner and J.K. Koelliker. 1980. Volatile ammonia losses from surface-applied sludge. J. WPCF, 52(9): 2340-2350.

Freney, J.R., J.R. Simpson and O.T. Denmead. 1983. Volatilization of ammonia. In: Gaseous Loss of Nitrogen from Plant-Soil Systems. J.R Freney and J.R. Simpson (eds.). Martinus Nijhoff / Dr W. Junk Publishers. pp. 1-32.

Groot Koerkamp, P.W.G., A. Elzing. 1996. Degradation of nitrogenous components in and volatilization of ammonia from litter in aviary housing systems for laying hens. Trans. ASAE 39(1): 211-218.

Hamelers, H.V.M. 1993. A theoretical model of composting kinetics. In: H.A.J. Hoitink and H.M. Keener (eds.). Science and engineering of composting: Design, environmental, microbiological and utilization aspects. Renaissance Publications, Worthington, OH. pp. 36-58.

Hansen, R.C., C. Marugg, H.M. Keener, W.A. Dick and H.A.J. Hoitink. 1991. Nitrogen transformation during poultry manure composting. ASAE paper No. 91-4014.

Hansen, R.C., H. M. Keener and H. A. J. Hoitink. 1989. Poultry manure composting: Design guidelines for ammonia. ASAE paper No. 89-4075.

Hashimoto, A.G. and D.C. Ludington. 1971. Ammonia desorption from concentrated chicken manure slurries. In: Proc. of Int. Symp. Livestock Wastes. Livestock Waste Management and Pollution Abatement. pp. 117-121 ASAE. Columbus. St. Joseph, MI.

Janzen, R.A., Feddes, J.J.R., Leonard, J.J., McGill, W.B. 1997 Composting for resource recovery - strategies to retain nitrogen. In: W.B. McGill (ed.), Sustainability of Manure Management: Nutrient Retention and Cost-benefit Analysis. p. 93-118.

Final Report, CAESA Project RES-056-93. Alberta Agriculture, Food and Rural Development, Edmonton AB.

Jayaweera, G.R. and D.S. Mikkelsen. 1990. Ammonia volatilization from flooded soil systems: a computer model. I. Theoretical aspects. Soil Sci. Soc. Am. J. 54: 1447-1455.

Juma, N.G. and E.A. Paul. 1981. Use of tracers and computer simulation techniques to assess mineralization and immobilization of soil nitrogen. In: M.J. Frissel, and J.A Van Veen (eds.). Simulation of Nitrogen Behavior of Soil-Plant Systems. Pudoc, Wageningen, The Netherlands. pp. 145-154.

Kaiser, J. 1996. Modeling composting as a microbial ecosystem: a simulation approach. Ecological Modeling. 91: 25-37.

Kirchmann, H. and E. Witter. 1989. Ammonia volatilization during aerobic and anaerobic manure decomposition. Plant and Soil. 115: 35-41.

Kőrner, I., R. Stegmann. 1998. Influence of biowaste composition and composting parameters on the nitrogen dynamics during composting and nitrogen contents in compost. In: Szmidt, R.A.K. (Ed.), Acta Horticulturae: Proceedings on the International symposium on composting and use of composted materials for hoticulture, Auchincruive, UK. vol. 469, ISHS, Drukkerij Van Damme, Beke, Brugge, Belgium, pp. 97-110.

Liang, Y., J. J. Leonard, J. J. Feddes, G. Qu and J. Franke. 1996. Ground expanded polystyrene as a nutrient diluent for broiler breeders. Part II: Effects on manure composting. CSAE paper. No. 96-503.

Maeda, T. and Matsuda, J. 1997. Ammonia emission from composting livestock manure. In: J.A. Voermans and G.J. Monteny (eds.). Proceedings of the international symposium. Ammonia and odour control from animal production facilities. p. 145-153. Vinkeloord, The Netherlands.

McGill, W.B., H.W. Hunt, R.G. Woodmansee and J.O. Reuss. 1981. Phoenix, a model of the dynamics of carbon and nitrogen in grassland soils. In: Terrestrial nitrogen cycles. F.E. Clark and T. Rosswall (eds.). Ecol. Bull. (Stockholm) 33: 49-115.

Morisaki, N., C.G. Phae, K. Nakasaki, M. Shoda and H. Kubota. 1989. Nitrogen transformation during thermophilic composting. J. Ferment. Bioeng. 67(1): 57-61.

Nakasaki, K., H. Yaguchi, Y. Sasaki and H. Kubota. 1993. Effects of pH control on composting of garbage. Waste Manage. Res. 11: 117-125.

Nakasaki, K., J. Kato, T. Akiyama and H. Kubota. 1987. A new composting model and assessment of optimum operation for effective drying of composting material. J. Ferment. Technol. 65(4): 441-447.

Parnas, H. 1975. Model for decomposition of organic material by microorganisms. Soil Biol. Biochem. 7: 161-169.

Parton, W.J., W.D. Grould, F.J. Adamsen, S. Torbit and R.G. Woodmansee. 1981. NH_3 volatilization model. In: M.J. Frissel and J.A. Van Veen (eds.). Simulation of Nitrogen Behaviour of Soil-Plant Systems. Pudoc, Wageningen, The Netherlands. pp. 233-244.

Sikora, L.J. and M.A. Sowers. 1985. Effect of temperature control on the composting process. J. Environ. Qual. 14: 434-439.

Stombaugh, D.P. and S.E. Nokes. 1996. Development of a biological based aerobic composting simulation model. Transaction of ASAE. 39(1): 239-250.

Van Veen, J.A. and M.J. Frissel. 1979. Mathematical modeling of nitrogen transformations in soil. In: J.K.R. Gasser (ed.). Modeling Nitrogen from Farm Wastes. Applied Science Publishers, London. pp. 133-157.

Witter, E. 1986. The fate of nitrogen during thermophilic composting of sewage sludge-straw mixture. Ph. D. Dissertation. University of London.

Witter, E. and J. Lopez-Real. 1987. The potential of sewage sludge and composting in a nitrogen recycling strategy for agriculture. Biological Agriculture and Horticulture 5: 1-23.

Chapter 3

Determination of Compost pH

3.1 INTRODUCTION

Ammonia emission during composting has been shown to be strongly influenced by the pH of the composting materials (Ekinci et al., 1998; Jackson and Line, 1997; Martins and Dewes, 1992). The equilibrium between molecular ammonia, which is subject to escape by means of air exchange, and the dissociated ammonia (i.e. NH_4^+) is dependent on pH. A higher concentration of molecular ammonia, affected by a higher pH value, will increase the potential for ammonia loss (chapter 2). Consequently, accurate measurements of pH in the composting cycle are critical in studying its relation with ammonia emission, as well as in developing possible management strategies and treatments to reduce ammonia emission. However, determining accurate pH values for the composting materials is difficult. Not only do the composting materials have large variations in pH within a composite sample, but also the method of measurement can influence the value obtained.

Due to a lack of a standard method of analysis, pH values of composting sample have been determined in different ways (McKinley and Vestal, 1985; Tseng et al., 1995; Villar et al., 1993), and two pH measurement methods (saturated paste and saturated paste extract) are specified by Leege and Thompson (1997). The methods described by the above varied in terms of sample sizes, dilution ratios, and standing times. In contrast, the method of pH measurement of soil samples is well established (Dolling and Ritchie, 1985; McLean, 1982) but may not be applicable to compost due to the difference between the nature of the two. Although soil and compost are both matrix-based systems with a partially dried and porous nature, compost has higher organic content, a more complex buffer capacity, and sometimes consists of bulky materials. Carnes and Lossin (1970) concluded that the presence of a complex system of buffers makes pH determination of compost slurries very sensitive to concentration variations. These researchers also recommended that reliable pH values can only be achieved at very high dilutions, such as a concentration of 10 grams of compost per 500 ml of water, mainly because large variations can occur at lower dilutions. However, the pH value obtained from a highly diluted slurry may not represent that of *in situ* compost. The question arises as to what dilution is appropriate so that the measured pH can represent that of the composting material, and whether it is possible to obtain a value corresponding to zero dilution.

The objective of this study was to establish a method of pH measurement for both fresh as well as matured compost. The purpose was to obtain accurate and precise pH values using standard laboratory equipment without being excessively costly or time consuming. To this end, specifications were required for: sample size and method of sampling; time between sampling and measurement; diluent; dilution rate; and extraction time. This paper describes a series of experiments carried out with the aim of obtaining suitable specifications for a protocol for measuring pH in compost that could be widely applied.

3.2 MATERIALS AND METHODS

3.2.1 Compost Materials

Both immature and mature compost were used in this study. The term "immature compost" used in this study indicates the materials under decomposition in composter, including the initial mixture. Mature compost means the stabilized compost after the curing stage.

For the immature compost, dairy manure and chopped barley straw were processed in a bench-scale composter (8 L) running continuously for 10 days. At the termination time, the compost had cooled back to room temperature and was transferred to a plastic bag and kept at room temperature. Two batches were used for the purpose of this experiment. In this chapter, the age of compost is referenced to the starting day of each batch. For example, Day 1 compost indicates material obtained during the first day of processing. Compost samples were collected every day or every other day from each run for the purpose of analysis. Composite samples of about 100 g were obtained by randomly grabbing several small samples from different locations within the composter or bag and were thoroughly mixed. Moisture contents varied from 65~76% (wet basis). Partly decomposed straw in the samples was cut to lengths of less than 50 mm to satisfy later use. Samples were kept in covered, 500 ml plastic containers until further analysis. Drying and grinding was avoided so as to minimize the effect of gas loss accompanying moisture loss.

The mature compost used in this study was 3-year-old compost that had also been made from dairy manure and barley straw.

3.2.2 Instrumentation

pH measurements were carried out using one of two digital pH meters (Beckman Model 4500, Irvine, CA or Accumet Model 815 MP) with combination electrodes. The pH meters were calibrated using two-point calibration. The first point was standardized at pH of 7.0 while the second point was at pH of 10.0 for a span adjustment. Buffered standard solutions at pH 7.0 and pH 10.0 (Fisher Scientific, Nepean, ON) were used. The two-point calibration was checked each day before use and adjustment of the instruments was made when necessary. Both calibrations and measurements were carried out at room temperature. Although two pH meters were used, calibration was carried out each time before use and linear responses were assumed to be established.

3.2.3 Preliminary Considerations

In order to measure the pH of a substance, liquid is required so that electrical conductivity can be established. Therefore, the only means of obtaining the pH of a solid or semi-solid dry material is by adding liquid and allowing the extraction of ions from the material into the liquid (Westcott, 1978). This immediately leads to two considerations: (a) the size of solid sample required, and (b) the type of liquid, or diluent, that should be used. Utilization of large sample sizes could result in the fast consumption of compost and large amounts of diluent being required. On the other hand, because compost is generally heterogeneous, if samples are too small, they might not be representative of the material under consideration. A preliminary study was carried out to compare sample sizes of 2 or 5 grams. The results indicated that pH readings from 2 g samples of compost tended to have relatively larger variations and, consequently, a 5 g sample size was selected for further use.

The two diluents considered for use in this study were distilled water and de-ionized distilled water. Calcium Chloride ($CaCl_2$) solution is used sometimes as a diluent in soil pH measurement (Dolling and Ritchie, 1985; Schofield and Taylor, 1955) but was not considered for compost samples in this study. The reason for $CaCl_2$ being used in soil pH analysis is that calcium compresses the electrical double layer, replaces $H^+{}_3O$ and gives a pH measurement closer to the pH at the surface of soil colloids. Further, the addition of salt as $CaCl_2$ renders the salt concentration in the soil sample negligible with respect to the amount of salt added in this solution. In general the necessity of using $CaCl_2$ is not as large in compost as in soil, unless measurements are being made on compost with high salt content.

In preliminary experiments, pH measurements using distilled water gave readings approximately 0.1 unit higher than those using de-ionized distilled water (DD water). This can be explained by the fact that some of the cations and anions are removed by de-ionizing systems. Thus, DD water was assumed to have less influence on the true compost pH and was selected as the diluent for use in the rest of this study.

As a result of the preliminary work, the following procedure was adopted for all subsequent sample preparations and measurements:

Approximately 5 g quantities of composite original compost samples were weighed into a plastic container (175 ml) and DD water was added to the compost to form a mixture. The mixture was gently stirred with a glass rod for one minute and pH readings were taken from these mixtures without centrifugation or filtration.

3.2.4 Test Methods

Having established a method for preparing samples for pH measurement, a number of other factors needed to be addressed. Firstly, because immature compost represents a dynamic ecosystem, and because pH is known to change during composting (Jackson and Line, 1997), it could be hypothesized that, because of ongoing biological activity in the sample, measurements could be influenced by the time between sampling and measurement. Secondly, once the compost sample has been prepared (i.e. diluted), it is possible that the pH will change with time as more ions come into solution. Thus, the dependence of pH reading on standing time of the prepared sample needed to be established. Finally, there was a need to establish how pH readings were influenced by the degree of sample dilution and what was the most appropriate degree of dilution.

The approaches taken to investigate these three factors are detailed below.

Sampling-Measurement Time

Typically, biological activity, as evidenced by temperature and gas concentration measurements, increases most rapidly during the first several days of composting. A change in pH due to biological activity would most likely occur in samples taken during the early part of the composting process. Consequently, composite, mixed samples were collected from the composter on days one and two during the processing of the second batch of compost. Each of these samples were split into two with one half being analyzed within one hour of sampling while the other half was allowed to sit in a container at room temperature for 24 hours before pH measurements were taken. In all cases three 5 g sub-samples were used for pH measurements

Dilution-Measurement Time

The effect of extraction time was investigated by taking pH measurements at intermittent times up to 2 h after adding water to compost as above. Three 5 g sub-samples of Day 12 compost from the second batch as well as 3-year-old samples were used, with 40ml DD water added as diluent. Before each measurement, the slurry was stirred manually with a glass rod.

Dilution Ratio

Dilution-pH Relationship

In order to determine a relationship between measured pH and dilution, pH values were measured at various dilution ratios by adding measured volumes of DD water successively to each sample. Mixtures were stirred manually for one minute and then allowed to stand for four to five minutes after each addition. In each case 5 g of fresh compost was made into slurry by adding 20 ml DD water and then the slurry was further diluted in stages. Some samples were diluted up to a final dilution of 5 g in 100 ml water, while others were made up to a final dilution of 5 g in 2000 ml water. The pH for each dilution was recorded and measurements were carried out in triplicate.

Two- and Three-point Determination

In practice it would be inconvenient to measure pH at a large number of dilution ratios. Thus, the use of a limited number of dilutions, instead of a series of dilutions was investigated. On the basis of the results from the dilution experiment described above, eight 5 g samples of 20-day compost were mixed into slurry and diluted with 20 ml, 30 ml and, finally 60 ml of DD water to determine pH values. The same procedure was applied to samples of 3-year-old compost.

3.2.5 Statistical Analyses

Statistical analysis was done using General Linear Models and Regression procedures of SAS (SAS 1996).

3.3 RESULTS AND DISCUSSION

3.3.1 Sampling-Measurement Time

Results of pH measurements, using 50 ml DD water for dilution, and taken within one hour after sample collection and 24 h later are shown in Table 3-1. Time between sampling and measurement had a slight influence on pH readings. The pH values measured within an hour of collection were significantly different (P<0.05) to those measured 24 h later. This suggests that the pH measurement needs to be carried out as soon as possible after sample collection for immature compost samples. Several hours delay appears to result in chemical or biological changes in the sample and consequent change of pH value.

Table 3-1. pH measurements within 1 h between collection and measurement and after 24 h *

Compost type	Sampling-to -measurement time	Mean pH (50ml DD water added to 5g sample)
1-day sample	Within 1 hour	9.1
	24 hour	9.0
2-day sample	Within 1 hour	9.0
	24 hour	8.9

* All results are based on measurements of three replicates diluted in stages.

3.3.2 Dilution-Measurement Time

Figure 1 shows the trend in pH measurements taken over a period of 2 h from initial dilution and mixing. Samples 1, 2 and 3 were fresh compost while sample 4 was 3-year compost. The general trends are slightly different between fresh samples and the 3-year-old sample. The differences between the three fresh samples in Figure 1 are indicative of the non-homogeneity of compost but all three samples show the same general trend. pH readings increased during the first several minutes but, after 15 minutes, the readings decreased continuously with all three samples. A possible explanation for this is that the mixture begins to absorb carbon dioxide from the atmosphere (Westcott 1978), possibly due to the nature of the mixture. As shown by Figure 3-1, the time taken to obtain a measurement after mixing fresh compost into a slurry makes a difference to the value obtained. The pH of mature compost increased at the beginning and then decreased more slowly than pH of fresh compost. In subsequent parts of this study measurements were taken 5 to 10 minutes after mixing. In all cases, stable readings were reached within 10 to 20 seconds of inserting the electrode in the compost slurry.

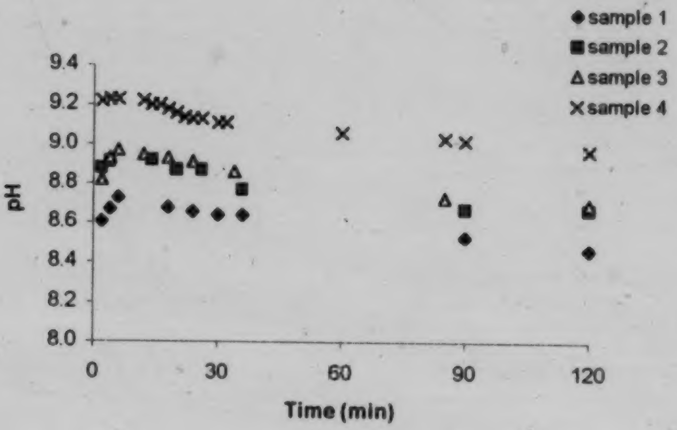

Figure 3-1. pH measurements vs. standing time (within 2 hours).

Samples 1, 2 and 3: Day 12 compost; Sample 4: 3-year-old compost

3.3.3 Dilution Ratio

The pH for each dilution of 5 g 3-year samples in up to 2000 ml water is plotted in Figure 3-2. Again, the non-homogeneity of the compost samples caused a large variation in measured pH at each dilution, but the trends for each sample were similar. In response to increases in dilution ratio, there were corresponding increases in pH reading. A plateau region was reached for all three samples after a dilution of 5 g per 750 ml water. Carnes and Lossin (1970) obtained similar result for their 0-d compost. According to the authors, compost contains a strong buffering system and the gradual rise in pH with increased dilution ratio could be attributed to the gradual release of buffers from the compost. While a constant pH reading appears to be approached at high dilutions, this is different to the pH in undiluted compost. A means of estimating undiluted pH values was sought using data obtained at lower dilution ratios.

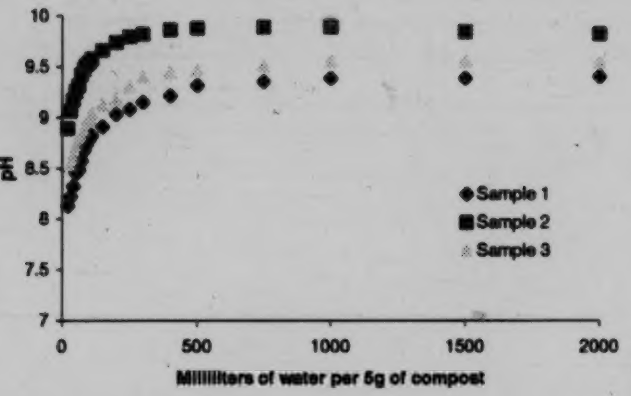

Figure 3-2. pH values of mature compost (diluted with up to 2000ml of DD water)

Measurements of pH at eleven lower dilution ratios (less than 100 ml) for 10-d compost are plotted in Figure 3-3. Simple linear regression analyses on data up to 100 ml water were carried out using the regression procedures of SAS (SAS 1996) and the linear relationships were significant ($P<0.01$). The regression equations for samples of 9-d and 10-d compost are presented in Table 3-2. From these equations it can be seen that the slopes are similar. Since there is a linear relationship between dilution ratio and pH, the pH value at zero dilution can be determined by extrapolating to zero, namely, by obtaining the intercepts of the linear regression equations. Theoretically, the intercept can be treated as the pH at zero dilution and should represent the actual pH in the compost matrix.

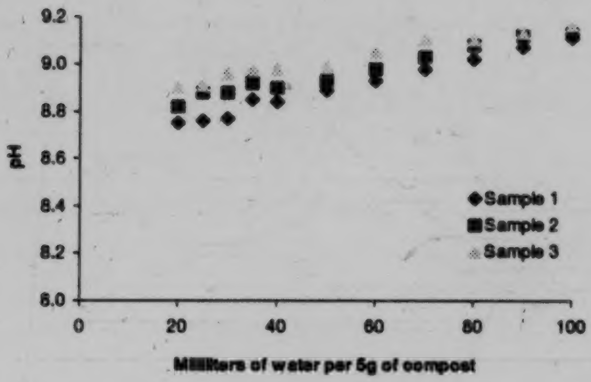

Figure 3-3. pH vlues for three replicates of 10-d compost (diluted with various amounts of DD water).

In order to combine data from several samples, the method of pH data analysis as presented by Murphy (1982) was applied in the data analysis. The author indicated that the calculation of a mean of observed pH's introduced a significant bias as compared to –log(mean[H^+]). Therefore, rather than averaging intercept pH values, hydrogen ion concentrations derived from the intercepts were averaged and the pH was reported as the negative logarithm of this mean hydrogen ion concentration, i.e., -log(mean[H^+]). The pH values shown in Table 3-2 represent the pH values, at zero dilution, for the two composts concerned. The errors were calculated as ± one standard deviation from the mean of the hydrogen ion concentration and then they were transformed to pH values. Notice that, because of this, errors obtained are no longer symmetrical.

Table 3-2. Linear regression relationships between dilution ratio (X) and pH (Y).

Compost type	Replicates	Regression equation	r^2	pH*
Day 9	Sample 1	$Y = 8.66 + 0.0045X$	0.87	8.6 (-0.08, 0.09)
	Sample 2	$Y = 8.67 + 0.0036X$	0.824	
	Sample 3	$Y = 8.53 + 0.0058X$	0.951	
Day 10	Sample 1	$Y = 8.85 + 0.0032X$	0.969	8.7 (-0.09, 0.11)
	Sample 2	$Y = 8.76 + 0.0038X$	0.974	
	Sample 3	$Y = 8.66 + 0.0046X$	0.988	

* Errors shown in parenthesis

3.3.4 Two- and Three-point Determinations

The advantage of using the intercept of the linear relationship is that any ambiguity about the level of dilution is removed. The disadvantage is that a number of pH determinations must be made, at different dilutions, in order to establish the linear relationship to determine the intercept. A study of two- and three-point determinations was carried out to verify that the pH-dilution relationship could be established from measurements at two or three dilution ratios rather than the ten dilutions used above. A convenient method would be to measure the pH value at two dilution ratios and from the slope of the points determine the intercept. In this case, measurements were made at three dilutions (20, 30 and 60ml) and compared with two dilutions (20 and 30 ml) or (30 and 60 ml) or (20 and 60 ml).

Table 3-3 shows the equations for each sample obtained when a straight line was fitted to two of the three points measured (20 and 60 ml dilution ratios). The pH at zero dilution for each type of compost was obtained by calculating the negative logarithm of the mean hydrogen ion concentration obtained from the intercepts of the eight equations.

To ensure that the pH value calculated by fitting lines to two points was independent of the specific points chosen, another two sets of lines were obtained by fitting to the 30ml and 60 ml dilution points as well as all three points. A comparison was made between the three estimated pH values obtained and this is shown in Table 3-4. There are no significant differences between pH values at zero dilution obtained from two dilution ratios or three dilution ratios ($P<0.01$). It can be concluded that pH values obtained using two-point determinations are independent of the number of dilution levels chosen for the determination.

Table 3-3. Estimation of pH by two-point determination (20ml and 60ml).

Compost type	Replicates	Equation	pH*
20-day-old	Sample 1	$Y = 8.70 + 0.0038X$	8.9 (-0.09, 0.12)
	Sample 2	$Y = 8.78 + 0.0032X$	
	Sample 3	$Y = 8.87 + 0.0017X$	
	Sample 4	$Y = 8.82 + 0.0028X$	
	Sample 5	$Y = 8.86 + 0.0035X$	
	Sample 6	$Y = 8.93 + 0.0028X$	
	Sample 7	$Y = 8.99 + 0.0032X$	
	Sample 8	$Y = 8.99 + 0.0020X$	
3-year-old	Sample 1	$Y = 8.51 + 0.0095X$	8.5 (-0.05, 0.05)
	Sample 2	$Y = 8.52 + 0.0095X$	
	Sample 3	$Y = 8.49 + 0.0087X$	
	Sample 4	$Y = 8.48 + 0.0080X$	
	Sample 5	$Y = 8.56 + 0.0082X$	
	Sample 6	$Y = 8.55 + 0.0063X$	
	Sample 7	$Y = 8.42 + 0.0088X$	
	Sample 8	$Y = 8.46 + 0.0078X$	

* Errors shown in parenthesis

Table 3-4. Comparison of pH vlaues calculated from two or three dilution points.

Compost type	Mean – DD water added (ml) to 5 g sample*		
	20 ml and 60 ml	30 ml and 60 ml	20 ml, 30 ml and 60 ml
20-day-old	8.9 (-0.09, 0.12)	8.9 (-0.06, 0.07)	8.9 (-0.08, 0.10)
3-year-old	8.5 (-0.05, 0.05)	8.5 (-0.03, 0.03)	8.5 (-0.05, 0.05)

* Errors shown in parenthesis

3.3.5 Effect of Number of Samples on Accuracy

Due to the heterogeneous nature of compost, it is necessary to take measurements for a large number of samples to minimize the error. The fewer the number of samples for which pH is measured, the more significant error there is. Using the data obtained for the two- and three-point determinations above, the standard deviations and errors associated with estimated pH values obtained with different sample numbers were calculated. Different sample numbers were obtained by progressively removing the sample with the pH value closest to the mean to obtain decreasing values of n. For example, to decrease the sample numbers from n=8 to n=7, sample 5 (measured pH of 8.86) was discarded, while from n=7 to n=6 sample 3 (measured pH of 8.87) was discarded, and so on. The relationship between root mean square (RMS) error and sample size for 20-day old and 3-year old compost is plotted in Figure 3-4, which shows that the error was lower for the 3-year old material than for the 20-day old material. This is to be expected since mature compost is likely to be much more homogeneous with regard to pH than fresh compost.

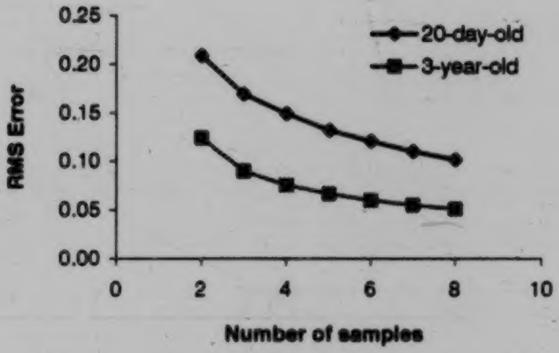

Figure 3-4. RMS error of pH using different sample sizes.

3.3.6 Determining the Number of Samples

The question of how many samples is appropriate to get a pH with a certain accuracy is of importance to researchers and operators alike. Before a sample number (n) can be determined, three components need to be specified. First, the level of confidence desired should be given, that is, the value of $100(1-\alpha)\%$ with α referred to as the probability that a confidence interval will not contain the true population mean (μ). Second, the maximum difference (D) desired between the estimate of the population mean ($\bar{x}$) and the true population mean (μ) must be given (Harnett 1982). The value of D (also known as limit of error, margin of error) is the maximum amount of "error" permitted in estimating the population parameter and is equal to the absolute value of ($\bar{x} - \mu$). Third, an estimate of the variability of the compost is required. This is provided by the population standard deviation (σ) or the sample standard deviation (s).

In Table 3-5 the standard deviations for 20-day and 3-year compost have been roughly estimated on the basis of the data in Table 3-3. Then, using standard statistical equations (Harnett, 1982) the values of n required for different confidence levels and error (D) were calculated.

Table 3-5. Sample size calculated based on desired confidence level and D using estimated population standard deviation (σ).

Compost type	σ	Confidence level	$D = \lvert \bar{x} - \mu \rvert$	n
20-day-old	0.10	95%	0.1	4
			0.05	16
		90%	0.05	11
3-year-old	0.05	95%	0.05	4
			0.025	16

Since there is a higher variation in pH values for fresh compost, more samples are required for pH determination for the same accuracy and the same confidence level compared with well-cured compost.

Generally, the population standard deviation (σ) of compost will not be known. In this case, an iterative procedure using the *t* variable can be used by assuming sample size n_e first, and then obtaining the critical value of *t* obtained from tables for the *t*-Distribution. Finally sample size n can be calculated. The discrepancy between the assumed n_e and the calculated n is used to assume a new value of n_e for the next iteration, and so on, until the n calculated equals the n_e assumed for the current iteration. Again standard deviation was assumed to have the value of error in the calculation. The results for 20-d compost are shown in Table 3-6.

Table 3-6. Sample size calculated based on desired confidence level and D using estimated sample standard deviation (s)

Compost type	s	Confidence level	$D=\lvert\bar{x}-\mu\rvert$	n
20-day-old	0.10	95%	0.1	7
			0.05	18

A comparison of the first two rows in Table 3-5 and Table 3-6 shows that, under the same confidence level and accuracy desired, more samples need to be taken when s rather than σ is assumed to be known (7 compared to 4 and 18 compared to 16).

3.4 CONCLUSIONS

It is also important to carry out pH measurements as soon as possible after sample collection. Linear relationships exist between dilution ratio (up to 100 ml/5 g compost) and pH. The pH value in undiluted compost can be obtained by extrapolating the linear relationship to the zero dilution. It is practical to estimate pH value of compost by taking measurements at two dilution points in the linear range for each sample. The number of samples depends on the accuracy required.

To this end, the following procedure is proposed:

1. Weigh 5 g wet compost sample and add 20 ml deionized (DD) water. Stir mixture gently with a glass rod, wait 5 minutes, insert the pH electrode into the slurry, and take the pH_{20} measurement;
2. Add 40 ml more DD water to the mixture and stir again, wait 5 minutes, insert the pH electrode into the slurry, and take the pH_{60} measurement;
3. Repeat Step 1 and 2 for other samples to get pH_{20} and pH_{60} for each sample;
4. Fit straight lines to pH_{20} and pH_{60} for each sample and calculate a mean hydrogen ion concentration at the intercepts;
5. Transform the mean hydrogen ion concentration to get the pH of the original undiluted compost matrix.

3.5 REFERENCES

Carnes, R.A. and Lossin, R.D., 1970. An investigation of the pH characteristics of compost. Compost Sci., 11: 18-21.

Dolling, P.J. and Ritchie, G.S.P., 1985. Estimates of soil solution ionic strength and the determination of pH in west Australian soils. Australian J. of Soil Res. 23: 309-314.

Ekinci, K., Keener, H.M. and Elwell, D.L., 1998. Composting short paper fiber with broiler litter and additives- alum, HiClay® alumina and sulfuric acid: I. Effect of initial pH and C/N ratio on ammonia emission. ASAE Paper, No. 984137.

Harnett, D.L., 1982. Statistical methods. Addison-Wesley Publishing Company. Reading, MA.

Jackson, M.J. and Line, M.A., 1997. Composting pulp and paper mill sludge – Effect of temperature and nutrient addition method. Compost Sci. and Util. 5(1): 74-81.

Leege, P.B. and W.H. Thompson (eds). 1997. Test Methods for the Examination of Composting and Compost. The U.S. Composting Council. Bethesda, MD, pp193-205.

Martins, O. and Dewes, T., 1992. Loss of nitrogenous compounds during composting of animal wastes. Bioresource Tech. 42: 103-111.

McLean, E.O., 1982. Soil pH and lime requirement. In: A.L. Page, R.H. Miller and D.R. Keeney (Eds), Methods of soil analysis. Part 2. American Society of Agronomy, Madison, WI. pp.199.

McKinley, V.L. and Vestal, J.R., 1985. Effect of different temperature regimes on microbial activity and biomass in composting municipal sewage sludge. Can. J. of Microbiology, 31: 919-925.

Murphy, M.R., 1982. Analyzing and presenting pH data. J. Dairy Sci. 65:161-163.

SAS. 1996. Version 6.12. Raleigh, NC: Statistical analysis system Institute Inc.

Schofield, R.K. and Taylor, A.W., 1955. The measurement of soil pH. Proc. Soil Sci. Am. 19: 164-167.

Tseng, D.Y., Chalmers, J.J., Tuovinen, O.H. and Hoitink, H.A.J., 1995. Characterization of a bench-scale system for studying the biodegradation of organic solid wastes. Biotechnology Progress 11: 443-451.

Villar, M.C., Beloso, M.C., Acea, M.J., Cabaneiro, A., González-Prieto, S.J, Carballas, M., Díaz-Raviña, M. and Carballas, T., 1993. Physical and chemical characterization of four composted urban refuses. Bioresource Tech. 45: 105-113.

Westcott, C.C., 1978. pH measurements. Academic Press. NY.

Chapter 4

The Influence of Carbon Availability and pH Modification on Ammonia Losses in Laboratory-Scale Composting of Manure and Straw

4.1 INTRODUCTION

During the composting process, aerobic, thermophilic bacteria break down organic materials and utilize available nutrients to produce microbial biomass. Of the major nutrients, nitrogen is often the key limiting factor to crop production in agricultural ecosystems, and has been cited as a crucial factor in increasing food production. Nitrogen loss can be severe when materials with high nitrogen contents are decomposed. Since finished compost is often used as a soil amendment, the nutrients in the compost would be of value from an agricultural standpoint. It would be desirable if the nitrogen could be converted to organic forms available to the environment over a longer period and causing fewer problems, such as excessive biological oxygen demands of surface water, leaching into groundwater, and odour problems.

Ammonia is produced from either aerobic or anaerobic decomposition of proteins and amino acids. In composting, ammonia emission is normally detected during the thermophilic stage of aerobic decomposition. A C/N ratio of about 30 is considered to be optimum for composting, since living organisms utilize about 25 to 35 units of carbon for every unit of nitrogen during active aerobic growth (Bishop and Godfrey, 1983). Generally, a low C/N ratio results in excess nitrogen loss by ammonia volatilization. However, when different types of organic materials are composted, a higher C/N ratio does not necessarily indicate an effective solution for preventing nitrogen loss. Several studies have been done with respect to the availability of carbon sources to microorganisms (Barrington et al., 1997; Brink, 1995; Mahimairaja et al., 1994; Mote and Griffis, 1980; Shin and Jeong, 1996; Subair et al., 1999; Witter, 1986). A readily available carbon source appeared to cause immediate immobilization of N when an appreciable amount of glucose was added to soils (Okereke and Meints, 1985). Subair (1995) found that a labile organic amendment (glucose) was effective in reducing NH_3 volatilization from liquid hog manure, whereas material resistant to decomposition (sawdust) was not. Losses of nitrogen during the composting of cattle manure and straw have been reduced by increasing the proportion of ground straw to chopped straw whilst maintaining a C/N ratio of 31.6 (Meyer and Sticker, 1983).

The process of ammonia volatilization in composting is influenced by several factors, such as ammoniacal N (the combined amount of nitrogen associated with both unionized, NH_3, and ionized, NH_4^+, forms in solution) concentration, pH, temperature, moisture content and aeration rate. Experimental data (Freney et al., 1983; Nakasaki et al., 1993) indicated that the most severe losses of NH_3 occurred when high pH values were measured. Since the molecular NH_3 portion of ammoniacal N increases as pH and temperature of compost increase, higher pH values increase the concentration of NH_3 present in both the compost solution and free air space, and therefore increase the potential for NH_3 loss. Inorganic chemicals have been used to inhibit ammonia volatilization by increasing the acidity of the compost mixture (Carey et al., 1998; Ekinci et al., 1998; Kithome et al., 1999). The addition of $Al_2(SO_4)_3$ (alum) has given reduction in ammonia losses in several studies (Kithome et al., 1999; Moore et al., 1995). The addition of sulfuric acid, which lowered initial pH below 7, also reduced ammonia losses, but the low pH may also have some influence on the heating process (Carey et al., 1998). Although a range of chemical amendments have been evaluated with regard to NH_3 volatilization, there is less information in the literature on the use of buffer materials to regulate pH at a certain range during the initial thermophilic stage of composting.

A simulation model describing the process of substrate decomposition and nitrogen volatilization in the high rate stage of composting was developed (Chapter 2). The unique features of this model are: (i) the substrate was partitioned into several sub-groups based on both the chemical components and different decomposition rates of raw materials; (ii) microbial biomass growth was related to the C and N dynamics and (iii) ammonia volatilization was related with interstitial carbon dioxide concentration, which was influenced by both microbial activity and air exchange rate, based on a calculation of a multisolute CO_2-NH_3-H_2O aqueous system. This model demonstrated that ammonia volatilization was associated with substrate composition, temperature, aeration, pH and moisture content.

Among the various control factors that can influence the fate of nitrogen during composting, two were chosen to be tested for the purpose of validating the model. This is described in Chapter 5. The experiments used in gathering the model validation data, however, provided additional insights into the composting process and are described here. The objectives of this study were (i) to quantify the dynamics of N losses through ammonia volatilization during composting of dairy manure and wheat straw mixtures; and (ii) to evaluate the effectiveness of two types of carbon amendments and two chemicals forming buffer solutions in reducing N losses.

4.2 MATERIALS AND METHODS

4.2.1 Vessel System

Composting experiments were conducted at the University of Alberta's Edmonton Research Station using a computer-controlled system very similar to that described by Franke (1997). The system consisted of eight 170 L, insulated, aerated vessels each fitted with temperature sensors and from which head-space gases could be sampled and analyzed. A block diagram of the system is shown in Figure 4-1. For sampling purpose three 10 cm diameter holes were made in the wall of each vessel on a vertical line as openings with one close to the top, one in the middle, and one close to the supporting steel grate. The holes were sealed by duct fittings when they were not in use. One aeration aquarium pump (Maxima, Rolf C. Hagen Inc., Montreal, QC) and one centrifugal fan (RB5, Rotom, Pickering, ON) were attached to the bottom of each vessel. The aquarium pump supplied a low airflow (4 L· min^{-1}) continuously through 6.4 mm OD flexible polyethylene tube to meet oxygen requirements in the composting vessel. The fan was used to cool the compost by delivering air through a 50 mm ID rigid PVC pipe when the temperature inside the vessel exceeded a set point of 55°C. The fan supplied approximately 20 L· min^{-1} air. Manually-actuated ball valves were located on the 50 mm lines to adjust the exact amount of air being delivered to the vessels. This was necessary because the flows into eight vessels needed to be adjusted to be identical after they were initially loaded in each experiment. An anemometer (Velocicalc 8350, TSI, St.Paul, MN) was used to measure the velocity of the air in the 50 mm lines once a day and, hence, to calibrate the ball valves used for flow control. The flows of the aquarium pumps were not checked after the installation since it was assumed that the flows were relatively insensitive to the variation of the pressure downstream.

Temperature Monitoring System

Two precision temperature sensors (LM335, National Semiconductor Corporation, Santa Clara, CA) were placed in each vessel to provide a temperature profile of the compost. The two sensors were fastened to a steel rod (5 mm in diameter and 635 mm in length), one at the bottom of the rod and the other in the middle (about 300 mm apart). The rods were pushed along the vertical centerline of the compost to equal heights for all the vessels. Leads from the sensors were connected to an external circuit board that multiplexed the analog signal to an analog-to-digital (A/D) converter. All temperature sensors were calibrated in a water bath prior to each experiment and the linear calibration equations derived were used in the data acquisition program to translate the digital voltage values into corresponding temperatures in degrees Celsius.

Gas Sampling System

Gas samples were drawn through 6.4 mm OD flexible polyethylene tubing running from the head space of each vessel to a gas sampling manifold. A solenoid valve (203X-3, Airmatic-Allied Inc., Wilmington, OH) was connected in each of the sample lines to control from which vessel gas was to be drawn as input to the manifold. The manifold was placed in an insulated, heated enclosure in order to maintain temperature of the gas in the sampling lines so as to minimize condensation of moisture. Temperature inside the enclosure was set in the range of the off gas temperature measured from the vessels. Gas coming out of a single shared output from the manifold was delivered to three gas analyzers that were in parallel (Figure 4-2).

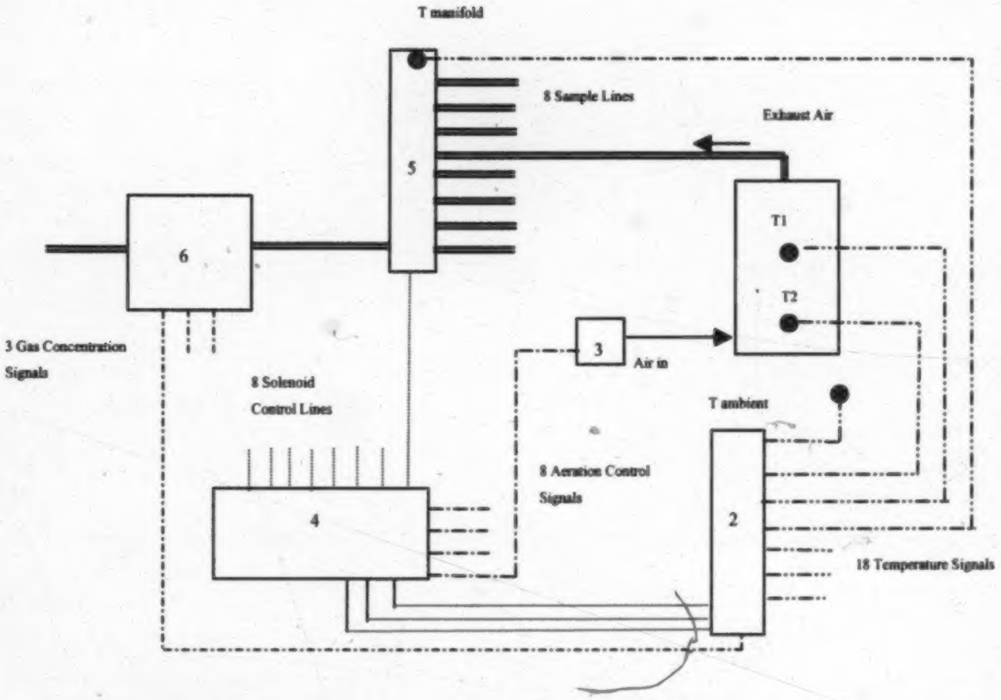
T manifold
8 Sample Lines
Exhaust Air
5
6
T1
T2
3 Gas Concentration Signals
3
Air in
8 Solenoid Control Lines
T ambient
8 Aeration Control Signals
4
2
18 Temperature Signals

Figure 4-1. Flow diagram of the composting system. 1. 8 vessels; 2. Multiplexer; 3. 8 Fans; 4. Data acquisition and control computer; 5. Valves and Manifold; 6. 3 gas analyzers.

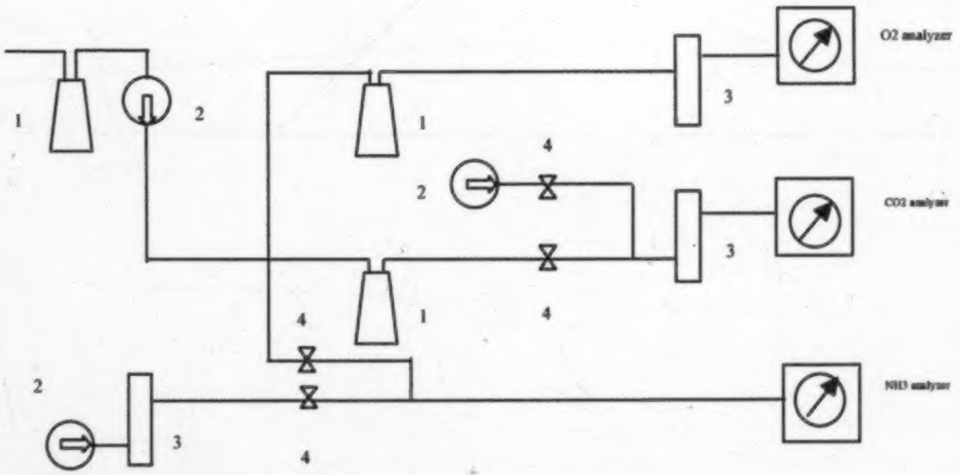
O2 analyzer
1
2
1
3
4
2
CO2 analyzer
3
4
1
4
4
2
NH3 analyzer
3
4

Figure 4-2. Gas Ssampling system. 1. Condenser; 2. Vacuum pump; 3. Dessicator; 4. Needle valve.

The concentration of oxygen (O_2), carbon dioxide (CO_2) and ammonia (NH_3) in the sample gases were measured by an oxygen analyzer (540A Industrial Oxygen Analyzer, Taylor Servomex, Sussex, Endland), a carbon dioxide analyzer (Model 870, Beckman, Fullerton, CA) and an ammonia analyzer (Model 880, Beckman, Fullerton, CA), respectively. All three analyzers were regularly calibrated with zero and span gases. The oxygen analyzer was calibrated with cylinders of air with O_2 concentration analyzed as 21.2%. The CO_2 and NH_3 analyzers were calibrated with cylinders of CO_2 gas at 3.49% and NH_3 gas at 0.138%, respectively. Cylinders of dry nitrogen (N_2) gas were used for zeroing of all three instruments. A vacuum pump was placed on the main line after the manifold and prior to the distributor to provide sufficient flow rate through each analyzer. Due to the low measurement ranges of both the carbon dioxide and ammonia analyzers, the gas samples to these were diluted at a ratio of 4:1 and 3:1 by volume, respectively, with fresh air from outside the building. Dilution air for the ammonia analyzer was passed through a filter of calcium sulphate ($CaSO_4$) to remove NH_3. Dilution air for each stream was drawn in by an aquarium pump (Optima, Rolf C. Hagen Inc., Montreal, QC). Needle valves were placed in series with sample and dilution air to ensure that the proper rate of air flow was being delivered. The needle valves were calibrated each day using a bubble meter and a stop-watch.

Due to the high relative humidity in the vessels' head spaces and the small diameter of tubing used, the gas sampling lines were insulated all the way from the head space of each vessel to the solenoid valve box in order to avoid any condensate plugging the gas lines. Lines were led through flexible electrical conduit wrapped with 26 $W \cdot m^{-1}$ heat tape and covered in a layer of duct insulation. This provided sufficient energy to maintain a temperature between 40~50°C inside the lines and prevented severe condensation forming.

Moisture in gas samples affects the accuracy of gas concentration readings, and also threatens to slowly decrease the performance of the gas analyzers over time. In an attempt to minimize this problem, condensate traps made from 1.5 L Erlenmeyer flasks were placed at three locations. One flask was connected between the manifold and the vacuum pump. The other two were positioned on the inlet lines to the CO_2 and O_2 analyzers. In addition, a desiccant column (W.A. Hammond Drierite Company, Xenia, OH) was put in the inlet lines to the CO_2 or O_2 analyzers to absorb any remaining moisture. Desiccant was changed regularly. Since indicating calcium sulfate ($CaSO_4$) was used as the drying agent and ammonia can react with $CaSO_4$ to reduce the ammonia concentration in the measured air stream, the column could not be used in series with the ammonia analyzer. Gas to the NH_3 analyzer was kept heated and insulated up to the inlet of the analyzer to make sure that any moisture remained in its vapor form.

Data Acquisition and Control System

Data acquisition and relay control were operated through software written in Qbasic running on a 80486 PC computer installed with a 12 bit analog-to-digital (A/D) converter board (DAS 1201, Keithley MetraByte/Asyst, Taunton, MA) and a high speed serial card (HSP–1P, Logicode Technology, Inc., Camarillo, CA). The A/D board, controlled by software, created the interface between the computer and instrumentation to control hardware and collect data into files. Three analog input lines were utilized from the A/D interface board to accommodate the 21 multiplexed analog signals produced by the 18 temperature sensors and three gas analyzers.

Temperature data, which were used to control the status of aeration fans, were continuously measured. They were stored into files at a predefined interval of 30min. Gas concentration data were sampled sequentially and stored into files at a predefined interval of 75 min.

Eighteen digital input/output (I/O) channels on the A/D board were allocated to digital output controls to operate 18 AC devices (8 solenoid valves, 8 aeration fans, one vacuum pump for gas sampling, and one heater for the manifold enclosure). They were actuated individually by solid state AC switching relays (PD2401, CP Claire Corp., Chicago, IL).

4.2.2 Experimental Conditions and Treatments

Four experiments were carried out to examine the retention of nitrogen during composting of mixed dairy manure and chopped wheat straw under different conditions. Two experiments were designed to investigate the influence of C availability while the other two were aimed at examining how NH_3 volatilization could be controlled by addition of buffering amendments. Wheat straw was used as the basic C source while, in the first two experiments, molasses and paper were used as alternative sources. The characteristics of raw materials are given in Table 4-1. The pH values of manure were between 8 and 9 from several measurements in different experiments. Manure was collected from the floor scraper at the Dairy Unit of the Edmonton Research Station of the University of Alberta. The scraper was operated twice a day and the manure contained some of the bedding materials (wood shavings and sawdust) used in the barn. A separate collection was done before each run. Non-weathered wheat straw was obtained from the Metabolic Research Unit of the Edmonton Research Station, and was chopped (5-10 cm) before each experiment. The composting mixture used was made up of a 3:1 ratio (wet weight) of dairy manure and wheat straw. The composition of the mixture was calculated to give a C:N ratio of approximately 25:1 and a moisture content of 70% (wet basis), with additional water added.

Table 4-1. Characteristics of raw materials

Ingredients	*Dry Solids Fraction (%)*	*Ash Content (%)*	*Carbon Content (%) (dry basis)*	*Nitrogen Content (%) (dry basis)*
Dairy Manure	16	15.0	42.3	3.46
Wheat Straw	90	10.0	42.2	0.456
Office Paper	99	13.5	43	0.06

In each experiment, four treatments were used, with each treatment duplicated.

At the time of loading, calculated amounts of manure, straw, and water or necessary amendment were mixed in a mortar mixer and placed in vessels. The rods with temperature sensors were pushed into each vessel and aquarium pumps, fans and gas sampling lines were connected. The data acquisition and control system was started running. Flows of ventilation ducts were checked every day for the first four days of each experiment, and the relevant flow rates were used for the calculation of the mass of each gas evolved.

Headspace gases were analyzed continuously for two weeks while the compost remained in the vessels, and was continuously aerated, for 3 to 4 weeks. The gas measurement period of Experiment 3 was only six days due to a malfunction of the carbon dioxide analyzer. This experiment was treated as valid since the period of maximum ammonia emission had occurred by that time. Vessels were weighed before emptying and the compost was left piled outside for curing. Samples of composting materials were taken immediately after mixing and then after two weeks and at emptying for measurement of dry matter contents, ash contents, TKN, pH, and soluble C for Experiments 1 and 2. In

Experiment 3 and 4, samples were taken once a day during the first five days to monitor pH values as well. When the system was running, compost was taken from the three holes in each vessel and mixed thoroughly in order to obtain representative samples. Each time, about 300 g of samples were taken for a series of analyses, while about 100 g was taken if only pH was to be determined. Samples for pH determination were measured as soon as possible while those for other tests were placed in sealed plastic bags and stored in a 4°C cold room until analysis.

4.2.2.1 Carbon Availability Experiments

Experiment 1 – Molasses Amendment

Molasses, with a composition of mainly sucrose, was chosen as the readily available C source to be added into the composting mixture. We hypothesized that the addition of molasses would increase N immobilization at the initial decomposition stage and cause less ammonia volatilization. In treatment 1A, only water was added, while in treatments 1B, 1C and 1D calculated amount of molasses were added after being dissolved in the same amount of water as used in 1A. Treatments 1B, 1C, and 1D received sucrose at rates of approximately 3, 6.6 and 10%, respectively, of the dry weight of the initial mixtures.

The soluble C content of 1A was assumed to be 0.02 kg of C per kg of initial dry matter based on some unpublished test results from Franke (1997). The additions to treatments 1B, 1C and 1D were calculated to provide approximately 0.02, 0.04, and 0.06 kg, respectively, of extra soluble C per kg of initial dry matter. The actual amount of compost placed in each vessel ranged from 47 ~ 49 kg.

Experiment 2 – Office Paper Amendment

Office paper, consisting mainly of cellulose, was chosen as a less readily available carbon source. Standard 216 mm × 280 mm sheets of paper were shredded to approximately 10mm in width prior to mixing with dairy manure and straw. Treatment 2A received water only. Treatments 2B, 2C and 2D received increased amounts of paper and decreased amount of straw in order to obtain the similar initial C/N ratio of approximately 25:1.

4.2.2.2 pH Buffering Experiments

A buffer solution is one that tends to maintain a constant pH when an acid or alkali is added to it. A buffer system usually consists of a weakly dissociated acid and the salt of that acid, or a weak base and its salt.

Our hypothesis was that buffer solution added to composting mixture would maintain the pH at a desired level and that this would influence ammonia volatilization.

A phosphate buffer was chosen because phosphate is present in most composting raw materials and has not shown any negative influence on microbial activities. The pK_a of the phosphate pair, $HPO_4^{=}$ and $H_2PO_4^{-}$, the dihydrogen and monohydrogen phosphate ions, is 7.2. Effective buffer systems have a range of approximately two pH units centered about the pK_a value (West et al., 1966). In this case, the effective range is approximately pH of 5.2 to 9.2.

The pH values of the buffer solution applied were chosen as 6, 7, and 8 because pH values of 6 to 9 are the appropriate pH range of compost (Nakasaki et al., 1993). The actual amount of chemicals added was determined by a preliminary trial as follows.

The molar proportion of the monohydrogen and the dihydrogen chemicals is specific for a buffer solution at a certain pH value. For example, for pH=7, the ratio is 31:69. By keeping this proportion and increasing the absolute amount of each chemical, the buffer strength of the solution increases. Various amounts of chemicals with the same proportion were mixed with 5 g of wet compost separately. Sufficient water was added to the mixture to form a slurry so that the pH value could be measured. Potassium hydroxide (KOH) was added into each mixture 1ml at a time with pH measured at each interval. A titration curve was obtained for each mixture with buffer solution, and the point where a sharp pH change occurred was noted. A typical titration curve is shown in Figure 4-3. The amount of KOH used to reach this point was recorded and calculated as number of moles of alkali accommodated. A series of these moles of KOH were obtained from all mixtures and scaled up from 5 g compost to approximately 50 kg of compost. Table 4-2 shows the details of this calculation.

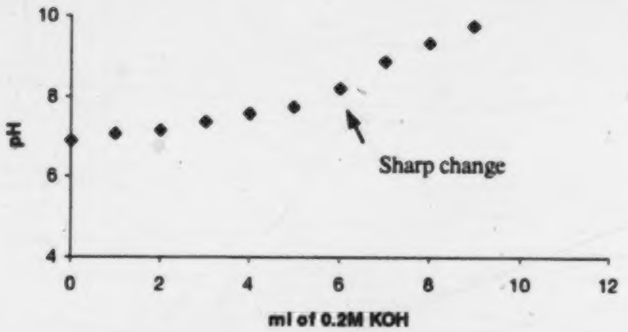

Figure 4-3. A titration curve of 0.3744 moles of monobasic phosphate and 0.5856 moles of dibasic phosphate mixed in 5 g of initial mixture.

Table 4-2. Calculation of equivalent amount of KOH that can be accommodated by 47 kg of mixture

Trial	5 g mixture			47 kg mixture
	Mono	Di	KOH point	Equivalent KOH in need
	moles			
1	0.1248	0.1952	0	0
2	**0.2496**	**0.3904**	$0.4*10^{-3}$	4
3	0.3744	0.5856	$0.6*10^{-3}$	6
4	0.6240	0.9760	$1.2*10^{-3}$	1.2

An estimate of approximately 3.5 moles (60 g) of NH_3 that could be emitted from 50 kg of wet compost was obtained from the previously developed model (Chapter 2). This estimate was compared with the numbers calculated from those derived from titration curves and the amount of chemicals used with the closest moles of alkaline (4 moles) was chosen as the buffer strength we used in Experiment 3. In this case, the amounts of chemicals used in trial 2 were chosen (0.2496 and 0.3904) and scaled up to the actual weight of composting material of each treatment.

Experiment 3 – Buffer (I)

Monobasic Sodium Phosphate ($NaH_2PO_4{\cdot}H_2O$) and Dibasic Sodium Phosphate ($Na_2HPO_4{\cdot}2H_2O$) were added to the basic mixture as buffer materials in the amounts shown in Table 4-3. The amount of each chemical was calculated to give the buffer solutions' pHs of 6, 7, and 8, while having the same molar concentration. Chemicals were dissolved into 9kg of water prior to mixing with the substrates.

Experiment 4 – Buffer (II)

Monobasic Sodium Phosphate ($NaH_2PO_4 \cdot H_2O$) and Dibasic Sodium Phosphate ($Na_2HPO_4 \cdot H_2O$) were again added to the basic mixture as buffer materials in the amounts shown in Table 4-3. The buffer solution used for each treatment has the same buffer pH of 7 but varied buffer strength. The amount of each chemical was doubled and tripled in treatment 4C and 4D, respectively, compared with treatment 4B, to allow the solutions to have increased buffer strengths while holding the buffer pH around 7. Chemicals were dissolved into 9 kg of water prior to mixing with the substrates.

Table 4-3. Experimental treatments.

Treatment	*Substrates*	*Additives*
1A	28.5 kg manure + 9.5 kg straw	9 kg H_2O
1B		9 kg H_2O + 0.5 kg molasses
1C		9 kg H_2O + 1.0 kg molasses
1D		9 kg H_2O + 1.5 kg molasses
2A	31.1 kg manure + 10.45 kg straw	9 kg H_2O
2B	31.1 kg manure + 8.4 kg straw	9 kg H_2O + 1.86 kg office paper
2C	31.1 kg manure + 6.4 kg straw	9 kg H_2O + 3.72 kg office paper
2D	31.1 kg manure + 4.3 kg straw	9 kg H_2O + 5.58 kg office paper
3A	28.5 kg manure + 9.5 kg straw	9 kg H_2O
3B		9 kg H_2O + 364 g Mono[1] + 66 g Di[2]
3C		9 kg H_2O + 162 g Mono + 326 g Di
3D		9 kg H_2O + 22 g Mono + 507 g Di
4A	31.1 kg manure + 10.45 kg straw	9 kg H_2O
4B		9 kg H_2O + 172 g Mono + 347 g Di
4C		9 kg H_2O + 344 g Mono + 695 g Di
4D		9 kg H_2O + 517 g Mono + 1042 g Di

[1] Monobasic Sodium Phosphate
[2] Dibasic Sodium Phosphate

4.2.3 Laboratory Analyses

Water Soluble C was extracted from original samples by shaking 20 g of compost with 150 ml of deionized water for 60 min. The mixture was filtered with suction through a 47-mm diameter, 0.2-µm metrical membrane filter. Water Soluble C was measured in the filtrates using a soluble carbon Analyzer (Astro 2001 System 2, Astro International Corp., League City, Texas). Moisture content was determined by drying the samples in an oven at 70°C for 24 h. Determination of ash content was made by heating pre-dried samples at 550°C for 8 h. TKN was measured by the Kjeldahl method (Bremner and Mulvaney, 1982).

The pH value was determined from three 5 g samples. For each sample, 30 ml of deionized distilled water was first added and mixed. Measurement of pH was made in the solution as pH_{30}. An additional 30 ml of water was added, mixed and measurement of pH was made in the solution as pH_{60}. Straight lines were fitted to pH_{30} and pH_{60} for each sample and a mean hydrogen (H^+) ion concentration was calculated from the three intercepts. The pH of the original undiluted compost was obtained by transforming the mean hydrogen ion concentration. A pH measurements were carried out using a digital pH meters (Accumet Model 815MP) with combination electrodes.

4.2.4 Statistical Analyses

Values of dry matter contents, ash contents, and ammonia emission associated with the treatments were compared using the General Linear Models procedure of SAS (SAS 1999).

4.3 RESULTS

4.3.1 Chemical Properties

Initial properties of the mixes are given in Table 4-4. Initial dry matter contents for all runs were not significantly different ($P<0.05$). In Runs 2 and 4, ash contents increased significantly with increased amounts of paper amendment or buffering chemicals added ($P<0.05$). Thus, the ash content of treatment A was lowest followed by those of treatments B, C and D. Total nitrogen contents of treatments in Experiment 4 were significantly different ($P<0.05$), since the treatments with increased amounts of inorganic chemicals used had larger dry matter contents, and, therefore, smaller nitrogen contents.

Table 4-4. Initial chemical properties of composting mixtures.

Experiment	DM (%)	Ash (%, db)	T-N (%, db)	pH
1A	29.5	11.7	1.59	8.8
1B	29.0	11.7	1.44	8.8
1C	28.5	12.0	1.55	8.6
1D	31.0	11.4	1.36	8.7
2A	30.0	11.3	1.72	8.4
2B	28.2	12.7	1.66	8.2
2C	30.4	14.5	1.58	8.3
2D	29.7	15.5	1.47	8.3
3A	29.4	12.4	1.59	8.6
3B	29.2	14.9	1.57	8.6
3C	29.9	14.9	1.55	8.6
3D	30.2	15.3	1.55	8.9
4A	28.5	12.3	1.62	9.1
4B	27.7	14.7	1.35	9
4C	28.7	17.3	1.31	8.7
4D	28.9	20.3	1.25	8.7

Final properties of the compost are presented in Table 4-5. Final ash contents and total nitrogen contents for all treatments were significantly higher than their initial values ($P<0.05$). Results showed no differences in pH values between initial and final compost.

Table 4-5. Final chemical properties of compost mixtures.

Experiment	DM (%)	Ash (%, db)	T-N (%, db)	pH
1A	24.2	17.4	1.95	8.6
1B	23.8	18.4	1.95	8.7
1C	23.9	18.4	2.05	8.7
1D	26.9	16.7	1.85	8.7
2A	24.0	20.9	2.62	8.8
2B	26.5	22.6	2.28	8.8
2C	24.0	27.2	2.52	8.8
2D	26.5	27.1	2.1	8.7
3A	24.2	19.1	2.03	8.5
3B	25.3	22.7	2.06	8.0
3C	25.2	21.9	2.16	8.5
3D	24.8	22.5	2.07	8.8
4A	24.2	20.7	2.30	8.8
4B	23.4	25.8	1.98	8.4
4C	26.2	25.3	1.70	8.8
4D	25.6	26.3	1.50	8.7

4.3.2 Temperature

The temperature profile for treatments in all experiments followed similar patterns. The average temperatures from two sensors in each vessel of Runs 2A, 2B, 2C and 2D are presented in Figure 4-4. Temperatures increased dramatically in all vessels. Temperatures of vessels that received medium and most paper (treatment 2C and 2D) exceeded 55°C within 30 h, which was approximately 10h earlier than vessels that received none and least paper (treatment 2A and 2B). Temperatures above 55°C caused centrifugal fans to turn on to remove excess heat. The maximum difference between temperatures measured by the upper sensor and lower sensor inside each vessel was as large as 20°C (data not shown) when the average temperature exceeded 55°C and centrifugal fans were actuated, indicating non-uniform conditions within each composting unit. The condition with large temperature difference measured lasted approximately two days. Material in the upper portion received warmer and moister air than that in the lower portion of the units, especially when large air flows were applied. The evaporative cooling and drying experienced by the lower portion during the first 100 h prevented this material from undergoing faster decomposition. A moisture difference existed between the top and the bottom portion in all composting vessels.

The secondary temperature peaks that occurred in some of the vessels (most significant in the paper treatment) were mainly a result of the delayed microbial growth in the lower portion of composting mixture in the vessels, either due to water leached from the top, or lower heat removal rate due to the predominance of smaller, constant aeration rate, or both.

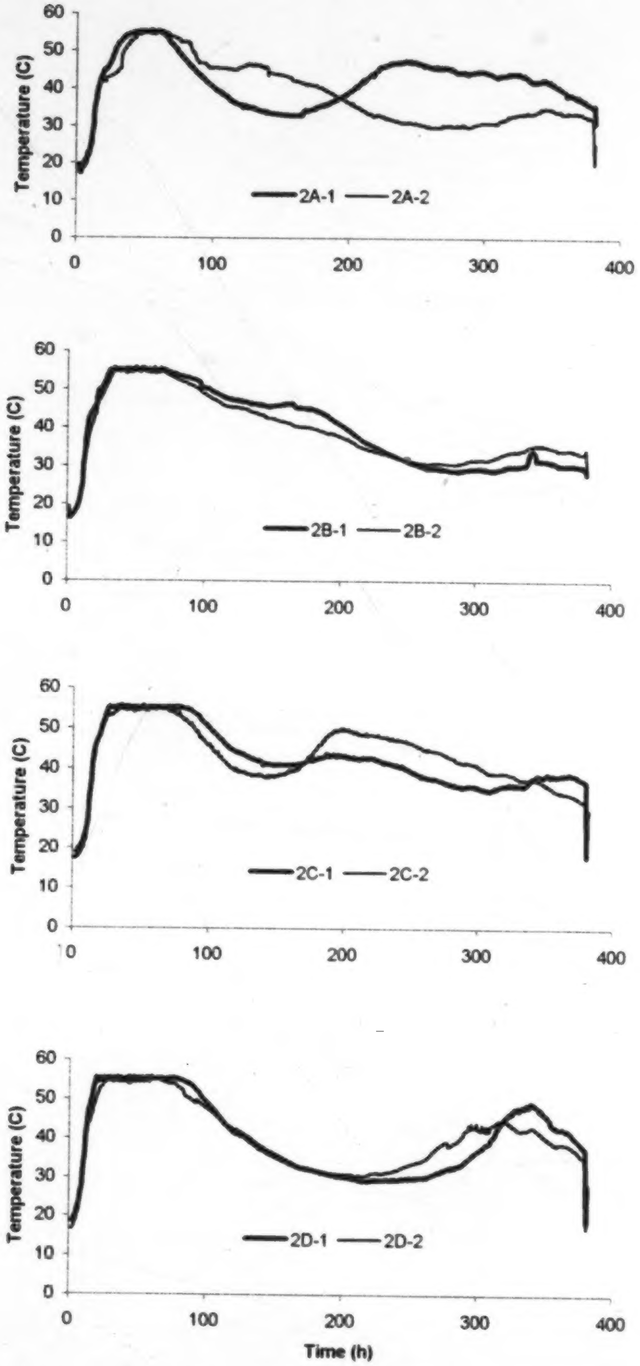

Figure 4.4. Average temperatures with paper treatments (Runs 2A, 2B, 2C and 2D)

4.3.3 Dry Matter Loss

Dry matter loss during composting without any amendments ranged from 38 to 45% (Table 4-12). This organic matter loss is consistent with the normal rage of 35 to 50% (Kithome et al., 1999).

4.3.4 Nitrogen Content

Final N contents were all higher than initial N contents. This was expected since nearly all N loss was less than the reduction in volatile solids due to biooxidation.

Ninety percent of the ammonia loss occurred before 100 h of reaction in all vessels. Hansen et al. (1989) reported that over 85% of total NH_3-N produced occurred during the first 4 days when composting poultry manure and ground corncobs mixtures.

4.3.5 pH

Figure 4-5 shows the pH values measured during Experiment 4 that represented the typical pH change of all experiments. There was a slight increase of pH value in the first one or two days and then a slight decrease afterwards. Although this pattern was typical of the other experiments, Experiment 4 was different from the others in that the treatments with more buffering chemical amendments showed lower initial pH values than those with less or no amendment but they were not significantly different ($P<0.05$).

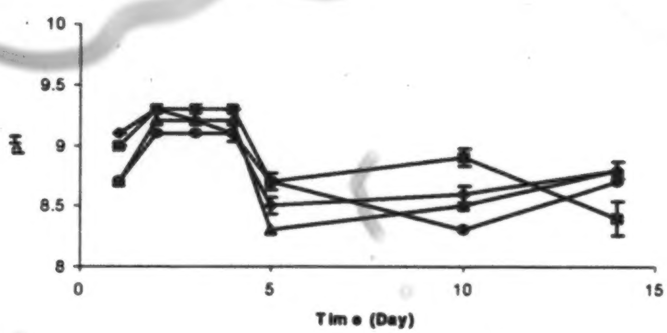

Figure 4-5. pH values of treatments with various amounts of buffer chemicals (Experiment 4). ◆ 4A; ■ 4B; ▲ 4C; ● 4D.

4.3.6 Ammonia Volatilization

All gas emissions were calculated by converting the volumetric concentrations (ppmv) measured by gas analyzers to mass concentrations (kg/m^3) and then multiplying by the ventilation rates to give emission rates (kg/h).

As with temperature, the ammonia emission from all vessels showed similar trends but the total loss varied among different vessels. Graphs of cumulative amounts of ammonia emitted over 300 h from the paper treatments are shown in Figure 4-6.

Most of the ammonia was emitted during the first 100 h and this period coincided with the highest temperatures and greatest amount of aeration. Cumulative ammonia emissions were related to the total ventilation air received by the vessels, as shown in Tables 4-6, 4-7, 4-8 and 4-9.

Cumulative ammonia emissions from vessels that received sucrose at 10% of initial dry matter (by weight) (Treatment 1D) were significantly less ($P<0.05$) than those from vessels that received sucrose at 6.6% of dry weight (Treatment 1C), which in turn were significantly less ($P<0.05$) than those from vessels that received sucrose at 3% of dry weight (Treatment 1B) and the control treatment.

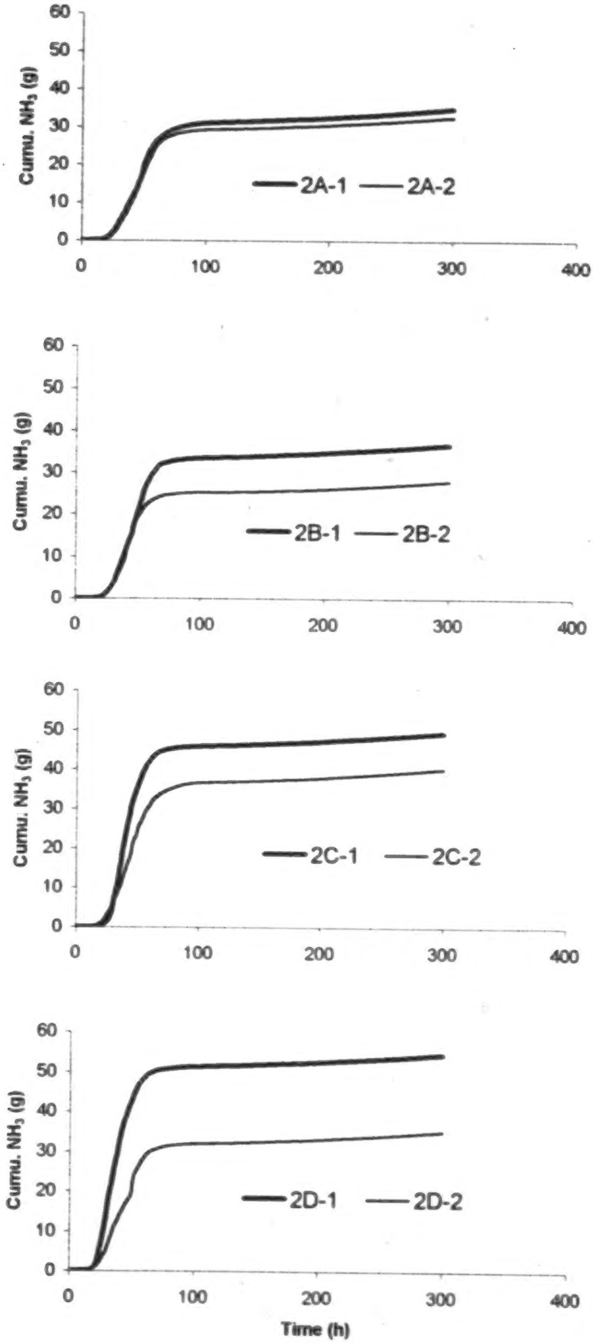

Figure 4.6. Cumulative ammonia emitted from vessels received various amounts of paper. 2A-1,2: None; 2B-1,2: 1.86kg each; 2C-1,2: 3.72kg each; 2D-1,2 5.58kg each.

Table 4-6. Ventilation air received and NH_3 loss during the first 100 h (molasses treatment)

Treatment	*High flow rate time (hour)*	*High flow rate (L/h)*	*Low flow rate time (hour)*	*Total air flow (m^3)*	*Cumulative NH_3 loss at 100th hour (g)*	*Cumulative NH_3 loss average (g)*[*†]
1A-1	8.8	1368	91.2	33.9	51.9	50.9 (±1.41) a
1A-2	7.8	1510	92.2	34.0	49.9	
1B-1	0.9	1212	99.1	24.9	30.4	30.8 (±0.49) b
1B-2	0.7	1368	99.3	24.7	31.1	
1C-1	1.1	1416	98.9	25.2	26.6	27.9 (±1.77) b
1C-2	0	1416	100	24.0	29.1	
1D-1	2.5	1368	97.5	26.5	20.8	21.4 (±0.85) c
1D-2	0.3	1320	99.7	24.3	22.0	

* Standard deviations shown in parenthesis

[†] Letters show multiple comparison. Means with the same letter are not significantly different at $P<0.05$

Table 4-7. Ventilation air received and NH_3 loss during the first 100 h (Paper treatment)

Treatment	*High flow rate time (hour)*	*High flow rate (L/h)*	*Low flow rate time (hour)*	*Total air flow (m^3)*	*Cumulative NH_3 loss at 100th hour (g)*	*Cumulative NH_3 loss average (g)*[* †]
2A-1	2.5	1272	92.6	26.6	31.0	30.1 (±1.27) a
2A-2	2.0	1368	96.7	26.2	29.2	
2B-1	7.4	1368	97.5	32.4	33.4	30.3 (±4.38) a
2B-2	3.3	1368	98.0	27.7	27.2	
2C-1	10.8	1272	89.2	35.2	45.9	41.2 (±6.58) a
2C-2	2.4	1416	97.6	26.8	36.6	
2D-1	14.6	1212	85.6	38.0	51.3	41.6 (±13.72) a
2D-2	2.5	1510	97.5	27.2	31.9	

* Standard deviations shown in parenthesis

[†] Letters show multiple comparison. Means with the same letter are not significantly different at $P<0.05$

Table 4-8. Ventilation air received and NH_3 loss during the first 100 h (Buffer treatment I)

Treatment	*High flow rate time (hour)*	*High flow rate (L/h)*	*Low flow rate time (hour)*	*Total air flow (m^3)*	*Cumulative NH_3 loss at 100th hour (g)*	*Cumulative NH_3 loss average (g)*[* †]
3A-1	15.8	1510	82.2	43.6	49.9	43.8 (±8.70) a
3A-2	6.6	1368	93.4	31.4	37.6	
3B-1	17.2	1212	82.8	41.7	41.3	39.0 (±3.25) a
3B-2	11.9	1272	88.1	36.3	36.7	
3C-1	9.6	1272	90.4	33.9	40.6	35.8 (±6.79) a
3C-2	5.5	1272	94.5	29.7	31.0	
3D-1	14.6	1272	85.4	39.1	41.3	39.8 (±2.19) a
3D-2	12.1	1368	87.9	37.6	38.2	

* Standard deviations shown in parenthesis

[†] Letters show multiple comparison. Means with the same letter are not significantly different at $P<0.05$

Table 4-9. Ventilation air received and NH_3 loss during the first 100 h (Buffer treatment II)

Treatment	*High flow rate time (hour)*	*High flow rate (L/h)*	*Low flow rate time (hour)*	*Total air flow (m^3)*	*Cumulative NH_3 loss at 100th hour (g)*	*Cumulative NH_3 loss average (g)** †
4A-1	9.2	1510	90.8	35.8	35.9	43.2 (±10.32) a
4A-2	29.2	1416	70.8	58.3	50.5	
4B-1	29.4	1272	70.6	54.4	41.8	39.2 (±3.75) a
4B-2	13.4	1510	86.6	41.0	36.5	
4C-1	18.5	1368	81.5	44.8	34.2	28.3 (±8.41) a
4C-2	2.1	1416	97.9	26.6	22.3	
4D-1	4.1	1212	95.9	28.2	31.3	26.8 (±6.36) a
4D-2	0.4	1272	99.6	24.4	22.3	

* Standard deviations shown in parenthesis

† Letters show multiple comparison. Means with the same letter are not significantly different at $P<0.05$

4.3.7 Carbon Dioxide Evolution vs. Ammonia Loss

Total and peak losses of carbon and nitrogen, and aeration demand are shown in Tables 4-10 and 4-11. The peak rate of ammonia nitrogen loss decreased slightly with increased amount of molasses added (Table 4-10), while the ratios of peak carbon to nitrogen loss were higher.

Nitrogen mass balances were constructed from the amounts of N initially present in mixture, NH_3 volatilized, total N in composts at the end of experiments, and the N removed at each sampling interval. Initial N, final N, N loss and NH_3-N emitted/N loss are presented in Table 4-12.

Nitrogen losses ranged from 12.1~24.6% of initial nitrogen contents in all treatments (Table 4-12). In the molasses experiment, nitrogen loss reduced incrementally with increased amounts of molasses (24.6 to 12.1%). In Experiment 3, treatments with buffer amendments (3B, 3C, 3D) showed slightly lower N loss than the one without any buffer amendment. In Experiments 2 and 4, the N losses were similar. Of these nitrogen losses, 60.2 to 99.7% was accounted for as ammonia loss.

Table 4-10. Carbon dioxide and ammonia losses over entire gas measurement time.

Runs	Gas Sampling Period (Day)	CO_2-C Loss Total* (g_C/kg d.s.)	CO_2-C Loss Peak* (g_C/hr.kg d.s.)	NH_3-N Loss Total* (g_N/kg d.s.)	NH_3-N Loss Peak* (g_N/hr.kg d.s.)	$\frac{\text{C Loss}}{\text{N Loss}}$ Total (-)	$\frac{\text{C Loss}}{\text{N Loss}}$ Peak (-)
1A-1	15	149.7	1.51	3.2	0.122	47.2	12.4
1A-2		161.5	1.50	3.1	0.102	52.9	14.6
1B-1		150.2	1.61	1.9	0.063	79.1	25.6
1B-2		138.3	1.61	2.0	0.064	69.8	25.0
1C-1		149.3	1.51	1.7	0.064	87.1	23.7
1C-2		129.4	1.36	1.9	0.052	69.7	26.3
1D-1		110.5	1.20	1.2	0.037	91.4	32.2
1D-2		126.8	1.20	1.3	0.036	100.4	32.9
2A-1	15	102.5	0.92	1.9	0.080	54.2	11.5
2A-2		95.3	0.80	1.8	0.050	54.0	17.4
2B-1		102.9	1.50	2.0	0.080	51.6	18.7
2B-2		84.8	1.23	1.6	0.080	52.1	15.3
2C-1		137.2	1.17	2.7	0.098	50.9	12.0
2C-2		124.5	0.94	2.2	0.060	56.8	15.8
2D-1		133.6	1.17	3.0	0.102	44.7	11.5
2D-2		115.5	1.14	1.9	0.068	60.1	16.8
3A-1	6	97.3	1.53	2.9	0.120	33.8	12.7
3A-2		83.9	1.29	2.2	0.093	37.4	13.9
3B-1		94.8	2.24	2.5	0.120	38.5	18.6
3B-2		79.3	1.35	2.2	0.077	36.7	17.6
3C-1		83.0	1.44	2.4	0.079	33.9	18.2
3C-2		69.2	1.29	1.8	0.066	37.4	19.5
3D-1		83.0	1.66	2.4	0.095	33.9	17.5
3D-2		98.8	1.32	2.3	0.086	42.5	15.4
4A-1	15	117.1	1.42	2.0	0.098	58.0	14.5
4A-2		148.3	1.64	2.8	0.170	53.1	9.7
4B-1		130.8	1.59	2.4	0.100	55.0	15.8
4B-2		127.0	1.43	2.1	0.091	61.7	15.7
4C-1		124.7	2.16	1.9	0.096	64.4	22.5
4C-2		101.3	1.29	1.3	0.046	78.9	27.8
4D-1		80.1	1.36	2.0	0.102	44.0	13.4
4D-2		97.3	0.96	1.3	0.036	74.1	27.1

* kg d.s. represents kg of initial dry solids.

Table 4-11. Carbon dioxide and ammonia losses, and aeration demand in the first 100h of composting.

Runs	CO_2-C Loss (g_C/kg d.s.)*	NH_3-N Loss (g_N/kg d.s.)*	C Loss /N Loss	C Loss/N Loss (Average)	Total Aeration (m^3/kg d.s.)*
1A-1	94.5	3.1	30.6	32.6 (±2.8)	2.4
1A-2	102.4	3.0	34.5		2.5
1B-1	92.9	1.8	51.2	46.9 (±8.1)	1.8
1B-2	79.1	1.9	42.6		1.8
1C-1	97.5	1.6	61.0	51.6 (±13.4)	1.8
1C-2	73.7	1.7	42.1		1.8
1D-1	74.3	1.1	65.3	68.8 (±4.9)	1.8
1D-2	87.0	1.2	72.3		1.6
2A-1	57.5	1.7	34.2	35.2 (±1.5)	1.8
2A-2	57.5	1.6	36.3		1.7
2B-1	70.4	1.8	38.7	37.0 (±2.4)	2.1
2B-2	52.3	1.5	35.3		1.8
2C-1	83.0	2.5	33.1	32.8 (±0.4)	2.3
2C-2	65.0	2.0	32.5		1.8
2D-1	83.0	2.8	29.5	33.3 (±5.4)	2.5
2D-2	65.0	1.8	37.1		1.8
3A-1	97.3	2.9	33.8	36.3 (±3.5)	3.0
3A-2	83.9	2.2	37.4		2.2
3B-1	94.8	2.5	38.5	38.1 (±1.6)	3.0
3B-2	79.3	2.2	36.7		2.6
3C-1	83.0	2.4	33.9	35.8 (±2.2)	2.5
3C-2	69.2	1.8	37.4		2.2
3D-1	83.0	2.4	33.9	38.5 (±6.8)	2.8
3D-2	98.8	2.3	42.5		2.7
4A-1	71.4	2.0	35.0	35.4 (±0.9)	2.4
4A-2	97.0	2.8	33.9		3.9
4B-1	63.5	2.4	26.1	32.5 (±7.9)	3.7
4B-2	78.5	2.1	37.1		2.8
4C-1	77.9	2.0	37.7	43.9 (±7.3)	3.2
4C-2	64.3	1.3	47.1		1.9
4D-1	49.6	1.8	24.9	39.7 (±17.3)	2.0
4D-2	66.8	1.3	49.3		1.7

* kg d.s. represents kg of initial dry solids.

Table 4-12. Comparison of nitrogen loss and NH_3-N emitted.

Treatment	Initial N	Final N	Dry Solid Loss	N Loss[1]	NH_3-N Emitted/ N Loss
	gN/kg init. d.s.	gN/kg final d.s.	%	%	%
1A	15.9	19.5	38.5	24.6	77.3
1B	14.4	19.5	37.3	15.1	84.5
1C	15.5	20.5	36.1	15.5	69.6
1D	13.7	18.5	34.9	12.1	70.6
2A	17.2	26.2	44.8	15.9	60.2
2B	16.6	22.8	38.9	16.1	61.7
2C	15.8	25.2	48.2	17.4	81.9
2D	14.7	21.0	45.0	21.4	72.4
3A	15.9	20.3	38.1	21.0	79.0
3B	15.7	20.6	35.6	15.5	98.1
3C	15.5	20.2	36.1	16.7	76.2
3D	15.5	20.7	36.7	15.5	96.2
4A	16.2	23.0	43.8	20.2	75.5
4B	13.5	19.8	43.5	17.1	99.7
4C	13.1	17.0	34.3	14.7	81.0
4D	12.5	15.0	30.0	16.0	74.1

[1] N loss (%) = 100* (Initial N -(1-dry solid loss)*Final N)/Initial N

4.3.8 Nitrogen Retention

Nitrogen retention was calculated by dividing the N-to-Ash ratio from final compost by the ratio from initial mixture (Table 4-13). N retention in Treatment 1A (82.4±0.5) was significantly lower ($P<0.05$) than Treatment 1B (86.9±0.6). N retention in Treatments 1B, 1C and 1D were numerically different but this difference was not significant ($P<0.05$). N retentions for all treatments in Experiment 2 were not different from each other. No significantly differences ($P<0.05$) in nitrogen retention between treatments were found from either Experiment 3 or Experiment 4.

Table 4-13. Retention of nitrogen.

Treatment	$N_{initial}/Ash_{initial}$	N_{final}/Ash_{final}	N retention % of $N_{initial}$
1A	0.136	0.112	82.4±0.5
1B	0.123	0.107	86.9±0.6
1C	0.129	0.112	86.8±4.9
1D	0.121	0.112	92.6±5.3
2A	0.152	0.125	82.2±0.3
2B	0.131	0.101	77.4±5.0
2C	0.110	0.092	83.6±0.4
2D	0.095	0.078	81.6±5.2
3A	0.128	0.106	82.8±2.9
3B	0.106	0.090	84.9±5.3
3C	0.105	0.096	91.4±2.4
3D	0.102	0.092	90.2±5.4
4A	0.132	0.111	84.1±8.2
4B	0.092	0.077	83.7±2.3
4C	0.076	0.067	88.1±0.4
4D	0.062	0.057	92.6±7.3

4.4 DISCUSSION

4.4.1 General

The initial parts of all temperature curves were typical of laboratory composting processes and indicated that the system was operating satisfactorily. The flow-back of the condensate from the inside of the lids of the vessels after the initial temperature peak may partly explain a resumption of microbial activity, which resulted in the secondary temperature peaks in some vessels. The secondary temperature peaks have been reported by several researchers (Ashbolt and Line, 1982; Shin and Jeong, 1996; Sikora and Sowers, 1985). They were either indicative of a recovered thermophilic microbial population or ascribed to the degradation of cellulose after readily degradable matter is consumed. No substantial difference was observed between treatments with regard to average temperatures in each experiment. This indicated that the additional amendments in all experiments did not have any negative influence on the heating process.

4.4.2 Influence of Aeration on Ammonia Volatilization

It is obvious that vessels receiving more air had larger NH_3-N loss, regardless of the treatments. This is consistent with reports in the literature that ammonia volatilization increased remarkably with the rise of air supply (Beck et al., 1997; Osada et al., 1997). A low airflow results in a reduction of the diffusion of ammonia, generated by the degradation of organic nitrogen, through the materials and leads to a build up of ammoniacal nitrogen in compost (Witter, 1986). On one hand this may result in a reduction in the rate of ammonia loss, on the other hand it increases the opportunity for adsorption of ammonia onto the solid materials and further possible nitrogen immobilization by microbial growth. While aeration provides oxygen to the composting process, it also decreases the carbon dioxide concentrations in the air space in the compost, which is an important factor affecting the equilibrium of the multisolute CO_2-NH_3-H_2O aqueous system. Since organic decomposition under low levels of oxygen may be qualitatively different from that at a higher oxygen concentration, aeration may have an effect on the balance between carbon dioxide and ammonia evolution (Witter, 1986).

Figure 4-7 shows the relationship between NH_3-N loss (g/kg of initial dry solids) and aeration demand for all four experiments. NH_3-N increased linearly (R^2=0.484, n=32) with increasing aeration. Käck (1996), as cited by Beck et al. (1997) found a positive correlation between ammonia volatilization and aeration rate (R^2=0.51) and indicated that aeration was the most important process parameter for ammonia volatilization during composting. Maeda and Matsuda (1997) also reported a linear relationship between ammonia trapped in boric acid as when studying ammonia emission from livestock manure. After converting the x and y variables of our regression equation to the same units as a percentage of initial total nitrogen and air supply (m^3/kg initial mass), the prediction by our equation was more accurate (R=0.743) than theirs (R=0.401). They investigated the ammonia emission conditions with varying C/N ratio from 15 to 45 under various levels of constant aeration, while we carried out our experiments under temperature-response aeration, which resulted in much larger total air supplies in our case.

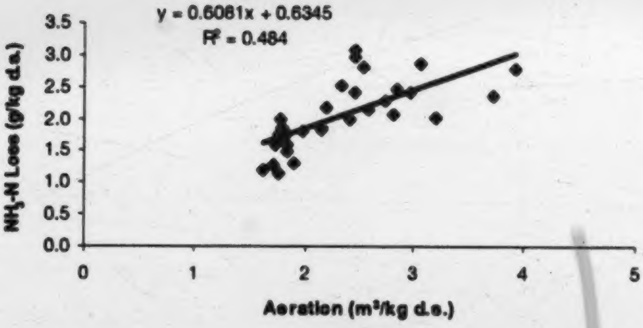

Figure 4-7. Relationship between NH_3-N emitted and aeration demand.

4.4.3 Effect of Carbon Amendments on Ammonia Volatilization

In the molasses treatment, comparison was made among 1B, 1C, and 1D, which received similar total air (24.0-26.5 m^3). The treatments with higher molasses doses had relatively lower ammonia emissions (Table 4-10). N loss was lowest at 12.1% with the most molasses treatment, while the highest N loss was 24.6% with no amendment. This can be explained by vessels with higher molasses having higher microbial availability of carbon, which contributes to the immobilization by micro-organisms and a resultant decreased nitrogen loss. This is supported by the results of Wilson and Hummel (1975) who composted dairy manure and straw with different mixing ratios. Witter (1986) measured an ammonia nitrogen loss with 1% sucrose amendment that was 67% lower than that without amendment. A very labile organic amendment is effective in reducing ammonia volatilization by stimulating microbial activity to work together with some more resistant organic material (Subair, 1995).

The addition of some organic amendments may produce acidic intermediate compounds under metabolism to decrease the pH of the compost mixture so that NH_3 loss can be reduced. This was found by Witter (1986) who observed that, when adding 4% sucrose dry weight to an initial sewage sludge-straw mixture, the composting process halted at 40°C, and the pH had fallen from 7.5 to 4.5. In this experiment, molasses was added at a maximum rate of 10% dry weight of initial mixture, but no significant pH reduction was detected. The reason for the higher pH values may be that an alkaline buffer compound could have been present in the dairy manure used in this experiment.

The ratio of peak carbon loss to peak nitrogen loss increased steadily with increased amount of molasses addition (Table 4-10, from 13.5±1.6 (1A) to 32.5±0.5 (1D)). During peak hours the ratio of approximately 13.5 from no amendment treatment may indicate that mainly proteinaceous materials were under decomposition, while a ratio of 32.5 from the most molasses treatment indicates that the more labile carbon form also underwent decomposition at the initial stage.

The ratio of total carbon loss to nitrogen loss in the molasses experiment increased steadily with increased amounts of molasses addition (from 50.0±4.0 to 95.9±6.3). During microbial growth in aerobic composting, about one-third the carbon utilized by organisms combines with nitrogen in the living cells, while the remaining two-thirds is respired as carbon dioxide (Bishop and Godfrey, 1983). As the cells die and decay as the composting process proceeds, the released nitrogen along with carbon is utilized by other organisms to produce cell protoplasm (Bishop and Godfrey, 1983). Total carbon loss to nitrogen loss ratios of 50 to 96 indicate that the nitrogen was retained and got recycled while the carbonaceous materials went on being reduced due to the loss as carbon dioxide. However, the total CO_2-C loss deceased steadily with increased amounts of molasses addition (from 155.6±8.4 g/kg d.s. (1A) to 118.7±11.5 g/kg d.s. (1D)), indicating that the carbon decomposition from molasses must have occurred at the expense of the decomposition of carbon compounds present in the manure-straw mixture.

The recoveries of nitrogen in Experiment 1 were generally larger than 80% (Table 4-13). A regression of N recovery on C:N ratio of composting materials derived from data in literature indicated that recovery of 80% nitrogen is associated with C:N ratio>25, with higher recovery rates resulting from higher C:N ratios (Janzen et al., 1997). In our experiment, C:N ratio was set at 25:1 by mixing straw with manure. But with higher amounts of molasses added into mixture, C:N ratio were slightly higher from Treatment 1A to Treatment 1D (26 vs. 30). The recovery of more nitrogen from 1D than 1C, 1B or 1A could be associated with either higher C:N ratio, or higher proportion of readily available form of carbon for microbial decomposition, or a combination of both.

In the paper experiment, there were no differences between treatments receiving similar total air (2A-1, 2A-2, 2B-2, 2C-2, 2D-2). However, when all data were pooled together, regardless of the total air supply received, Experiments 2C and 2D, with the medium and most amounts of paper, had significantly higher ($P<0.1$) ammonia losses than Experiments 2A and 2B, with none and the least amount of paper. Peak rates of CO_2 evolution, and total CO_2 losses of the three treatments with paper amendment were similar to the control treatment. When the composting mixtures were placed into the vessels, the volumes occupied by the mixtures were different. The more paper that was added, the smaller volume was occupied by the mixture due to the higher bulk density caused by moist paper. It is possible that the denser structure of the mixture with more paper resulted in more heat accumulation in the initial stage, evidenced by the earlier rise to 55°C in treatment 2C and 2D (Figure 4-4), and therefore encouraged ammonia evolution by earlier high temperatures and more air supplied.

When paper and straw were tested as extra carbon sources in composting food waste, Brink (1995) observed that straw gave good nitrogen retention with various mixing ratios with food while paper retained N when added in smaller amounts but not with larger amounts. Witter (1986) postulated that the addition of cellulose to a sewage-straw mixture appears to have stimulated the decomposition of nitrogenous compounds at the expense of carbonaceous compounds.

The addition of carbon sources had a marked impact on N loss by volatilization (Table 4-11). The amendment of different amounts of molasses in composting materials not only increased the theoretical C:N ratio slightly (26 to 30), but also increased the actual C:N ratio of the organic material available to microorganisms, which was at any time lower than the theoretical (total) C:N value. The organic carbon from lignin in straw was actually unavailable to microbial decomposition during the initial high-rate composting process. Only after the readily degradable substrates are utilized, will the more recalcitrant material be attacked. It has been pointed out that the initial C:N ratio is not a good indicator of the subsequent transformation of the ligno-cellulose residues (Baca et al., 1992).

4.4.4 Effect of Buffering Chemicals on Ammonia Volatilization

The volatilization of ammonia from composting mixtures results from the difference in the partial pressure of ammonia between the air space in the compost and the atmosphere, while the pH can influence the ammonia concentration in the air space by controlling the distribution of ammonia and ammonium concentration in the aqueous phase. Lowering the pH in solution will reduce the ammonia concentration in the aqueous and gas phase, thus reducing volatilization.

The initial pH values of 4C and 4D were slightly lower than those of 4A and 4B. This lasted till the second day, when the ammonia volatilization rate was highest. This may be one of the reasons that reduced total ammonia volatilizations were measured in 4C and 4D (1.3-2.0 gN/kg d.s.) compared with 4A and 4B (2.0-2.8 gN/kg d.s.), although Ekinci et al. (1998) claimed that NH_3-N loss decreased rapidly below pH=7 and increased rapidly for pH above 8. However, the reason why the addition of high doses of buffering material didn't lower the pH of the composting mixture as desired is unclear.

The patterns of ammonia volatilization in treatments of Experiment 4 were not significantly different from each other. Both the ratios of total C losses/N losses and ratios of peak C losses/N losses in the four treatments were similar. The addition of higher amounts of buffer chemicals, aiming at increasing buffer strength in solution, resulted in substantially lower dry matter losses (Table 4-13, 30~34.3% in 4C, 4D compared with 43.5~43.8% in 4A and 4B). The slower decomposition rate in 4C and 4D may have been due to the higher salt content, resulting in high electrical conductivity, causing a different balance of carbon and nitrogen losses than with the faster decomposition rate observed in 4A and 4B.

4.4.5 Ammonia Emitted vs. Nitrogen Loss

In all experiments, NH_3 volatilization losses accounted for 60.2~99.7% of N losses during composting processes. The unaccounted loss represented a larger proportion of initial nitrogen, than the 10.1% reported by Janzen et al. (1997), who carried out their experiments using similar materials and under similar conditions. In an incubation experiment using poultry manure with different amendments under aerobic conditions, an unaccounted loss of approximately 50% of total initial N was found by Mahimairaja et al. (1994). The authors suggested that the unaccounted N loss was due to denitrification, which is a microbial reduction of nitrate and nitrite with the release of nitrous oxide (N_2O) and molecular nitrogen (N_2). This was possibly caused by aerobic nature of certain denitrifying bacteria or the existence of anaerobic microenvironments within the compost due to high moisture. In our study high moisture (>73.0%) and low aeration (4

L/min·vessel) at the mesophilic stage after the first week were the dominant conditions, and denitrification could have occurred.

4.5 LIMITATIONS AND SOURCES OF ERROR

The results reported in this study should be interpreted in terms of the experimental conditions described in Section 4.2. In an attempt to protect the gas analyzers and increase the accuracy of gas concentration readings, a condensate trap was used before off gases were distributed to the three analyzers. The gas stream to the ammonia analyzer was continuously heated and insulated up to the inlet of the analyzer because the desiccant used with other streams (drierite) was reactive with NH_3. A second condensate trap was placed before each desiccant column leading to the CO_2 or O_2 analyzer. The condensate collected was not analyzed because in a composting study using similar materials and mixing ratio under similar experimental configuration, Janzen et al. (1997) reported the dissolved nitrogen in the condensate was less than 1% of the detected NH_3-N. Errors in gas measurements, especially NH_3 and CO_2 gases, could have occurred through this unknown loss, especially in the thermophilic stage when condensate were in high quantity.

However, Sikora and Sowers (1985) reported that condensate from composting a mixture of raw, limed sewage sludge and woodchips contained approximately 80% of the total NH_3 lost. Sikora (1999) determined that the N loss in condensate as 30-40% of the total N lost from the composters in a study of composting immature municipal solid waste compost and dairy manure. Meada and Matsuda (1997) also measured ammonia emission both in the condensate (NH_3-C) and in the boric acid trap (NH_3-B) when composting swine, dairy cattle, and poultry manure separately, mixed with varying amount of sawdust under varying constant aeration. Their data from the successful composting (in terms of achieving desirable thermophilic temperature) showed that NH_3-C contributed at least 60% of total NH_3 emission. If the condensate could have been analyzed in this study, the evolution rates of both ammonia and carbon dioxide would have been higher, possibly at the initial thermophilic stage, which would have led to higher cumulative NH_3 and CO_2 evolution.

4.6 CONCLUSIONS

Nitrogen losses amounted to 12 to 25% of initial nitrogen, of which 90% was lost during peak activity at the early stage. Most of the N losses could be accounted for as ammonia nitrogen. Readily available form of carbon amendment had a marked influence on ammonia volatilization. The treatment received sucrose at a rate of 10% the dry weight of the initial mixture reduced 100% N losses (24.6% vs. 12.1%). The amendment of cellulose didn't have much influence on ammonia volatilization. The lowered pH by the addition of buffering material slightly reduced the N losses. Under the temperature response aeration in this study, the ammonia volatilization was linearly correlated with the total air supply (R=0.696). It indicated that the aeration was a very important process parameter for ammonia volatilization during composting.

4.7 REFERENCES

Ashbolt, N.J. and Line, M.A. 1982. A bench-scale system to study the composting of organic wastes. J. Environ. Qual. 11(3): 405-408.

Baca, M.T., Fornasier, F. and De Nobili, M. 1992. Mineralization and humification pathways in two composting process applied to cotton wastes. J. of Ferment. and Bioeng. 74(3): 179-184.

Barrington, S. F., Choiniere, D., Trigui, M., Wasay, S., Knight and W. 1997. In: J.A. Voermans and G.J. Monteny (Eds), Proceedings of the international symposium. Ammonia and odour control from animal production facilities. p. 579-584. Vinkeloord, The Netherlands.

Beck, J., Käck, M., Hentschel, A., Csehi, K. and Jungbluth, T. 1997. Ammonia emission from composting animal wastes in reactors and windrows. In: J.A. Voermans and G.J. Monteny (Eds), Proceedings of the international symposium. Ammonia and odour control from animal production facilities. p. 381-388. Vinkeloord, The Netherlands.

Bishop, P.L. and Godfrey, C. 1983. Nitrogen transformations during sludge composting. Biocycle 24: 34-39.

Bremner, J.M and Mulvaney, C.S. 1982. Nitrogen-Total. In: A.L. Page. et al. (eds.). Methods of soil analysis, Part 2, 2nd edition, 595-624. Agronomy Series No. 9. Madison, Wisconsin.

Brink, N., 1995. Composting of food waste with straw and other carbon sources for nitrogen catching. Acta. Agric. Scand. Sect. B, Soil and Plant Sci. 45: 118-123.

Carey, D.S., Keener, H.M and Elwell, D.L. 1998. The effect of ammonium sulfate addition to partially composted poultry manure. ASAE paper. No. 98-4099. St. Joseph, MI. 20p.

Ekinci, K., Keener, H.M. and Elwell, D.L. 1998. Composting short paper fiber with broiler litter and additives-alum, Hiclay, alumina and sulfuric acid: I. Effect of initial pH and carbon/nitrogen ratio on ammonia emission. ASAE paper. No. 98-4137. ASAE, St. Joseph, MI. 21p.

Franke, J.O., 1997. Cold climate composting: the influences of sub-zero ambient and ventilating temperatures. M.Sc. Thesis, University of Alberta, Edmonton, AB.

Freney, J.R., Simpson, J.R. and Denmead, O.T. 1983. Volatilization of ammonia. In: J.R Freney and J.R. Simpson (Eds.). Gaseous Loss of Nitrogen from Plant-Soil Systems. Martinus Nijhoff / Dr W. Junk Publishers. Hingham, MA. pp. 1-32.

Hansen, R.C., Keener, H.M., and Hoitink, H.A.J., 1989. Poultry manure composting: Design guidelines for ammonia. ASAE paper, No. 89-4075. ASAE, St. Joseph, MI. 10p.

Janzen, R.A., Feddes, J.J.R., Leonard, J.J. and McGill, W.B. 1997 Composting for resource recovery - strategies to retain nitrogen. In: W.B. McGill (Ed.), Sustainability of Manure Management: Nutrient Retention and Cost-benefit Analysis. p. 93-118. Final Report, CAESA Project RES-056-93. Alberta Agriculture, Food and Rural Development, Edmonton AB.

Käck, M. 1996. Ammoniakemissionen bei der Kompostierung separierter Feststoffe aus Flüssigmist in belüfteten Rottereaktoren. Diss., Hohenheim, Forschungsbericht Agrartechnik, MEG-Nr. 285.

Kithome, M., Paul, J. W. and Bomke. A.A. 1999. Reducing nitrogen losses during simulated composting of poultry manure using absorbents or chemical amendments. J. Environ. Qual. 28: 194-201.

Maeda, T. and Matsuda, J. 1997. Ammonia emission from composting livestock manure. In: J.A. Voermans and G.J. Monteny (Eds.), Proceedings of the international symposium. Ammonia and odour control from animal production facilities. p. 145-153. Vinkeloord, The Netherlands.

Mahimairaja, S., Bolan, N.S., Hedley, M.J., Macgregor, A.N. 1994. Losses and transformation of nitrogen during composting of poultry manure with different amendments: an incubation experiment. Bioresource Technology 47: 265-273.

Meyer, M. and Sticher, H. 1983. The significance of straw content for the retention of nitrogen during the composting of cattle manure. Z. Pflanzenernaehr. Bodenk. 146: 199-206.

Moore, P.A., Jr., Daniel, T.C. Edwards, D.R. and Miller, D.M. 1995. Effect of chemical amendments on ammonia volatilization from poultry litter. J. Environ. Qual. 24:293-300.

Mote, C.R. and Griffis, C.L. 1980. Variation in the composting process for different organic carbon sources. Agricultural Wastes 2: 215-223.

Nakasaki, K., Yaguchi, H. Sasaki, Y. and Kubota, H. 1993. Effects of pH control on composting of garbage. Waste Manage. Res. 11: 117-125.

Okereke, G.U. and Meints, V.W. 1985. Immediate immobilization of labeled NH_4^+ sulfate and urea nitrogen in soils. Soil Sci, 140:105-109.

Osada, T., Kuroda, K. and Yonaga, M. 1997. N_2O, CH_4 and NH_3 emission from composting of swine waste. In: J.A. Voermans and G.J. Monteny (Eds), Proceedings of the international symposium. Ammonia and odour control from animal production facilities. p. 373-380. Vinkeloord, The Netherlands.

SAS. 1999. Version 6.12. Statistical Analysis Systems Institute Inc.

Shin, H. and Jeong, Y. 1996. The degradation of cellulosic fraction in composting of source separated food waste and paper mixture with change of C/N ratio. Environ. Technol. 17: 433-438.

Sikora, L.J. and Sowers, S.E. 1985. Effect of temperature control on the composting process. J. Environ. Qual. 14:434-439.

Subair, S. 1995. Reducing ammonia volatilization from liquid hog manure by using organic amendments. MSc. Thesis. McGill University, Montreal.

Subair, S., Fyles, J.W. and O'Halloran, I.P. 1999. Ammonia volatilization from liquid hog manure amended with paper products in the laboratory. J. Environ. Qual. 28: 202-207.

West, E.S., Todd, W.R., Mason, H.S. and Van Bruggen, J.T. 1966. Textbook of biochemistry. The MacMillan Company, NY.

Willson, G.B. and Hummel, J.W. 1975. Conservation of nitrogen in dairy manure during composting. In: Conf. proc. of 3rd International Symposium on Livestock Wastes. ASAE. St. Joseph, MO.

Witter, E. 1986. The fate of nitrogen during high temperature composting of sewage sludge-straw mixtures. Ph.D. thesis. University of London.

Chapter 5

Performance of a Simulation Model Describing Ammonia Volatilization during Composting

5.1 INTRODUCTION

A mathematical model was developed to simulate compost substrate decomposition and nitrogen loss in the high rate stage of composting (Chapter 2). Mineralization, volatilization and immobilization were the main processes taken into consideration and N loss was assumed to be mainly via gaseous losses, especially ammonia volatilization. A simplified flow chart of the simulation model is presented in Figure 5-1.

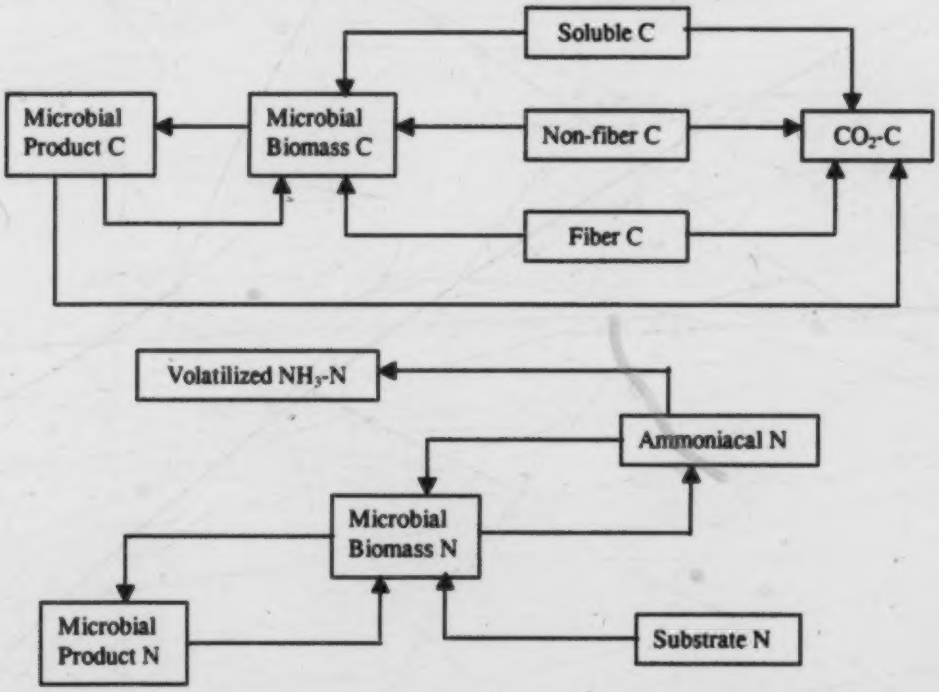
Soluble C
Microbial Product C
Microbial Biomass C
Non-fiber C
CO_2-C
Fiber C
Volatilized NH_3-N
Ammoniacal N
Microbial Biomass N
Microbial Product N
Substrate N

Figure 5-1. Flow chart of C and N transfers in the simulation model (adopted from Chapter 2)

In this model, the carbon was assumed to be present as substrate C, microbial biomass C, microbial product C, and C in respired carbon dioxide (CO_2-C). Similarly, the nitrogen was present as substrate N, microbial biomass N, microbial product N, ammoniacal N in compost solution, and N in volatilized ammonia (NH_3-N). Complex C substrates were represented by three components: Soluble C, Non-fiber C and Fiber C. The partitioning of substrate was based on both the chemical components and different decomposition rates of compost raw materials. Nitrogen was treated as a single variable and was assumed to be associated with, and decomposed at the same rate, as Non-fiber C. The microbial products represented microbial metabolic products and organic materials consisting of dead organisms. The variable of ammoniacal nitrogen in solution accounted for ammonium ions and molecular ammonia associated with the compost solution.

In the development of the model, the growth of the biomass on substrate C was described using Michaelis-Menten kinetics. The three C components were treated as homogenous, independent variables, exhibiting different resistances to microbial decomposition. Oxygen was treated as a rate-limiting factor similar to substrates. Rate of reduction factors for temperature, moisture content and pH were incorporated to correct for sub-optimal environmental conditions. Independent action of these three factors was assumed, and was realized by multiplication. The transfer of microbial biomass C to microbial product C was described using first-order kinetics.

Immobilization describes the rate at which inorganic N (mineral N) is transferred to microbial biomass N. The immobilization of inorganic N by microbes depends on both the concentration of ammoniacal N and the microbial C/N ratio. Mineralization occurs concurrently with immobilization. Ammonia volatilization was related with interstitial carbon dioxide concentration, which itself was influenced by both microbial activity and air exchange rate. This inter-relationship was represented by a CO_2-NH_3-H_2O multisolute aqueous system.

The model demonstrated that ammonia volatilization was associated with substrate composition, temperature, aeration, pH and moisture content. However, in order to check the validity of the model, its performance was tested with a data set obtained by using a laboratory-scale, manure-and-straw composting system (Chapter 4). The model was used: (i) to quantify temperature profiles, carbon dioxide (CO_2) and ammonia (NH_3) evolution; and (ii) to evaluate the effect of different C sources and buffering materials on ammonia volatilization. Two experiments were carried out to investigate the influence of C availability. Molasses and office paper were tested as additional carbon source. The other two experiments were aimed at examining how ammonia volatilization could be controlled by addition of buffering amendments, in which two chemicals forming buffer solution were used.

5.2 MODEL APPLICATION

In the original model (Chapter 2), the heterogeneity of raw materials was accounted for by partitioning the substrate C into three C variables with different associated decomposition parameters. For this study, in order to account for the cellulose content in paper, which was added in one experiment (paper experiment) to replace some of the straw, a major change to the model was the addition of a Cellulose C variable. The

Cellulose C was assumed to decompose independently. Only the cellulose content in paper was considered as the Cellulose C portion.

The initial values of variables for the simulation of different experimental runs are presented in Table 5-1. The values of Soluble C contents were chosen based on the actual results of laboratory analyses on samples from initial mixtures. The nitrogen was calculated on the assumption that 30% of TKN is present as ammoniacal N (NH_3-N and NH_4-N) in cow manure. This was based both on the data presented in Martins and Dewes (1992) and on the fact that approximately 60% to 97% of the total N in animal manure is present in organic forms (Mahimairaja et al., 1990). Of the total nitrogen 40 to 60% is in compounds such as urea and uric acid (Bouldin et al., 1984). Urea nitrogen represents approximately 97% of the total nitrogen in urine from cattle, and can be quickly and easily converted to ammoniacal forms by urease enzymes, possibly within a few hours depending on temperature (Schulte, 1997; Varel, 1997). The remaining 70% of TKN was assumed to be Non-fiber N. Non-fiber C was derived by multiplying the Non-Fiber N value by a ratio of four. The C:N ratio of protein is close to 2.6 (Jakobsen, 1992), and a ratio of four was chosen to account for some other C containing materials that show similar decomposition rate as protein, i.e polysaccharides. Although manure and straw also have cellulose content, Cellulose C was only calculated based on the proportion of paper used in different treatments, because of its significant amount. In the paper treatment, the Volume variable varies since the more paper was added, the smaller the volume that the composting mixture occupied due to the higher bulk density caused by moist paper. The Initial mass, Ash content, Volume and pH are based on actual measurements from the experiments. In the buffer experiment (4A to 4D), greater amounts of buffering materials added resulted in higher ash contents, which caused slightly lower C contents (kg C per kg dry matter).

Table 5-1. Initial variables used in the model

	Experiment Number							
	1A	*1B*	*1C*	*1D*	*2A*	*2B*	*2C*	*2D*
Soluble C†	0.010	0.014	0.018	0.022	0.010	0.012	0.015	0.018
Non-fiber C†	0.0464	0.0448	0.0421	0.0408	0.048	0.0464	0.044	0.040
Cellulose C†	0	0	0	0	0	0.0577	0.1127	0.1667
Fiber C†	0.3600	0.359	0.356	0.3536	0.3622	0.2997	0.2374	0.1763
Ammoniacal N‡	0.0050	0.0048	0.0047	0.0044	0.0051	0.0050	0.0050	0.0050
Non-fiber N‡	0.0116	0.0112	0.0105	0.0102	0.012	0.0116	0.011	0.010
Initial mass (kg)	47	47	47	47	50	50	50	50
Ash Content (%)	12	12	12	12	11.3	12.7	14	15.4
Volume (m^3)	0.137	0.137	0137	0.137	0.137	0.127	0.117	0.107
pH	8.7	8.7	8.7	8.7	8.4	8.4	8.4	8.4

	Experiment Number							
	3A	*3B*	*3C*	*3D*	*4A*	*4B*	*4C*	*4D*
Soluble C†	0.01	0.01	0.01	0.01	0.01	0.01	0.01	0.0091
Non-Fiber C†	0.0464	0.0444	0.0444	0.0444	0.0464	0.0424	0.040	0.0375
Cellulose C†	0	0	0	0	0	0	0	0
Fiber C†	0.3600	0.3486	0.3486	0.3486	0.3600	0.3533	0.344	0.3326
Ammoniacal N‡	0.0044	0.0044	0.0044	0.0044	0.0044	0.0044	0.0042	0.0040
Non-Fiber N‡	0.0116	0.0111	0.0111	0.0111	0.0116	0.0105	0.0100	0.0094
Initial mass (kg)	47	47	47	47	50.0	50.5	51.0	51.5
Ash Content (%)	12	15	15	15	12.0	14.5	17.0	20.0
Volume (m^3)	0.137	0.137	0.137	0.137	0.137	0.137	0.137	0.137
pH	8.6	8.6	8.6	8.9	9.1	9.0	8.7	8.7

† Unit of $kg_C\ kg^{-1}$ initial dry matter
‡ Unit of $kg_N\ kg^{-1}$ initial dry matter

Table 5-2 shows the values of other parameters used in the model. Most of these are the same as those outlined in Chapter 2. However, the Maximal growth rates and Microbial maintenance coefficients of μ_{maxi}, β_{maxi} were decreased by 20% to account for the large composting mass and the consequent non-uniform decomposition within the vessels, especially along the depth.

Table 5-2. Parameters used in the model.

Symbol	*Parameter description*	*Value*	*Units*
$\mu_{max,1}$	Maximal growth rate on Soluble C	0.40	h^{-1}
$\mu_{max,2}$	Maximal growth rate on Non-fiber C	0.40	h^{-1}
$\mu_{max,3}$	Maximal growth rate on Cellulose C	0.03	h^{-1}
$\mu_{max,4}$	Maximal growth rate on Fiber C	0.03	h^{-1}
$\beta_{max,1}$	Microbial maintenance coefficient on Soluble C	0.064	h^{-1}
$\beta_{max,2}$	Microbial maintenance coefficient on Non-fiber C	0.064	h^{-1}
$\beta_{max,3}$	Microbial maintenance coefficient on Cellulose C	0.0048	h^{-1}
$\beta_{max,4}$	Microbial maintenance coefficient on Fiber C	0.0048	h^{-1}
$K_{S,1}$	Half saturation constant for Soluble C	0.05	$kg\ kg^{-1}_{DM}$
$K_{S,2}$	Half saturation constant for Non-fiber C	0.17	$kg\ kg^{-1}_{DM}$
$K_{S,3}$	Half saturation constant for Cellulose C	0.10	$kg\ kg^{-1}_{DM}$
$K_{S,4}$	Half saturation constant for Fiber C	0.40	$kg\ kg^{-1}_{DM}$
K_{O2}	Half saturation constant for oxygen	0.00003	$kg\ kg^{-1}_{DM}$
δ	Microbial death rate	0.025	h^{-1}
k_p	Rate constant for microbial uptake of Product C	0.002	h^{-1}
$Y_{X/SC}$	Yield coefficient of biomass from Soluble C	0.35	$kg_X\ kg^{-1}_C$
$Y_{X/PC}$	Yield coefficient of biomass from Non-fiber C	0.35	$kg_X\ kg^{-1}_C$
$Y_{X/CC}$	Yield coefficient of biomass from Cellulose C	0.3	$kg_X\ kg^{-1}_C$
$Y_{X/FC}$	Yield coefficient of biomass from Fiber C	0.3	$kg_X\ kg^{-1}_C$
$Y_{X/P}$	Yield coefficient of biomass from Product C	0.35	$kg_X\ kg^{-1}_C$
$Y_{W/S}$	Conversion factor	0.56	$kg\ H_2O\ kg^{-1}_S$
$Y_{O2/S}$	Conversion factor	1.37	$kg\ O_2\ kg^{-1}_S$
$Y_{H/S}$	Conversion factor	19100	$kJ\ kg^{-1}_S$

The model was run for a simulated time of 200h and time step of 0.01h with the initial conditions and parameter values detailed in Tables 5-1 and 5-2. The outputs from the model (temperature, CO_2 and NH_3 emission, etc.) were compared with data obtained from the laboratory experiments described in Chapter 4.

5.3 RESULTS

Temperature

Figures 5-2 (a, b, c) shows the comparison of model outputs and experimental data of temperature in the paper, buffer I and buffer II experiments. Complete temperature data for molasses experiment are not available due to a hardware malfunction at 60 h of running that caused errors in all temperature readings from the lower sensors in all eight vessels.

The model output was in close agreement with the experimental temperature profiles. The readily degradable substrate was decomposed initially followed by the more resistant cellulose and fiber material, represented by the raised temperature of over 55°C between 25 to 70 h, and rapid decline afterwards. Temperatures of model outputs before 50h exceeded 55°C for a short period. These high temperatures result from the fast decomposition of compost substrate and cause a continuous high air flow to be applied in the model. The second temperature peak observed experimentally was not predicted by the model.

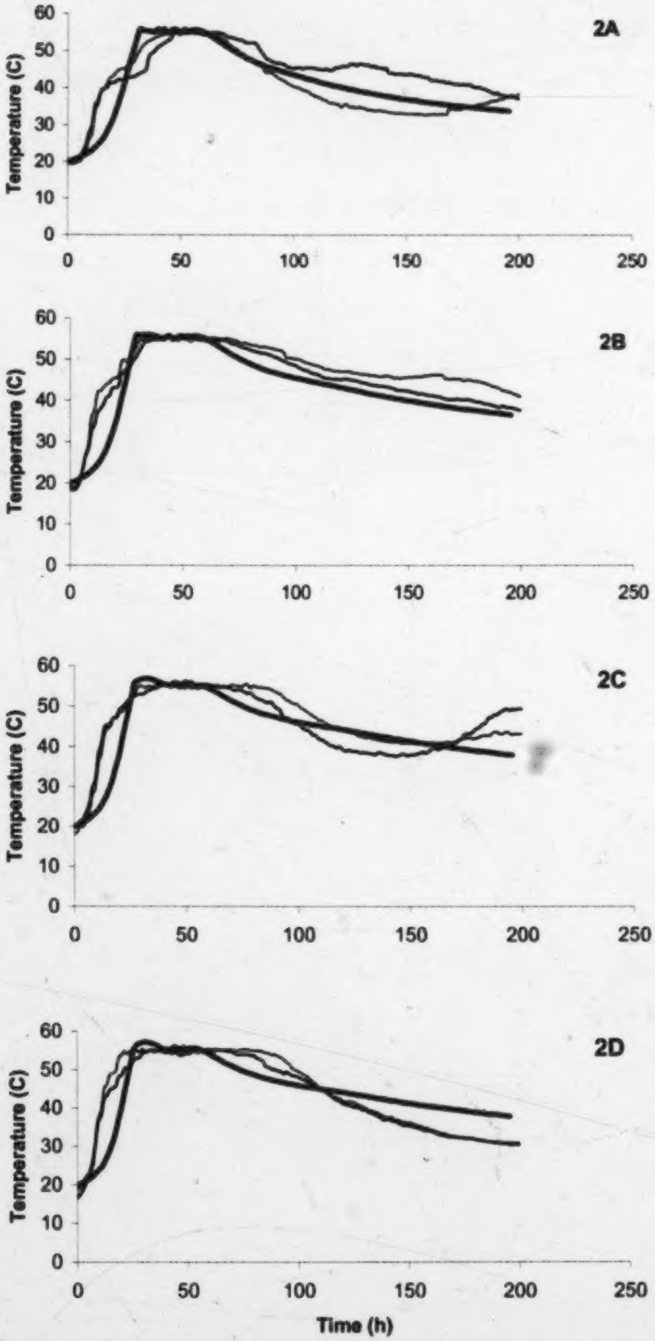

Figure 5.2a Model output (thick line) and experimental data (thin lines) for temperature in paper experiment

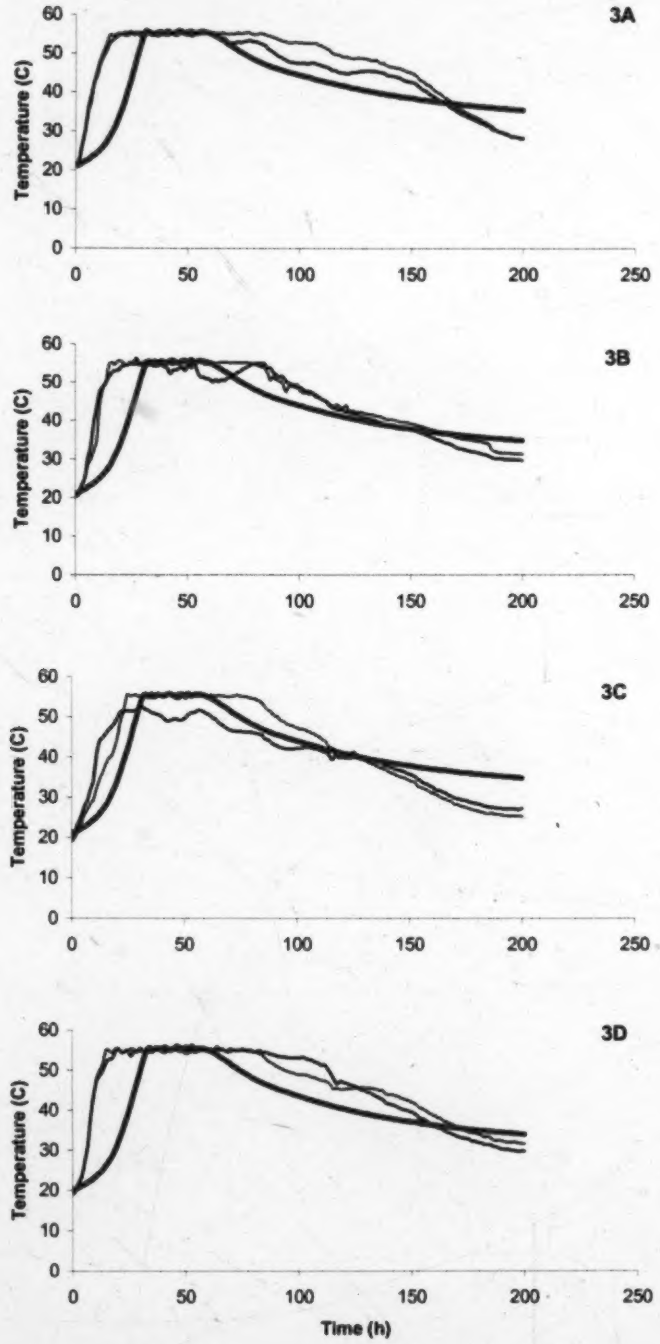

Figure 5.2b. Model output (thick line) and experimental data (thin lines) for temperature in buffer I experiment

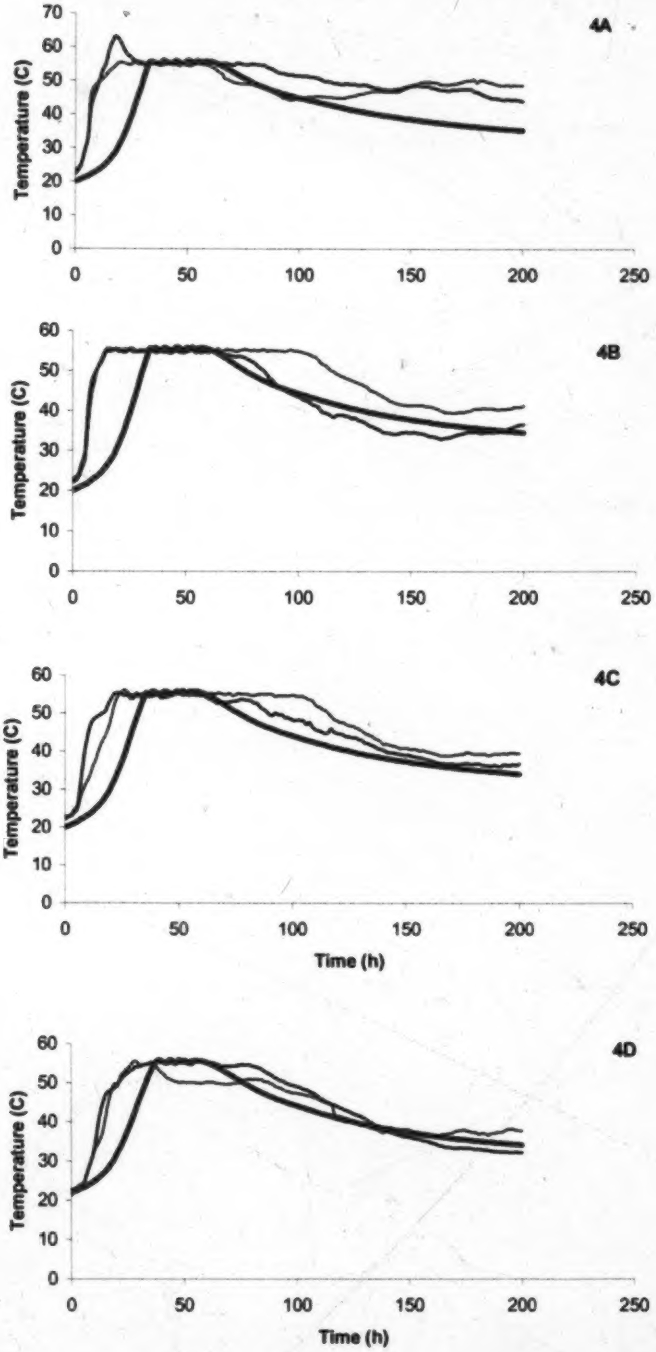

Figure 5.2c. Model output (thick line) and experimental data (thin lines) for temperature in buffer II experiment

Average temperatures of Experiments 1 to 4 and the model outputs are presented in Table 5-3. Average temperature, derived by summing the recorded temperatures for each compost vessel in a specific range and dividing by the number of records, can reflect substrate availability and heat retention, particularly within the thermophilic stage. Simulated average temperatures in the paper treatments were close to the experimental measurements. Simulated average temperatures in both buffer experiments were up to 14% lower than the experimental measurements. Generally, the model output is in good agreement with experimental data with regard to the temperature in all vessels.

Table 5-3. Average temperatures of experimental data and model outputs at 200h (°C)

	Experimental		Simulated		Experimental		Simulated
1A-1	-		41.7	2A-1	40.7	(42.8)	41.4
1A-2	-			2A-2	44.8		
1B-1	-		41.0	2B-1	47.5	(46.5)	43.3
1B-2	-			2B-2	45.4		
1C-1	-		42.0	2C-1	46.5	(46.0)	44.3
1C-2	-			2C-2	45.5		
1D-1	-		42.5	2D-1	43.9	(43.5)	44.3
1D-2	-			2D-2	43.0		

	Experimental		Simulated		Experimental		Simulated
3A-1	47.3	(46.5)	41.7	4A-1	48.3	(48.3)	42.2
3A-2	45.6			4A-2	48.3		
3B-1	45.1	(44.6)	41.3	4B-1	47.1	(44.8)	41.7
3B-2	44.0			4B-2	42.5		
3C-1	41.8	(41.1)	41.3	4C-1	45.4	(44.6)	41.3
3C-2	40.3			4C-2	43.7		
3D-1	46.1	(46.0)	41.3	4D-1	42.0	(41.8)	40.7
3D-2	45.9			4D-2	41.6		

Note: Values in parenthesis are averages of two replicates of each treatment

The final moisture contents in the simulation were approximately 2% higher than their initial values (data not shown). This agrees with the fact that the final dry matter contents measured in experiments were always 3-5% lower than their initial dry matter contents (Chapter 4, Tables 4-3, 4-4).

Carbon Dioxide Evolution

Comparisons of model outputs and experimental data of carbon dioxide evolution in all experiments are shown in Figures 5-3, 5-4, 5-5 and 5-6. Comparisons of carbon dioxide evolutions at 200 h (except where otherwise mentioned) are also shown in Table 5-4.

Table 5-4. Cumulative carbon dioxide evolutions (g) of experimental data and model outputs at 200h

	Experimental		Simulated	Error+		Experimental		Simulated	Error+
1A-1	5555	(5734)	3961	30.9%	2A-1	3567	(3601)	4311	-19.7%
1A-2	5912				2A-2	3634			
1B-1	5618	(5229)	4143	20.8%	2B-1	4367	(3811)	4334	-13.7%
1B-2	4840				2B-2	3254			
1C-1	5470	(4940)	4218	14.6%	2C-1	5218	(4787)	5008	- 4.6%
1C-2	4410				2C-2	4356			
1D-1	4565	(5029)	4363	13.2%	2D-1	5141	(4654)	4989	- 7.2%
1D-2	5490				2D-2	3999			

	Experimental*		Simulated*	Error+		Experimental		Simulated	Error+
3A-1	5088	(4732)	3393	28.3%	4A-1	4563	(5374)	4175	22.3%
3A-2	4377				4A-2	6186			
3B-1	4913	(4518)	3263	27.8%	4B-1	5039	(4827)	3939	18.4%
3B-2	4122				4B-2	4615			
3C-1	4297	(3945)	3263	17.3%	4C-1	4438	(4054)	3800	6.3%
3C-2	3594				4C-2	3671			
3D-1	4226	(4630)	3263	29.5%	4D-1	3177	(3481)	3570	- 2.6%
3D-2	5033				4D-2	3786			

Note: Values in parenthesis are averages of two replicates of each treatment
*Numbers shown are at 143h when carbon dioxide analyzer malfunctioning
+Error = (Mean experimental value – model value)/ Mean experimental value * 100

The carbon dioxide evolutions of model outputs are in trend with the experimental data in all experiments. However, some differences can be seen in the molasses and both buffer experiments. In molasses and both buffer experiments, the carbon dioxide evolution rates (slopes of the curves) from model outputs after 60h closely match those from experiments in most of the treatments, but deviate at the beginning. For example, in experiments 1A, 3A, 3B, 3D, 4A, 4B, simulated carbon dioxide evolution rates were lower than the measurements in the first 25 h, which were possibly caused by the prediction of lagged substrate decomposition, represented by lagged temperature rises. The slopes of the predicted curves caught up the experimental data afterwards, mainly resulting from some temperature overshoot at this stage. The errors between the model values and the experimental values are within –20% to 31%. Generally, the model predicted well the CO_2 production during the high rate period.

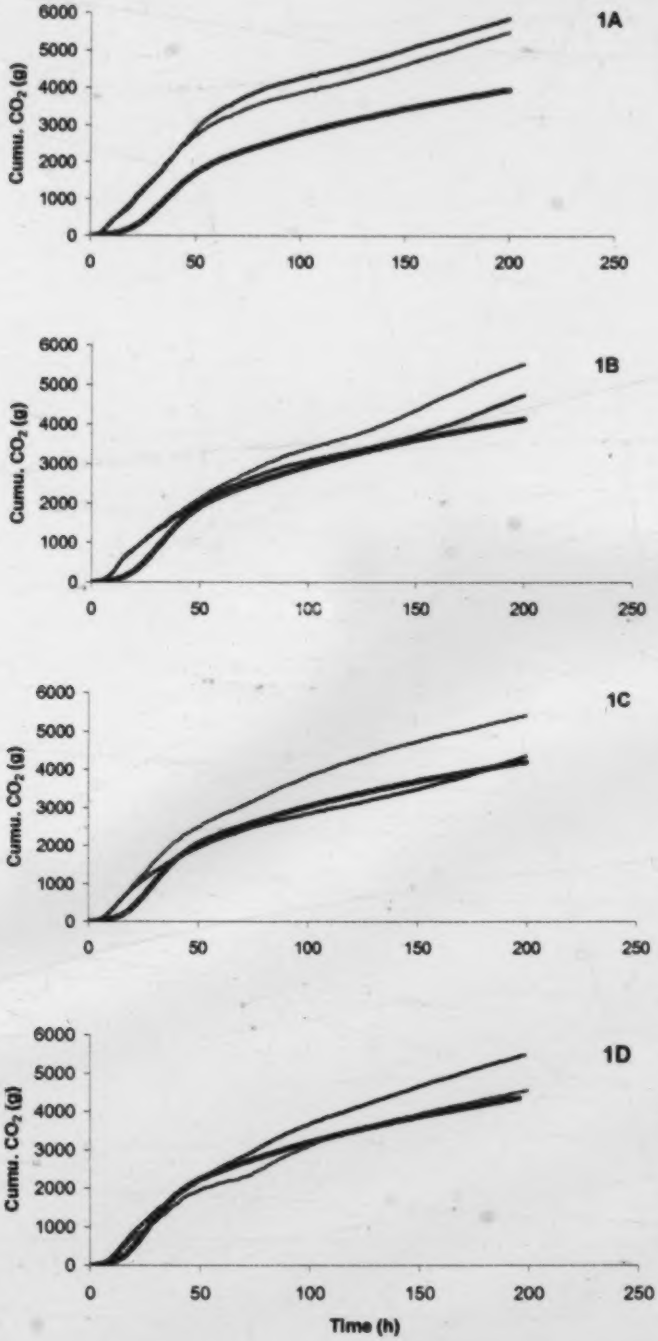

Figure 5.3. Model output (thick line) and experimental data (thin lines) for CO_2 evolution in **molasses** experiment

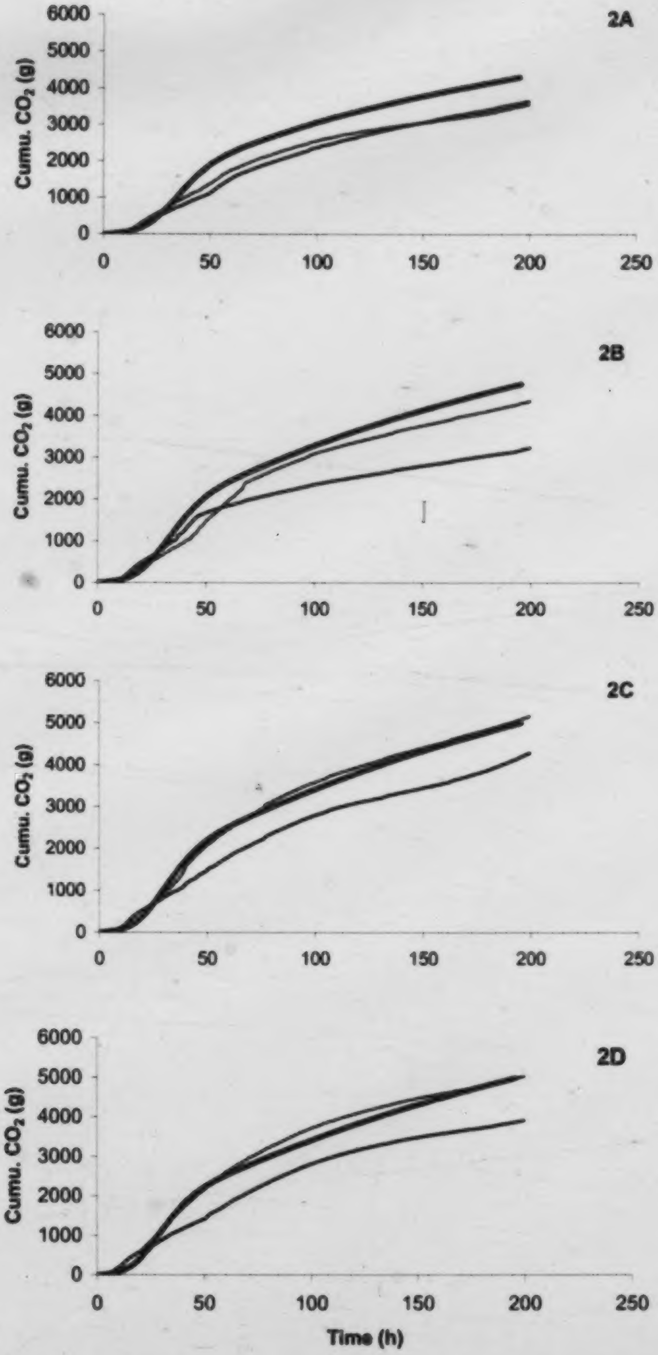

Figure 5.4. Model output (thick line) and experimental data (thin lines) for CO$_2$ evolution in **paper** experiment

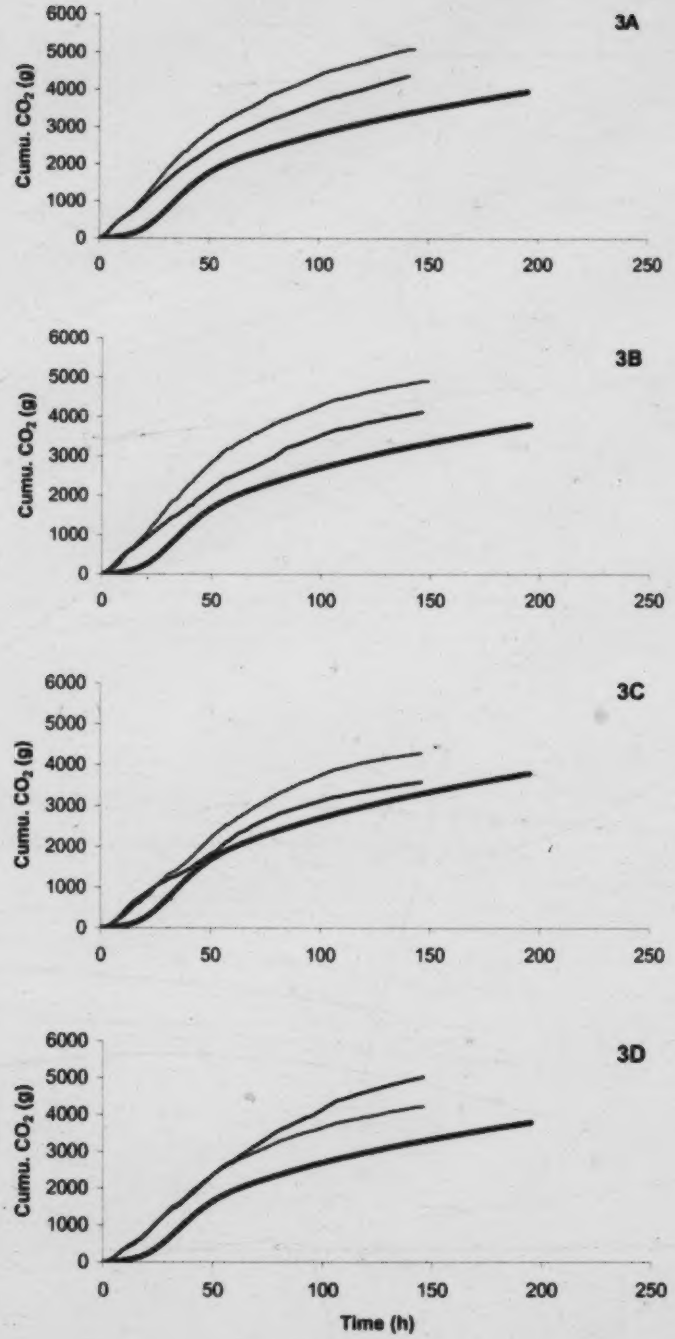

Figure 5.5. Model output (thick line) and experimental data (thin lines) for CO_2 evolution in **Buffer I** experiment

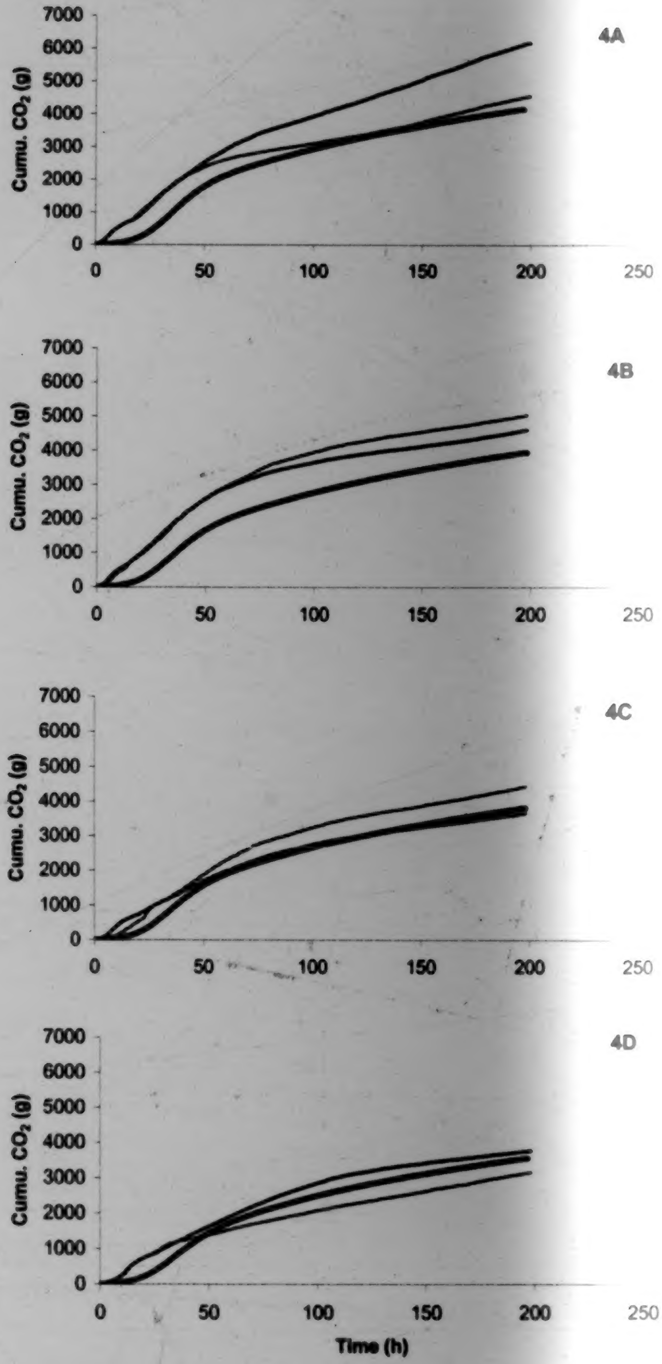

Figure 5.6. Model output (thick line) and experimental data (thin lines) for CO$_2$ evolution in Buffer II experiment

Aeration

The timing of the cooling-fan-on period predicted by the model were in agreement with the experimental measurements, as seen in Figures 5-2 (a, b and c). Model outputs are compared to experimental data with regard to cooling-fan-on time in Table 5-5. Cooling-fan-on time represents the time during which high aeration flow was actuated. The reason that the cooling-fan-on time of experimental measurements from buffer treatments were generally higher than those from molasses and paper experiments lies in the adjustment of sensor location. In molasses and paper experiments, the temperature sensors were pushed all the way into the composting materials and resulted in possibly exposure of the lower sensors to the ventilation plenum at the bottom of the composters. Later adjustment was made to leave approximately 15 cm distance for the lower sensors when pushing the temperature sensors in the buffer experiments, to make sure that they were covered by the composting materials. This led to higher average temperature readings in the two buffer experiments, resulting in longer cooling-fan-on time.

Table 5-5. Cooling-fan-on time (h) of experimental data and model output

	Experimental		Simulated		Experimental		Simulated
1A-1	8.8	(8.3)	13.5	2A-1	2.5	(2.3)	15.0
1A-2	7.8			2A-2	2.0		
1B-1	0.9	(0.8)	15.2	2B-1	7.4	(5.4)	17.7
1B-2	0.7			2B-2	3.3		
1C-1	1.1	(0.5)	16.4	2C-1	10.8	(6.6)	19.2
1C-2	0			2C-2	2.4		
1D-1	2.5	(1.4)	18.3	2D-1	14.6	(8.6)	18.2
1D-2	0.3			2D-2	2.5		

	Experimental		Simulated		Experimental		Simulated
3A-1	15.8	(11.3)	14.6	4A-1	33.3	(21.0)	14.7
3A-2	6.7			4A-2	8.7		
3B-1	17.2	(17.2)	11.9	4B-1	19.7	(16.6)	10.0
3B-2	17.1			4B-2	13.4		
3C-1	9.6	(7.6)	11.9	4C-1	18.6	(10.4)	7.5
3C-2	5.5			4C-2	2.1		
3D-1	14.6	(13.4)	11.1	4D-1	4.1	(2.3)	4.6
3D-2	12.1			4D-2	0.4		

Note: Values in parenthesis are averages of two replicates of each treatment

In molasses and paper experiments, the experimental records of cooling-fan-on time were substantially lower than the simulated values. Measurements of Treatments 1B, 1C and 1D were at least one magnitude lower than those of the simulations. In buffer experiments, the model outputs are more close to the experimental data.

Ammonia Emission

In the molasses treatment, simulation results of ammonia emission show similar trends but a slight decrease with increasing amount of molasses, as illustrated in Figure 5-7. NH_3-N losses increased with time but the rates of losses decreased with time.

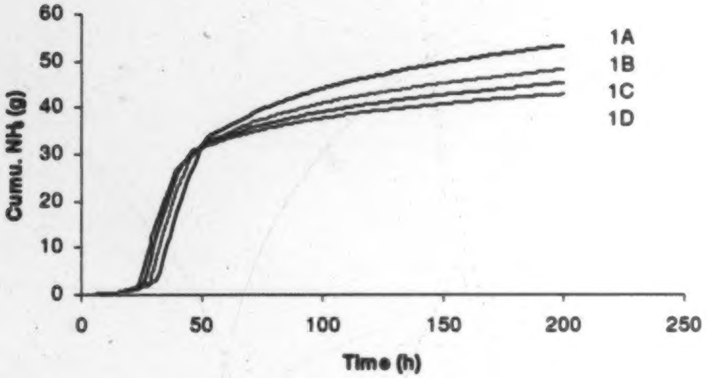

Figure 5-7. Simulation outputs of ammonia emission from **molasses** experiment. 1A: no molasses; 1B, 1C, 1D: increased molasses.

However, the difference of measured ammonia emission from four treatments were significantly different ($P<0.05$, Chapter 4). This results in fairly large discrepancies in the comparison of simulation outputs and experimental data as seen in Figure 5-8. The simulated curve of Treatment 1A matched the measurements quite well for the first 60 hours and then the rates of losses in the simulation exceeded those from measurements (Figure 5-8, 1A). In all other treatments (1B, 1C and 1D), the simulated results were always higher than the experimental data. In these treatments, the simulated emission rates between 20 to 60 h were much higher than those from the experiment.

In the **paper** experiment, the simulation outputs for all four treatments are very similar, as shown in Figure 5-9 (53~58 g). The slopes in the initial high rate period (20~60 h) in treatments 2C and 2D matched the experimental data closely, while those in treatments 2A and 2B are larger than the experimental measurements. The slopes after 60 h are generally higher in the simulation results. The simulated cumulative ammonia emissions after 200 h are approximately twice as large as the measurements in Treatments 2A and 2B (Figure 5-9 2A, 2B).

The comparison of model outputs and experimental data for ammonia emissions in the **buffer I** experiment is shown in Figure 5-10. The simulation results (four thick lines) are similar for all treatments due to the similar variables used in simulation (Table 5-1), based on similar composition of raw materials and similar initial pH values measured. There are slight differences between simulation and measurements, mainly because the simulated ammonia emissions lagged several hours in the initial stage (<60 h).

Figure 5-11 shows the comparison of model outputs and experimental data for ammonia emissions in the **buffer II** experiment. The curves matched the experimental data quite well in most treatments. It is obvious that the ammonia emissions decrease steadily from treatments 4A to 4B, 4C and 4D in the simulation (52~33 g).

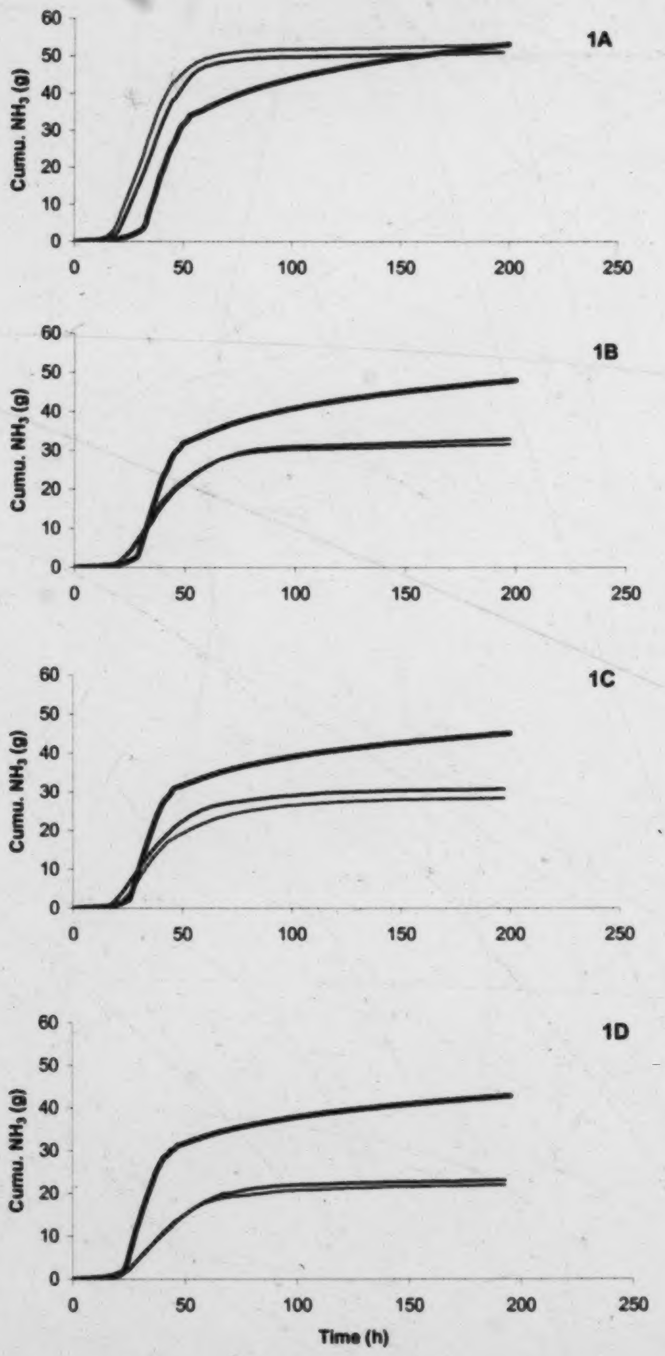

Figure 5.8. Model output (thick line) and experimental data (thin lines) for NH_3 emission in **molasses** experiment

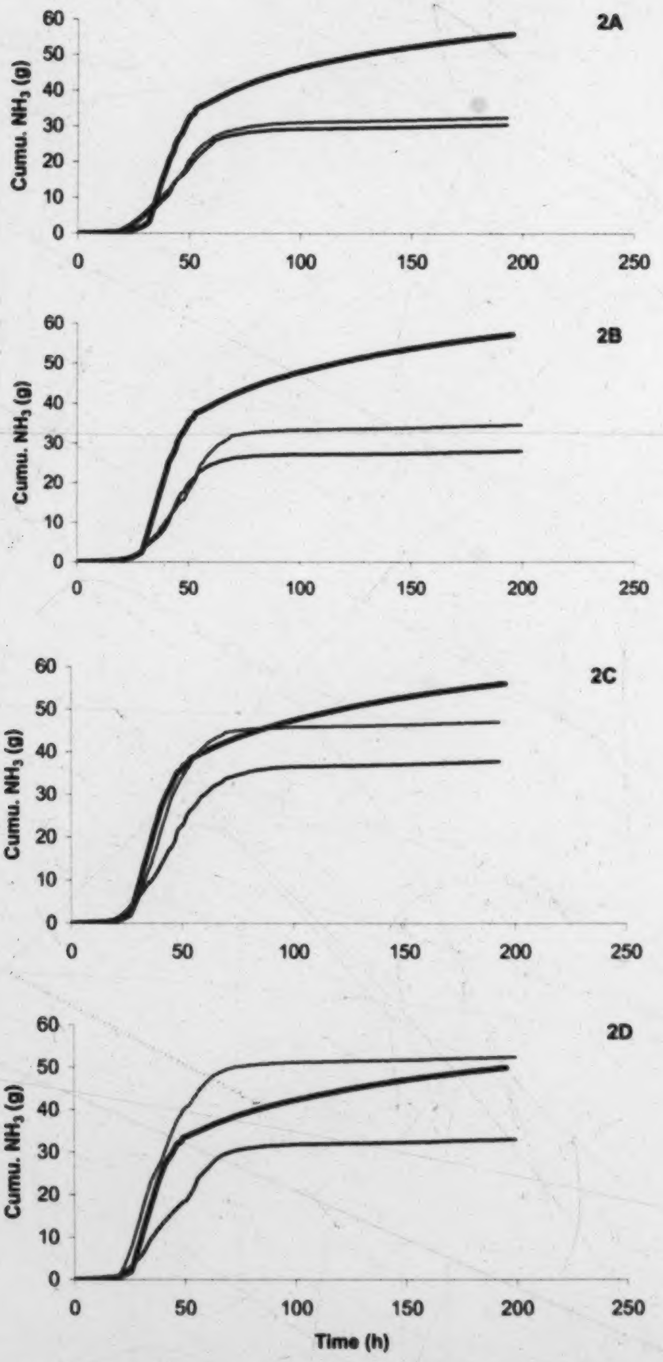

Figure 5.9. Model output (thick line) and experimental data (thin lines) for NH$_3$ emission in **paper** experiment

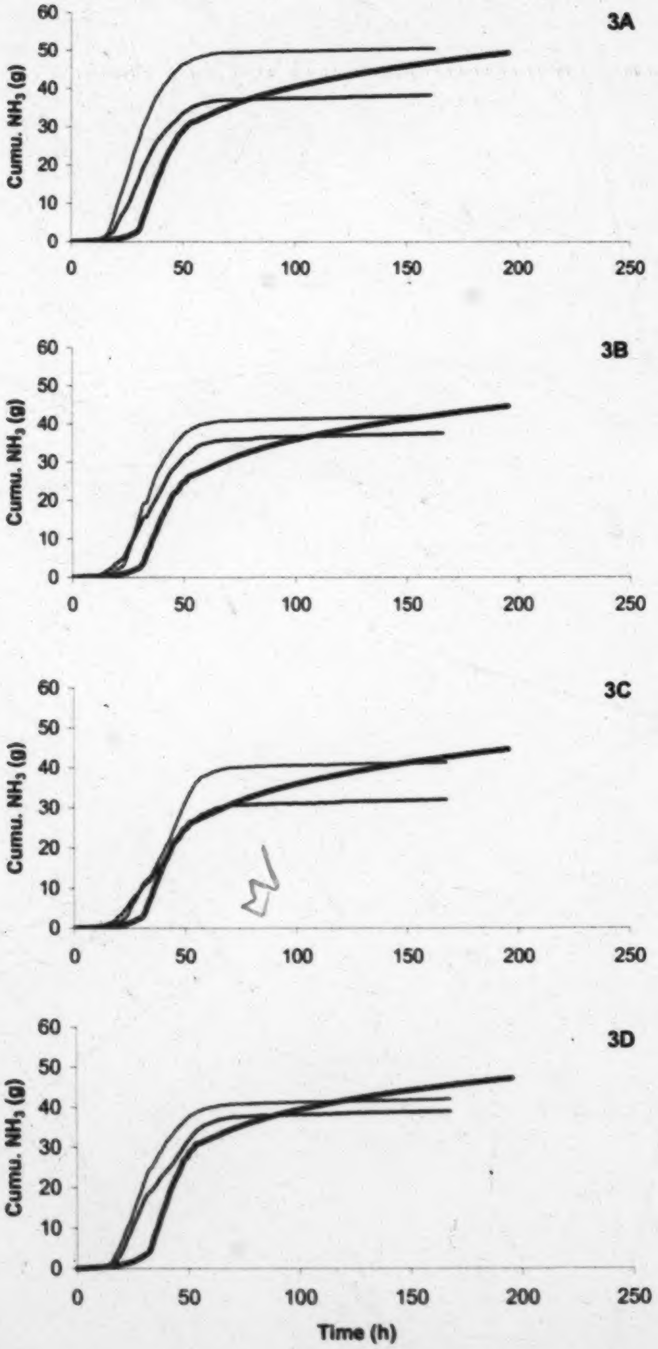

Figure 5.10. Model output (thick line) and experimental data (thin lines) for NH_3 emission in **buffer I** experiment

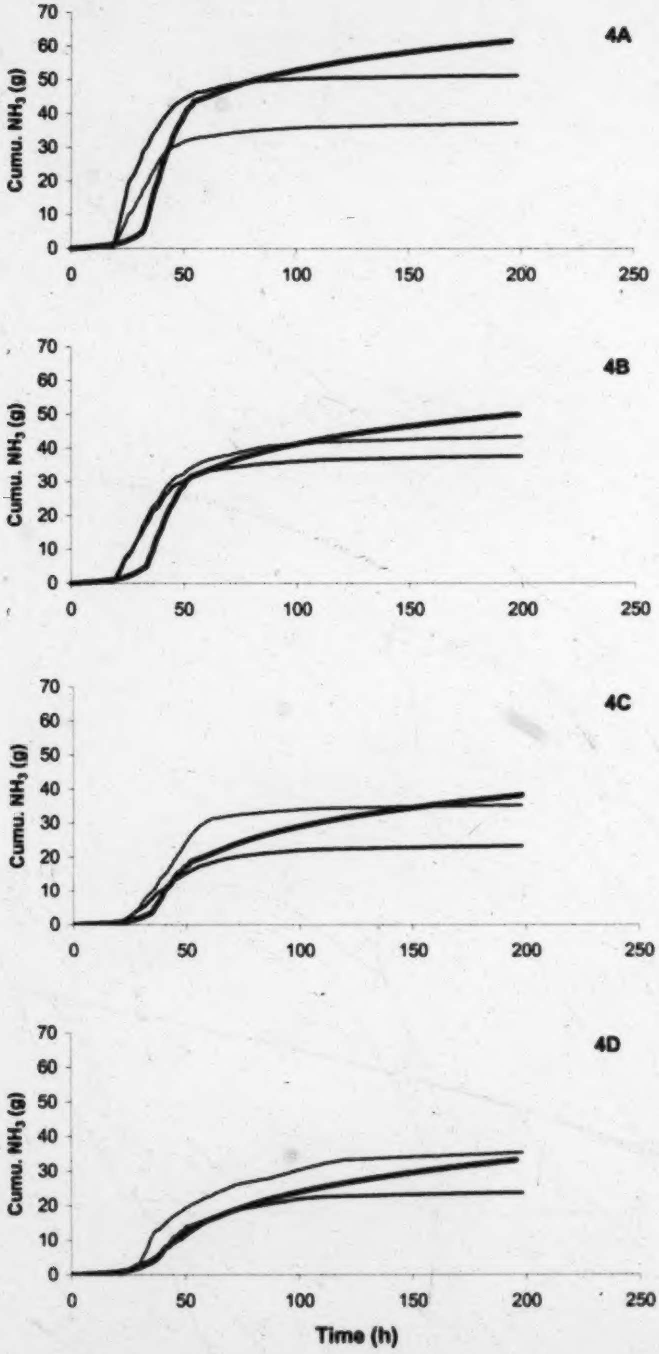

Figure 5.11. Model output (thick line) and experimental data (thin lines) for NH_3 emission in buffer II experiment

The cumulative ammonia emissions at 200 h are also summarized in Table 5-6. The difference between simulation and experimental values vary from –2% (1B) to –90% (1D).

Table 5-6 Ammonia emissions (g) of experimental data and model outputs at 200 h

	Experimental		Simulated	Error+		Experimental		Simulated	Error+
1A-1	53.2	(52.2)	53.3	- 2.1%	2A-1	32.4	(31.4)	56.0	-78.3%
1A-2	51.2				2A-2	30.4			
1B-1	31.7	(32.3)	48.1	-48.9%	2B-1	34.7	(31.4)	57.3	-82.5%
1B-2	32.9				2B-2	28.0			
1C-1	28.4	(29.6)	45.2	-52.7%	2C-1	47.1	(42.5)	56.1	-32.0%
1C-2	30.8				2C-2	37.8			
1D-1	22.1	(22.6)	42.9	-89.8%	2D-1	52.4	(42.7)	49.9	-16.9%
1D-2	23.0				2D-2	33.0			

	Experimental*		Simulated*	Error+		Experimental		Simulated	Error+
3A-1	50.7	(44.6)	47.2	- 5.8%	4A-1	37.3	(44.4)	61.7	-39.0%
3A-2	38.4				4A-2	51.4			
3B-1	42.1	(39.9)	42.3	- 6.0%	4B-1	43.5	(40.6)	50.0	-23.2%
3B-2	37.6				4B-2	37.7			
3C-1	41.4	(36.8)	42.3	-14.9%	4C-1	35.4	(29.4)	38.2	-29.9%
3C-2	32.1				4C-2	23.4			
3D-1	42.1	(40.6)	43.7	- 7.6%	4D-1	35.4	(29.6)	33.3	-12.5%
3D-2	39.1				4D-2	23.8			

Note: Values in parenthesis are averages of two replicates of each treatment
*Numbers shown are at 143h when carbon dioxide analyzer malfunctioning
+Error = (Mean experimental value – model value)/ Mean experimental value * 100

pH

pH measurements were carried out at the beginning and end of the molasses and paper experiments and so experimental data of pH variation with time are not available for these cases. However, simulation outputs of pH values from Treatment 4A in the Buffer II experiment are compared with experimental measurements in Figure 5-12. Simulated pH values were generally lower than the measurements in all treatments (4A–4D) (data not shown). The initial increase of pH was not predicted in the model.

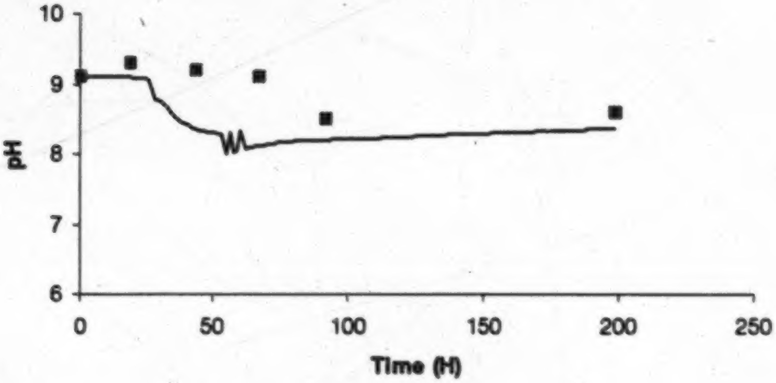

Figure 5-12. Comparison of model outputs (line) and experimental data (symbols) for pH from Treatment 4A in buffer II experiment

5.4 DISCUSSIONS

5.4.1 Limitations

The data collected using a laboratory-scale composting system (Chapter 4) were used to validate the model, by comparing temperature profiles, carbon dioxide evolutions and ammonia emissions. A large variability existed in the experimental data. For example, the cumulative carbon dioxide evolutions from all control treatments (totally eight vessels) up to 200 h (Table 5.4, 1A-1, 1A-2, 2A-1, 2A-2, 3A-1, 3A-2, 4A-1, 4A-2) varied from 3567 ~ 6186 g. A slight weight difference between the total initial materials used (47 ~ 51 kg) couldn't have resulted in the large variation. The variation could have resulted from a series of sources. First, the dairy manure was collected separately prior to each experiment. The physical and chemical properties can be slightly different. Even within the same bulk material, each mixing load can consist of manure with different moisture content and lumpiness, which could further influence the mixability and then the homogeneity of the mixture among vessels. Secondly, the loading density of the mixture in the composting vessels could be different due to the large volume of straw used and the bulky nature of the straw. This could influence the heat capacity and thermal conductivity of the materials, which would cause the temperature of some vessels to increase faster than others and the cooling-fan-on times could have varied. This in turn could have influenced the decomposition rate due to varied aeration conditions received. Furthermore, the height of temperature sensors could also affect the temperature readings that regulate cooling fans. There also could be some uncontrollable errors from vessel construction (i.e. height of plenum, tightness of lids, etc.).

With regard to the model, some parameters used were arbitrarily chosen. As seen in the sensitivity analysis of Chapter 2, substrate decomposition (represented by temperature, carbon dioxide evolution, and ammonia emission) is more sensitive to some parameters than others. Certain parameter values could have caused some of the discrepancy between model output and experimental measurements.

5.4.2 Model Verification

Substrate Decomposition

The partitioning of composting substrate did help predict the microbial growth and resulted in accurate temperature profiles in the simulation model. The readily degradable substrates (Soluble C and Non-fiber C) reached their maximum decomposition rates as groups, not as individual particles actually present in composting materials. This resulted in several hours' decomposition delay in the beginning and the overshoot of temperature above the set point afterwards. In the experiments, the average temperature, used to regulate the aeration rates, was a combined value from the sensors at two vertical positions in the vessels. The non-uniform decomposition in the experiments resulted in a lower peak heat generation compared with the simulation in the model. Thus, in the model aeration was unable to remove excess heat and temperature overshot the set-point.

The simulation of carbon dioxide evolution was associated with substrate decomposition. Since the model predicted substrate decomposition later than what actually occurred in the experiment, the carbon dioxide evolution rate was correspondingly lower than the measurement before the time when temperature reached set-point, represented by smaller slopes of almost all curves before 25 h (Figures 5-3 through 5-6). But the slopes caught up afterwards.

The difference between the predictions and the experimental measurements of temperature, moisture content and carbon dioxide evolution were in the range of –2% to 13%, 0 to 3% and –20% to 31% of the experimental measurements, respectively. This indicated that the simulation model gave a reasonable picture of the biological activity of the composting process.

Ammonia Emission

Ammonia emission was closely related with aeration. A longer cooling-fan-on time compared with its corresponding experiment generally resulted in larger ammonia emission, i.e., 1B, 1C, 1D, 2A, 2B (Figures 5-8, 5-9, Table 5-5).

The buffer experiments were predicted better partly due to the more closely predicted aeration, mainly represented by the cooling-fan-on time. In the buffer experiments, the differences of the simulation results among the treatments were due to both the slight difference of initial C contents and initial pH values (Table 5-1) used in the model. The lower values of initial C contents resulted in relatively less heat generation and lower temperature levels in the thermophilic stage, represented by the less cooling-fan-on time associated with more buffer chemicals added (Table 5-5). Consequently, less aeration may have contributed to lower ammonia emissions in the model.

In temperature-response-aeration composting, aeration is closely related with substrate decomposition, and ammonia emission was related with cooling-fan aeration due to the predominant high temperature and high decomposition rate of proteinaceous components in the thermophilic stage. Therefore the course of substrate decomposition largely controls the fate of nitrogen in the high rate stage of composting.

The model demonstrated some ability of relating these processes together. However, due to the large number of parameters that need to be estimated, a certain difficulty exists in obtaining complete and accurate predictions for a relatively large quantity of materials.

It was hypothesized that more labile C sources in the composting mixture would increase the microbially available C/N ratio and increase N immobilization during the initial stage so as to reduce ammonia volatilization. On the other hand, the addition of cellulose C would not have much impact on the NH_3-N loss. The model represented this hypothesis in that molasses addition did reduce ammonia loss although the reductions were not as profound as those observed in the experiments.

The model generally overestimated ammonia emissions and this discrepancy could be due to errors in measuring ammonia losses under experimental conditions or to model shortcomings, or both.

In the model, the drying conditions of the lower portion in composting vessels by the ventilation air were not accounted for. The model assumed uniformly distributed moisture when, in fact, the moisture in the compost was non-homogeneously distributed within vessels after the end of each experiment. The upper part was substantially moister and darker than the lower part, which indicated a better decomposition in the upper part. On one hand, if drying did take place within the lower portion of composting material at an early stage, that material could have become wholly or partially inactivated for decomposition, and could not have contributed to ammonia emission. On the other hand, the redistribution of the water from the lower portion to the upper portion by the aeration may have resulted in a beneficial condition for trapping (retaining) molecular ammonia into solution, which would be less subject to air stripping. In order to test these possibilities, the model was run under the previous assumption of 1B for 50 h, after which 1/3 of the composting materials were forced to quit participating in further decomposition. Also the humidity of inlet air was doubled from then on, to simulate the air being moistened by the lower inactivated materials. The resulting modified simulated ammonia emission is compared with the original output in Figure 5-13. The resulting curve showed about 10% lower cumulative ammonia emission, and indicates that moisture migration in the experimental treatments could explain at least some of the discrepancy between measured and simulated data. This phenomenon was observed experimentally by Hansen et al. (1993) who reported that a more uniform moisture distribution could result in more ammonia loss due to more complete decomposition, when applying reversed-direction airflow in a laboratory-scale composting vessel.

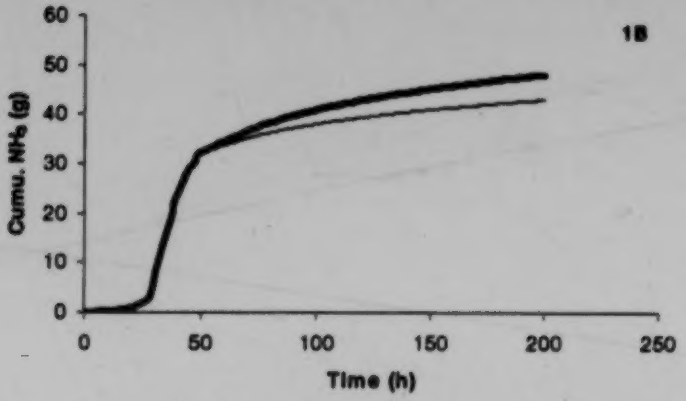

Figure 5-13. Comparison of model outputs, original (thick line) vs. that under modified assumption of partial material participating decomposition after 50h (thin line).

With respect to the development of the model, there also could be an incomplete understanding of the mechanisms related to activity of ammonia after being mineralized into ammoniacal forms. For example, in the calculation of CO_2-NH_3-H_2O multisolute aqueous system, the gas-liquid equilibrium of ammonia was assumed not reached, considering the high gas exchange rate during high rate stage composting. However, this was not based on any solid information. As well, if nitrification was considered in the cooling stage in this model, it could have accounted some of the nitrogen form as nitrite and/or nitrate and resulted in less ammonia concentration in compost. Morisaki et al. (1989) found that only 5.4% of their calculated NH_3 concentration was actually volatilized in their experiment. A possible explanation for this is that the dissolved NH_3 or water soluble NH_4^+-N exists mostly in the intracellular water phase rather than in free water in compost and is less likely subject to air stripping by aeration. The mechanism of adsorption and equilibrium of ammonia onto solid substrates was incorporated as a theory by Liberty and Taraba (1999) and a partition coefficient was applied in their calculation for nitrification in a biofilter. The binding of ammonia to the solid materials was not considered in this model. When investigating an abrupt drop in ammonia content in the compost that coincided with a change in cellulase activity, Shin and Jeong (1996) proposed a pathway for ammonia transformation that occurred in an initial stage of humification facilitated by the degradation of cellulose. These mechanisms need to be investigated in future development of the model.

The selected parameter values also influence the output of the simulation model. Adjustment of certain parameters, i.e. microbial death rate (δ), heat transfer coefficient (U) and maximum microbial growth ($\mu_{max,2}$), could decrease the predicted ammonia emission. However, due to the interrelated effect of the temperature, moisture, aeration on substrate decomposition and nitrogen loss, the adjustment is not easily made without further effort to investigate the interaction between the sensitive parameters.

pH

In the model the pH values were calculated from the multisolute CO_2-NH_3-H_2O aqueous system. The initial increase of CO_2 partial pressure, which resulted from the increased microbial activity and constant low aeration before temperatures reached 55°C, caused a slight decline in pH values in the first 30 to 50 h or so. This was followed by the rising pH values when temperature reached 55°C, and high aeration was in demand and applied. The fluctuated pH values at about 50 h were caused by the on-off application of the cooling-fan when the temperature was around 55°C, and consequent sharp changes of CO_2 partial pressure.

However, during the initial stage when there is fairly low microbial activity, the predominant factor influencing the compost pH may not be the composition of carbon and nitrogen species, but possibly some other materials, (e.g. organic acids generated in association with glucose degradation at the early stage of reaction, or unknown chemicals in original mixtures, exerting some buffering effect) unrecognized by the model. Therefore, as a simplification, the calculation of pH values from the multi-solute system was replaced by the pH measurement of the initial compost mixture at time zero. This measured pH value was forced to steadily approach the pH values calculated from the multi-solute system each time step, until they met at a certain point. By doing this, the initial measured pH value played a relatively important role in deriving pH values at the mesophilic stage, while pH calculated from the multi-solute system took over afterwards when the decomposition of carbon and nitrogen is more significant. The speed of approaching was chosen arbitrarily due to unavailable information.

The complicated composition of compost materials makes the simulation of buffering effects difficult. With the existing buffering capacity of raw materials unknown, the model was unable to fully predict the process except by using the initial pH measured.

5.4.3 Further Research Need

Further research is needed to consolidate some of the parameters required in this model. For example, experimental data of microbial biomass can be collected to validate some parameters related with microbial growth. This would provide more solid foundation for prediction using the current model.

5.5 CONCLUSIONS

Mathematical modeling of composting provided a dynamic link between microorganisms and the C and N decomposition in order to explain the complex interactions occurring in composting processes. The following conclusions can be made on the performance of this simulation model:

(1) The partitioning of the composting substrate effectively represented the organic matter decomposition. The simulated temperatures and moisture contents were in the range of 87% to 102% and 97 to 100% of the experimental measurements, respectively.

(2) The simulated carbon dioxide evolutions were within the 69 to 120% range of the experimental data, with an average difference of 89%. Much of this error is attributed to initial decomposition lag predicted in the model.

(3) The utilization of the multisolute aqueous system of CO_2-NH_3-H_2O predicted the ammonia volatilization in a reasonable range. The simulated ammonia emission ranged from 102% to 190% of the experimental data, with an average difference of 134%. The discrepancies between the model and experimental data could arise from:

a) inaccurate estimates of some kinetics parameters, resulting in errors in decomposition prediction; (b) incomplete understanding or interpretation of nitrogen transformation in the composting process; (c) the existence of chemical reactions other than the CO_2-NH_3-H_2O aqueous system recognized by the model.

5.6 REFERENCES

Bouldin, D.R. S.D Klausner and W.S. Reid. 1984. Use of nitrogen from manure. In: Hauck, R.D. (ed.) Nitrogen in crop production. American Society of Agronomy. Madison, WI.

Hansen, R.C., H.M. Keener, C.Marugg, W.A.Dick and H.A.J.Hoitink. 1993. Composting of Poultry Manure. In: H.A.J. Hoitink and H.M. Keener (eds.). Science and engineering of composting: Design, environmental, microbiological and utilization aspects. pp.131-153.

Jakobsen, S. T. 1992. Chemical reaction and air change during decomposition of organic matters. Resources, Conservation and Recycling 6: 259-266.

Liberty, K.R., and Taraba, J.L., 1999. Solid-state biofilter for nitrification. ASAE paper No. 99-4030. St. Joseph, MI.

Mahimairaja, S., Bolan, N.S., Hedley, M.J., Macgregor, A.N. 1990 Evaluation of methods of measurement of nitrogen in poultry animal manures. Fert. Res. 24:141-148.

Morisaki, N., Phae, C.G., Nakasaki, K., Shoda, M. and Kubota, H. 1989. Nitrogen transformation during thermophilic composting. J. of Ferment. and Bioeng. 1:57-61.

Schulte, D.D. 1997. Critical parameters for emission. In: J.A. Voermans and G.J. Monteny (eds.), Proceedings of the international symposium. Ammonia and odour control from animal production facilities. p. 579-584. Vinkeloord, The Netherlands.

Shin, H. and Jeong., Y. 1996. The degradation of cellulosic fraction in composting of source separated food waste and paper mixture with change of C/N ratio. Environ. Technol. 17:433-438.

Varel, V.H. 1997. Use of urease inhibitors to control nitrogen loss from livestock waste. Bioresource Technol. 62: 11-17.

Chapter 6

Synthesis

6.1 SUMMARY

The high rate stage of composting is characterized by high metabolic activity, represented by high rates of carbon dioxide and ammonia production, and of heat generation. In a laboratory-scale, this period lasts one to two weeks, while in a technical scale it lasts two to four weeks.

In this study, nitrogen retention in the high rate stage of composting processes was studied by simulating the substrate decomposition and nitrogen loss by the development of a mathematical model. Mineralization, volatilization and immobilization were the main processes taken into consideration and nitrogen loss was mainly via gaseous losses, especially ammonia volatilization. The unique feature of this model is: (a) substrate was partitioned into several groups based on both the chemical components and different decomposition rates; (b) ammonia volatilization was related with interstitial carbon dioxide concentration, which was influenced by both microbial activity and air exchange rate. The ammonia concentration in the free air space of composting materials was calculated based on the analysis of a CO_2-NH_3-H_2O multisolute aqueous system.

Initial runs of the model indicated good qualitative agreement with experimental results. A sensitivity analysis illustrated the influence of some parameters on the simulation output. To obtain a quantitative validation of the model, the next stage of this study required setting up an experimental system so that model outputs could be measured under known input conditions.

In the process of model development, it was recognized that pH, being an important control factor in the composting process, also influences the fate of nitrogen in the composting materials. Ammonia emission during composting has been shown to be strongly influenced by the pH of the compost (Körner and Stegmann, 1997; Nakasaki et al., 1993). While pH value was a well-established concept in chemistry, a representative method of pH determination for composting materials has not been investigated thoroughly. An effort was made in this work to reveal some phenomena related to carrying out pH measurement, and influencing factors such as sample size, diluent rate and extraction time were investigated. A protocol was developed for pH measurement of compost.

First, decide the number of samples to be measured based on the accuracy required. Secondly, for each sample, weigh 5 g original compost sample and add 20 ml deionized water. Stir mixture and wait for 5 minutes before pH_{20} *measurement is taken. Add an additional 40 ml deionized water, mix and take* pH_{60} *measurement. Thirdly, fit straight lines to* pH_{20} *and* pH_{60} *for each sample and calculate a mean hydrogen ion concentration at the intercepts. Finally, transform the mean hydrogen ion concentration to get the pH of the original undiluted compost material.*

Among the various control factors that influence the fate of nitrogen during composting, two were chosen to be tested for the purpose of validating the model. These include the influence of two types of carbon amendments and two chemicals forming buffer solutions on N losses.

The experiments were carried out in a laboratory-scale, manure-and-straw composting system and the data collected were used to validate the simulation model, by comparing temperature profiles, carbon dioxide evolutions and ammonia emissions. The model outputs were in good agreement with experimental measurement with regard to substrate decomposition, represented by temperature, moisture content and carbon dioxide evolution. The model generally overestimated ammonia emissions compared to those observed from the laboratory-scale experiment.

6.2 CONCLUSIONS

1. The model succeeded in reflecting well-known phenomena of the composting technologies. It reflected experimental results showing that ammonia volatilization is associated with substrate composition, C/N ratio, aeration, temperature, pH and moisture content.
2. pH measurements are influenced by sample size, type of diluent, dilution level, time between sampling and measurement, time between dilution and measurement. A recommendation was proposed as a guideline of successful pH determination of composting materials.
3. In the laboratory-scale composting experiment, nitrogen losses amounted to 12 to 25% of initial nitrogen, of which 90% was lost during peak activity in the early stage. Most of the N losses could be accounted for as ammonia nitrogen.
4. Amendment with a readily available form of carbon had a marked influence on ammonia volatilization. The treatment receiving sucrose at a rate of 10% the dry weight of the initial mixture reduced N losses by 100% (12.1% vs. 24.6% of initial N). Amendment with cellulose had little influence on ammonia volatilization.
5. The addition of buffering chemicals did not reduce the pH values significantly. This indicates that it may be difficult to adjust pH with buffers for some composting

materials. The lowered pH values resulting from the addition of buffering materials slightly reduced the N losses.

6. Under the temperature response aeration in this study, the ammonia volatilization was linearly correlated with the total air supply (R=0.696). This indicated that aeration is a very important process parameter for ammonia volatilization during composting.
7. The simulation model gave a good picture of the biological activity of the composting process. The simulated temperatures and moisture contents were in the range of 87 % to 102% and 97 to 100% of measured values, respectively. The simulated carbon dioxide evolutions were within 69% to 120% of the experimental data, with an average of 89%.
8. The prediction of the ammonia volatilization from the simulation model ranged from 102% to 190% of the experimental data, with an average of 134%.

6.3 FUTURE CONSIDERATIONS

1. Little data were available to either confirm or reject the predicted microbial biomass levels, even though the growth and death of microbial biomass was closely linked with substrate decomposition and nitrogen transformation, and was simulated in this model. More studies, including quantifying the microbial activity in composting, are required to further validate the current model.
2. Based on the sensitivity analysis of Chapter 2, appropriate values of certain parameters (i.e. microbial growth rate, microbial death rate, heat transfer coefficient, etc.) used in the model need to be determined experimentally to increase the accuracy of the model.

3. The ammonia volatilization was calculated based on the CO_2-NH_3-H_2O multisolute aqueous system. In the calculation, the gas-liquid equilibrium of ammonia was assumed not to be reached, because of the high air exchange rate during high rate stage of composting. However, this was not based on any solid information. An investigation is warranted for further modification.
4. In developing the model, the predominant mechanism for N loss was assumed to be gaseous N losses, especially ammonia volatilization. It would be more realistic to incorporate nitrification into the model so that the model can also predict nitrate and nitrite formation in the cooling stage.
5. While the model gave reasonable predictions for a relatively small and homogeneous system, it is uncertain whether it is capable of simulating a technical- or field-scale process. This deserves further study.

6.4 REFERENCES

Körner I., and R. Stegmann. 1998. Influence of biowaste composition and composting parameters on the nitrogen dynamics during composting and nitrogen contents in compost. In: Szmidt R.A.K. (ed.). Acta Horticulturae: Proceedings on the international symposium on composting and use of composted materials for horticulture, Auchincruive, UK. Vol. 469, ISHS, Drukkerij Van Damme, Beke, Brugge, Belgium, pp. 97-110.

Nakasaki, K., J. Kato, T. Akiyama and H. Kubota. 1987. A new composting model and assessment of optimum operation for effective drying of composting material. J. Ferment. Technol. 65(4): 441-447.

APPENDIX A

C Code of Simulation Model

```
/*************************************************************/
/* Function: growth()                                        */
/* Purpose : Calculation of microbial growth parameters.     */
/* Reference: Stella model                                   */
/* Input : temperature, moisture, pH, etc.                   */
/* Output: mui, and betai                                    */
/*************************************************************/
#include "header.h"
#include "main.h"
#include <stdio.h>
#include <math.h>
void muBeta(float temperature, float moisture, float pH,
          float SolubleC, float NonFiberC, float CelluloseC, float
FiberC,
          float O2con,
          float &muSC, float &muPC, float &muCC, float &muFC,
          float &betaSC, float &betaPC, float &betaCC, float &betaFC)
{
   float mumaxSC=.4;     // per hour.
   float mumaxPC=.4;    // per hour.
   float mumaxCC=.03; //smaller pool than FiberC, receiving high
rate,Sept99
   float mumaxFC=.03; // per hour.
   float KSC=.05;        // saturation constant.
   float KPC=.170;
   float KCC=.1;
   float KFC=.4;
   float KO2=.00003;       // unit: kg/kg d.m.
   float betamaxSC=.064;
   float betamaxPC=.064;
   float betamaxCC=.0048;
   float betamaxFC=.0048;
   float ktemp1, ktemp2, kH2O, kpH1, kpH2;

      /* temperature correction factor ktemp1 */
   if ((temperature>0.) && (temperature<30.)) ktemp1=temperature/(30.-
0.);
   else{
      if ((temperature>30.) && (temperature<55.)) ktemp1=1.;
      else  ktemp1=3.75-(temperature/(30.-10.));   // 55-75C
   }

      /* temperature correction factor ktemp2 */
   if ((temperature>0.) && (temperature<30.)) ktemp2=temperature/(30.-
0.);
   else{
      if ((temperature>30.) && (temperature<45.)) ktemp2=1.;
      else  ktemp2=(70.-temperature)/(70.-45.);  // 45C-75C
   }
      /* moisture correction factor kH2O */
   if (moisture>0. && moisture<.20)  kH2O=0.;
   else{
      if (moisture>.20 && moisture<.40)  kH2O=moisture/.2-1.;
      else  kH2O=1.;
   }

      /* pH correction factor kpH1: assigned for Soluble and Fiber */
   if (pH<5.|| pH>12.)  kpH1=0.;
   else if (pH>=5. && pH<6.) kpH1=pH-5.;
       else if (pH>=6. && pH<=9.1) kpH1=1.;
            else kpH1=-1.111*pH+11.11;

      /* mu, /hr */
   muSC=mumaxSC*(SolubleC/(SolubleC+KSC))
               *(O2con/(O2con+KO2))*ktemp1*kH2O*kpH1;
   muPC=mumaxPC*(NonFiberC/(NonFiberC+KPC))
               *(O2con/(O2con+KO2))*ktemp1*kH2O*kpH1;
   muCC=mumaxCC*(CelluloseC/(CelluloseC+KFC))
               *(O2con/(O2con+KO2))*ktemp2*kH2O*kpH1;
   muFC=mumaxFC*(FiberC/(FiberC+KFC))
               *(O2con/(O2con+KO2))*ktemp2*kH2O*kpH1;
      /* beta, /hr */

betaSC=betamaxSC*(SolubleC/(SolubleC+KSC))*(O2con/(O2con+KO2))*ktemp1*k
H2O;
betaPC=betamaxPC*(NonFiberC/(NonFiberC+KPC))*(O2con/(O2con+KO2))*ktemp1
*kH2O;
betaCC=betamaxCC*(CelluloseC/(CelluloseC+KCC))*(O2con/(O2con+KO2))*ktem
p2*kH2O;
betaFC=betamaxFC*(FiberC/(FiberC+KFC))*(O2con/(O2con+KO2))*ktemp2*kH2O;
}

/**************************************************************/
/* Function: carbon()                                         */
/* Purpose : Calculation of temp and CO2 partial pressure.   */
/* Reference: Stella model                                    */
/* Input : NH3conc -> from value()                            */
/* Output: temperature ->                                     */
/*         CO2 pPressure -> CO2 partial pressure              */
/**************************************************************/
#include <stdlib.h>
carbon(float NH3conc, float NH3ppm,
       float &CO2pPressure, float &temperature, float
*fStoichiometricConc)
{
  FILE* output_file;
    /* kinetic parameters */
  float deathRate=.025;  //   kd, per hour.
  float kp=0.002;  // 1st order rate constant of microbial growth on
product.
    /* property and parameter values */
  float ambientTemp=20.;
  float cw=4180.;
  float cvs=1480.;
  float cnvs=840.;
  float conductionK=4000.;  //J/K-m2/h.  U=1/R
  float area=1.76;    //m2
    /* yield coefficients */
   float Yxsc=-.35;    // kg cells produced / kg substrate consumed.
   float Yxpc=-.35;
   float Yxfc=-.3;
   float Yxp=-.35;      //Yield on microbial product C
   float YO2s=1.37; //YCO2s=2.;   // kgO2/kgS.
   float Yws=.56;     // kgH2O/kgS.
   float Yhs=1.91E07; // J / kg S.

    /* Input initial values from Yi's experiment, unit: kg/kgd.m. */
   float microBiomassC=1.5*0.186E-3;
   float microbialN=1.5*.031E-3; // initial microCN=4.
   float SolubleC=.014; // Total C=0.465,
   float NonFiberC=.0448;
   float NonFiberCN=4.; // proteinN=.0126(0.014-.0014) kg/kg d.m.
   float CelluloseC=0.;
   float FiberC=0.359;
   float nvs=.12;
   float waterCont=2.333; //71%. 2.333;
   float initMass, initDM=14.1;   // kg in 0.0123 m3.
   float volume=.137; //effective volume,  // m3.
   float BulkDensity=47./volume;  // kg/m3, initial value.
   float pHc=8.7, ammoniacalN=0.0048;
   float iniSolC, iniNonC, iniFibC, iniCluC;
   float microProdC=0.;
   float microProdN=0.;
   float ProductCN=6.;
   float O2conc=.2992; // CO2conc=.00059;   // kg/m3 air.
   float time=0., FanOn=0.;
   float porosity=.30;   // 30%,
   float flowRate;   // kgair/kgDMi
   float NonFiberN, microbialCN, Ca, Cu;
   float inorganicN;
   float dmNdt, dbNdt, dNdt, dpNdt, damNdt, dNH3dt, dammoNdt, dimmoNdt;
   float NH3cumulate=0.,NH3g=0.,NH3g2=0., Tcumu=0., Taverage,
sumdNH3dt=0., dNH3dtAV;
   float iniSubC=SolubleC+NonFiberC+CelluloseC+FiberC;
   float ratioCN, ratioCN2;         // initialized as 1.(pH >9)
   float HactCoeff=.87, HactCoeff2, ratiopH, ionH, ionH0, ionHlast;
   float fraction=.474, vSubs, DM, moisture;//C Fraction, kgC/kg
volatile substrate
   float muSC,muPC,muCC,muFC, betaSC,betaPC,betaCC,betaFC;
   float dmBCdt, dpdt;
   float dSCdt,dPCdt,dCCdt,dFCdt, dSCdt1, dPCdt1, dCCdt1, dFCdt1,
SCtemp,PCtemp,FCtemp;
   float dCO2dt,dCO2dt2, dCO2Cdt, dCO2Cwatdt, dO2dt, dWCdt, dTdt;
   float O2content, CO2mol, CO2pPLast, cumuCO2C=0.,CO2g=0.,O2consumRate,
O2consum=0.;
   float tdrybulb, tdewpoint;
   float airdensity=1.286;     //kgair/m3
   float humidin, humidout;    /* humidity ratio kg H2O/kgda. */
   float LatentLoss, SensibleLoss, heatResidual, heatVaporization;
   float humidair, enthalair, volumeair, rhomix, vmix;
   float cond, gmass, totalmass, oxidizedC, oxidizedS;
   float O2molFrac, CO2molFrac, nvCO2;
   float pH, pHlast, pHadjusted, Hactivity, kpH;
   float R=0.082;
   float maxBioC, PctvSubs, PctDM, PctTM, maxTemp;
```

```
  float logRatio, sign;

    /* time step */
  float delt=0.01;    // hour.
  int pHflag=0;

    /* calculate and save initial values */
  iniSolC=SolubleC*1.001;
  iniNonC=NonFiberC;
  iniCluC=CelluloseC;
  iniFibC=FiberC;
  initMass=iniSubC/fraction+nvs+waterCont;  // kg of mass/kgdm
  moisture=waterCont/initMass;
  O2content=O2conc*porosity/BulkDensity/(1.-moisture);
         // .08976 kgO2/m3 compost when porosity=30%
  temperature=20.;
  NonFiberN=NonFiberC/NonFiberCN;
  microbialCN=microBiomassC/microbialN;

  flowRate=.02; //  kgair/kgDM
  if ((output_file=fopen("largeControl.txt", "w"))== NULL)
  {
     printf("*** output.txt could not be opened for write. \n");
     exit(1);
  }
  else
  {  // print any interested variables.
      fprintf(output_file, " time ");
      fprintf(output_file, " temp");
      fprintf(output_file, " moist");
      fprintf(output_file, " cumuCO2C ");
      fprintf(output_file, " CO2g ");
      fprintf(output_file,  "NH3cumu ");
      fprintf(output_file,  "NH3g ");
      fprintf(output_file, "\n");
  }

  for(int i=0; i<20000; ++i)
  {
    time+=delt;

    muBeta(temperature, moisture, pHc,SolubleC, NonFiberC, CelluloseC,
FiberC,
      O2content, muSC,muPC,muCC,muFC, betaSC, betaPC,betaCC, betaFC);

      /* Rate of change in X (biomass) */
    dmBCdt=(muSC+muPC+muCC+muFC-deathRate)*microBiomassC
      + kp*microProdC;    //+(1./Yxdc+1.)*kp*microProdC, negative
result
    microBiomassC+=dmBCdt*delt;

    if (microBiomassC<0.)  microBiomassC=0.;
      /*  RATE OF CHANGE OF MICROBIAL PRODUCT */
    dpdt=deathRate*microBiomassC-
kp*microProdC+(1./Yxsc+1.)*kp*microProdC ;
    microProdC+=dpdt*delt;
    dpNdt=deathRate*microBiomassC/microbialCN
        +(1./Yxp)*kp*microProdC/ProductCN;
    microProdN+=dpNdt*delt;

      /* Rate of change in volatile substance, C and N */
    dSCdt=(1./Yxsc)*(muSC*microBiomassC)-betaSC*microBiomassC;
    if (dSCdt>0.) {
       dSCdt=0.;
    }
    SolubleC+=dSCdt*delt;
    dPCdt=(1./Yxpc)*(muPC*microBiomassC)-betaPC*microBiomassC;
    if (dPCdt>0.) {
       dPCdt=0.;
    }
    NonFiberC+=dPCdt*delt;
    if (NonFiberN>1E-06){
      dNdt=dPCdt/NonFiberCN;
      NonFiberN+=dNdt*delt;
    }
    else  dNdt=0.;
    dCCdt=(1./Yxfc)*(muCC*microBiomassC)-betaCC*microBiomassC;
    if (dCCdt>0.) {
       dCCdt=0.;
    }
    CelluloseC+=dCCdt*delt;
    dFCdt=(1./Yxfc)*(muFC*microBiomassC)-betaFC*microBiomassC;
    if (dFCdt>0.) {
       dFCdt=0.;
    }
    FiberC+=dFCdt*delt;
    vSubs=(SolubleC+NonFiberC+CelluloseC+FiberC)/fraction;  //volatile
substrate
    PctvSubs=1.-vSubs*fraction/iniSubC;
    DM=vSubs+nvs+microBiomassC+microProdC;
    PctDM=1.-
(vSubs+nvs+microBiomassC+microProdC)/(iniSubC/fraction+nvs);
    PctTM=1.-(vSubs+nvs+waterCont)/initMass;
    BulkDensity=(vSubs+nvs+waterCont)*initDM/volume;
      // oxidized substrate was used instead of substrate consumption,
change.
           //kgC/kg d.m.-hr.
    dCO2dt=(1./Yxsc+1.)*muSC*microBiomassC
        +(1./Yxpc+1.)*muPC*microBiomassC
        +(1./Yxfc+1.)*muCC*microBiomassC
        +(1./Yxfc+1.)*muFC*microBiomassC
        +(1./Yxp+1.)*kp*microProdC;
    dCO2dt2=dCO2dt-(betaSC+betaPC+betaCC+betaFC)*microBiomassC;
      //  CO2 generation kgCO2C/kgD.M.-unit time.
      cumuCO2C-=dCO2dt2*delt;   // kgCO2C/kgD.M.
    //if (time<50) { //Assumption tested for Chapter 5 - partially
drying
        CO2g-=dCO2dt2*delt*(1.-PctDM)*initDM*44./12.;
    //  }
    // else CO2g-=dCO2dt2*delt*(1.-PctDM)*initDM*44./12.*2./3.;

    oxidizedS=dCO2dt2/fraction;    // negative value
```

```
      /* Rate of change in O2 */
    dO2dt=YO2s*oxidizedS+(flowRate/airdensity)*(.2992 -
O2conc);//kgO2/kgD.M./h
    O2content+=dO2dt*delt;                    //kgO2/kgD.M.
    O2conc=O2content*(1.-moisture)*BulkDensity/porosity;   // kgO2/m3
da
                          // actural Bulkdensity/porosity
    if (O2conc<.0001)  O2conc=.0001;
    if (O2conc>.294)  O2conc=.294;
    O2consumRate=(.21*32./22.4-O2conc)*(flowRate/1.286*15.);
    O2consum+=O2consumRate*delt;
    O2molFrac=(O2conc/32.)*22.4;  // liter /liter air
    CO2molFrac=.2095-O2molFrac;   // .2095 is O2 mol-fraction in dry
air
    nvCO2=CO2molFrac/22.4;
    CO2pPressure=nvCO2*R*(temperature+273.15);  /* p=(n/V)RT, atm */
    if (CO2pPressure<0.) CO2pPressure=0.000327;   // value of 20C.
    tdrybulb=ambientTemp;
 //   if (time<50) { //Again assumption tested for Chapter 5
       tdewpoint=10.;          /* inlet air */
 //   }
 //   else tdewpoint=20.;
    psychro(tdrybulb, tdewpoint,
             humidair, enthalair, volumeair, rhomix, vmix);
    humidin=humidair;                 // kg water/kg da
    tdrybulb=temperature;
    if (moisture<.18)  tdewpoint=10.;    // saturated
    else  tdewpoint=temperature;
    psychro(tdrybulb, tdewpoint,
             humidair, enthalair, volumeair, rhomix, vmix);
    humidout=humidair;       // saturated humidity ratio, kg water/kg
da.
      /* RATE OF CHANGE IN WATER CONTENT */
    dWCdt=-Yws*oxidizedS-flowRate*(humidout-humidin); //kgH2O/kgD.M.
    waterCont+=dWCdt*delt;
    gmass=cvs+nvs*cnvs+waterCont*cw;  // J/K-kg d.m.
    cond=conductionK*area*(temperature-ambientTemp)/((1.-
PctDM)*initDM);
                         // J/kg d.m.-h
      /* heat of vaporization, approximate */
    if (temperature<30.)  heatVaporization=2455.;
    else{
      if ((temperature>=30.)&&(temperature<40.))
heatVaporization=2431.;
      else{
        if ((temperature>=40.)&&(temperature<50.))
heatVaporization=2407.;
        else{
          if ((temperature>=50.)&&(temperature<60.))
heatVaporization=2383.;
          else{
            if (temperature>=60.)  heatVaporization=2359.;
          }
        }
      }
    }
      /* RATE OF CHANGE IN TEMPERATURE */
    LatentLoss=heatVaporization*1.E03*(humidout-humidin)*flowRate;
//J/kg d.m.
    SensibleLoss=( (1.0*1006.+humidout*4187.)*temperature
              -(1.0*1006.+humidin *4187.)*ambientTemp )*flowRate;
    heatResidual=(-Yhs*oxidizedS-LatentLoss-SensibleLoss-cond);
    dTdt=heatResidual/gmass;
    temperature+=dTdt*delt;
    if (i>15000 && temperature<=ambientTemp)  temperature=ambientTemp;
      /* NEW TOTAL MASS and MOISTURE CONTENT */

totalmass=(SolubleC+NonFiberC+CelluloseC+FiberC)/fraction+nvs+waterCont
;
    moisture=waterCont/totalmass;
      /* N transformation */
    dNH3dt=NH3conc*flowRate/airdensity;  // kgN/kg d.m.-hr
    inorganicN=(ammoniacalN/waterCont); // kg N/kq Water
    fStoichiometricConc[0]=inorganicN*1000./14.;   // mol N/kg Water
    sumdNH3dt+=dNH3dt;
    if(i%100==0) {
      dNH3dtAV=sumdNH3dt/100.;    // NH3 rate average in an hour.
      sumdNH3dt=0.;
    }
    if(microbialCN<4.) dmNdt=microbialN-microBiomassC/4.;
    else {
      if (microbialCN>6.5) {
        Ca=0.;
        Cu=1.;    // encourage immobilization
      }
      else  {           // 5.<microbialCN<9.
        Ca=(1./3.)*(7.-microbialCN);
        Cu=(1./3.)*(microbialCN-4.);     //4-7   //E4
      }
      if (NonFiberC/iniNonC>0.2) {
         dammoNdt=0.03*microbialN*Ca;
         dimmoNdt=0.015*microBiomassC*inorganicN/(0.02+inorganicN)*Cu;
      }
      else {
         dammoNdt=0.;
         dimmoNdt=0.015*microBiomassC*inorganicN/(0.02+inorganicN)*Cu;
        // Monod equation 0.0042 kgN/kgC-hr  immobilizing .02 gN/kgH2O
      }
      dmNdt=dammoNdt-dimmoNdt;
    }  // end of else

    if (ammoniacalN>1E-06) {
       damNdt=dmNdt-dNH3dt;
       ammoniacalN+=damNdt*delt;  // kgN/kg D.M.compost
    }
    else ammoniacalN=1E-06;
    dbNdt=-dmNdt-(1./Yxsc)*kp*microProdC/ProductCN
            -deathRate*microBiomassC/microbialCN-dNdt;
     //  dbNdt=-dmNdt-dpNdt-dNdt;  // unit: kg N/m3-hour
    microbialN+=dbNdt*delt;
    NH3cumulate+=dNH3dt*delt;
//    if (time<50) { //Again assumption tested for Chapter 5
       NH3g+=dNH3dt*delt*(1.-PctDM)*initDM*17./14.;
//    }
//   else NH3g+=dNH3dt*delt*(1.-PctDM)*initDM*17./14.*2./3.;
   NH3g2+=dNH3dt*delt*initDM*17./14.;

      /* C:N ratio */

ratioCN=(SolubleC+NonFiberC+CelluloseC+FiberC+microBiomassC+microProdC+
nvs*
fraction)
          / (NonFiberN+microbialN+microProdN+ammoniacalN);

ratioCN2=(SolubleC+NonFiberC+CelluloseC+FiberC+microBiomassC+microProdC
)
          / (NonFiberN+microbialN+microProdN+ammoniacalN);
      // Average temperature
    Tcumu+=temperature;
    Taverage=Tcumu/(i+1);
      // For next time step
    microbialCN=microBiomassC/microbialN;
    ProductCN=microProdC/microProdN;
    if (temperature< 55.)  flowRate=0.02;  //
    if (temperature> 56.) {
      flowRate=0.10;    //0.301;
    }
    if (flowRate>.099)   FanOn+=delt;
    // temperature-response aeration
    if ( (i%136 ==0))
    {
      fprintf(output_file, "%4.1f  ", time);
      fprintf(output_file, "%4.1f", temperature);
      fprintf(output_file, " %5.3f", moisture);
      fprintf(output_file, " %5.3f ", cumuCO2C*1000. );
      fprintf(output_file, " %5.3f ", CO2g*1000. );
      fprintf(output_file, " %6.3f ", NH3cumulate*1000.);
      fprintf(output_file, " %6.2f ", NH3g*1000.);
//   fprintf(output_file, "\n");
    }  // End of if  (i%100=0)

    if (i) pHlast=pH;
    else pHlast=9.5;
    if (fStoichiometricConc[0]>1E-05){
      multsolu(NH3conc, NH3ppm, pH, ionH, HactCoeff2, 1.,
      CO2pPressure, temperature, fStoichiometricConc);
    } // HactCoeff2 was replaced by H coefficient at each time step
      // for current time step use.
    if ( (i%136 ==0))  //||(i>9000 && i%50==0 ) )
    {
      fprintf(output_file, " %5.3f", pH);//pH from CN
      fprintf(output_file, "\n");
    }
    if (i>8000 && pHc<7.4)  pHc=7.4;

 if (!pHflag) {
  if (pH<=pHlast) {//pH calculated from CN decline each time step
   if ((pH-pHc)>=0.1 && i<10000 ) {//pH from CN large than pHcompost
       // run only when pH difference is large enough
      float increment=.002;
      pHadjusted=pHc+increment*(pH-pHc);
      printf("\n pHadjusted=%f ", pHadjusted);
      Hactivity=pow(10., -pHadjusted);
      multpH(NH3conc, NH3ppm, pHc,
          Hactivity, HactCoeff, temperature, fStoichiometricConc);
   }
   else {
     Hactivity=pow(10., -pHc);
      multpH(NH3conc, NH3ppm, pHc,
          Hactivity, HactCoeff, temperature, fStoichiometricConc);
   }
  } //End of if
  else {//pH calculated from CN incline each time step, later on
    if (pH<pHc) { //most case
      float increment=.001;
      pHadjusted=pHc+increment*(pH-pHc);//pH-pHc<0, result in negative
value
      printf("\n pHadjusted=%f ", pHadjusted);
      Hactivity=pow(10., -pHadjusted);
      multpH(NH3conc, NH3ppm, pHc,
          Hactivity, HactCoeff, temperature, fStoichiometricConc);

    }
    else {  // rare case
      pHflag=1;
      pHc=pH;
    }
  }//End of else
 } //End of if (pHflag==0)
 } // End of for(i=0; i<18000; ++i)
  fprintf(output_file, "\nTaverage = %f", Taverage);
  fprintf(output_file, "  FanOn = %f", FanOn);
  printf("Taverage = %f", Taverage);
  printf("FanOn = %f", FanOn);
  printf("done!\n");
  return 0;
}

#define SQR(X) ((X)*(X))
#include <math.h>
#include <stdio.h>
void psychro(float tdryb, float tdewp,
      float &wair, float &hair, float &vair, float &rhomix, float
&vmix)
{
  float patm=(740./760.)*101325.;  // Pa. under 740 mmHg
  float R=22105649.25;
  float A=-27405.526;
  float B=97.5413;
  float C=-.146244;
  float D=.12558E-3;
  float E=-.48502E-7;
  float F=4.34903;
  float G=.39381E-2;
  float vaporPressure;
  tdryb+=273.15;   // kelvin
  tdewp+=273.15;
```

```
   /* saturation line when tdewp>273.15, ASAE 1994 p44 */
  vaporPressure=R*exp( (A+B*tdewp+C*SQR(tdewp)+D*tdewp*SQR(tdewp)
       + E*SQR(tdewp)*SQR(tdewp))/(F*tdewp-G*SQR(tdewp)));

  wair=.62198*vaporPressure/(patm-vaporPressure);  // kg water/kg dry
air
   /* v=mRT/Patm, R(dry air)=287 J/kg-K */
  vair=(287.055*tdryb/patm)*(1.+1.6078*wair); //air specific volume
m3/kgda

  rhomix=(1./vair)*(1.+wair);  //  kg mix/m3
  vmix=1./rhomix;              //  m3/kg mix
   /* Enthalpy of air-vapor mixture */
  hair=1000.*((tdryb-273.15)+wair*(2501.+1.805*(tdryb-273.15)));
}

#include <dos.h>
main()
{
  nosound();
  //return 0;
  float  CO2pPressure, temperature, fStoichiometricConc[2];
  float  NH3conc=.00001;   // kg/m3 air
  float  NH3ppm=1.;
  carbon(NH3conc, NH3ppm, CO2pPressure, temperature,
fStoichiometricConc);
  sound(500);
  sleep(1);
  nosound();
  return 0;
}


#include <string.h>
#include <stdio.h>
#include <stdlib.h>
#include <math.h>
#include <dos.h>
#include "header.h"
#include "main.h"
#define GASCONST 0.082
/*==========================================================*/
/* Function: multsolu()                                     */
/* Purpose: Calculation of NH3ppm, NH3conc, pH, ionic strength */
/*          total conc.(Stoichiometric) of C.               */
/* Input :  fConcMolality[] -> calculation of 8 species conc.  */
/* Output:  NH3ppm, NH3conc -> NH3 conc.in air, pH ->       */
/*          NH3conc has unit of kgN/m3 da.                  */
/*==========================================================*/

void multsolu(float &NH3conc, float &NH3ppm, float &pH, float &ionH,
       float &HactCoeff2, float ratiopH,
       float CO2pPressure, float temperature, float
fStoichiometricConc[])
{
  float fGama[9]; /* fGama[] is to store outputs from fActivityCoef().
*/
```

```
  float fBeta[9][9], fBetax[9][9];
  float fCm[2], fSMol[3], fConcMolality[8];
  float kelvin, fRT;
  // float CO2pPressure=.00039872;     //atm.
  float fEquConst[5], fHnry[3];
  float PPNH3, PPCO2;
  struct species_Rank species[9]; //Defines an array of structure
variables.
       //Can also be defined as "species_Rank  species[]".

  float  fI, NH3molL; //
       //  fStoichiometricConc[0]=.2500;  // [1]: to be calculated.
       // The total concentration, regardless of ionization or other
       //     chemical equilibria.
       // units: moles/kg H2O.
  kelvin=273.15+temperature;
  fRT=GASCONST*kelvin;
  ewequl(fEquConst, kelvin);
  fHnryl(fHnry,  kelvin);
  iniflash(fCm, fSMol, fConcMolality,
         fHnry, fStoichiometricConc, fEquConst, CO2pPressure);
  rank(species);
  fAssignBeta(fBeta, fBetax, kelvin);
  CalcMolecularSpeciesConc(fGama, fBeta, fBetax, kelvin, fConcMolality,
      fI,
fEquConst,fStoichiometricConc,ratiopH,species,fHnry,CO2pPressure);
  ionH=fConcMolality[6];
  pH=-log10(fConcMolality[6]*fGama[6]);
  HactCoeff2=fGama[6];   // Replaced by H coefficient at each time step
  PPNH3=fHnry[0]*fGama[0]*fConcMolality[0]; // *.969629;
  PPCO2=fHnry[1]*fGama[2]*fConcMolality[2]; // *.847981; // fPHI[1]
  NH3molL=0.5*PPNH3/fRT;       // mol/liter of air //.5* 50%
  NH3ppm=NH3molL*22.4E6;   //  ppm.
  NH3conc=NH3molL*14.;     // gN/litre da. or kgN/m3 da.
}

/********************************************************************/
/* Function: CalcMolecularSpeciesConc.cpp                           */
/* Purpose: Calculation of molecular conc of 8 species,             */
/*          when total conc.(Stoichiometric) of C unknown.          */
/* Reference: 1.Computer program TIDES;                             */
/* Input: fBeta,fBetax -> interaction para from AssignBate().       */
/*        kelvin -> Absolute temperature T.                         */
/*        fConcMolality[] -> from fInitialEstimates.                */
/*        fStoichiometricConc[0] -> N conc. in solution.            */
/*        fEquConst[] -> from ewequl.                               */
/*        ppCO2 -> CO2 partial pressure from Stella.                */
/* Output: fConcMolality[] -> calculation of eight species conc.    */
/*       pH -> log10(aH), fI -> ionic strength of solution          */
/********************************************************************/
void CalcMolecularSpeciesConc(float fGama[9], float fBeta[9][9],
     float fBetax[9][9], float kelvin, float fConcMolality[8],
     float &fI, float fEquConst[5], float fStoichiometricConc[2],float
ratepH,
     struct species_Rank species[9], float fHnry[], float ppCO2)
{
  int i, j, iteration=0, dFLAG=TRUE, cFLAG=TRUE;
  float fCTemp1, fCTemp2;
  float fAlfaMatrix[9][9], fBetaMatrix[9];
  float fDGama[8][8]={0.};
  float fAlfa;
  fAlfa=dhdata(kelvin);
  while(cFLAG)
  {
    fI=fIonicStrength(species, fConcMolality);
    fActivityCoeff(fGama, fBeta, fBetax, fConcMolality,
               species, fAlfa, fI);
      /*  The following step is important for speeding up.  */
    if(dFLAG)
    {
      fActivityDerivative(fGama, fBeta, fBetax, fConcMolality,
            species, fDGama, iteration, fAlfa, fI);
      dFLAG=FALSE;
    }
    iteration++;
    setupABmatrix(fAlfaMatrix, fBetaMatrix, fGama, fConcMolality,
      fStoichiometricConc, fEquConst, ratepH, species, fDGama, fHnry,
ppCO2);
    ludcomposition( 9, fAlfaMatrix, fBetaMatrix);
    cFLAG = FALSE;
    for(i=0; i<8; i++)
    {
      if (fBetaMatrix[i]>=0.)  fConcMolality[i]+=fBetaMatrix[i];
      else
      {
      fCTemp1=fConcMolality[i]*exp(fBetaMatrix[i]/fConcMolality[i]);
      fCTemp2=1.E-3*fConcMolality[i];
      if (fCTemp1<fCTemp2)  fConcMolality[i]=fCTemp2;
      else  fConcMolality[i]=fCTemp1;
      }
      if ( fabs(fBetaMatrix[i]) > 1.E-3*(fConcMolality[i]) )
         dFLAG=TRUE;
        /*--------------------*/
        /*  Convergence Check  */
        /*--------------------*/
      if ( fabs(fBetaMatrix[i]) > 5.E-3*(fConcMolality[i]) )
        cFLAG = TRUE;
    } // End of for(i=0; i<8; i++)

    if (fBetaMatrix[8]>=0.)  fStoichiometricConc[1]+=fBetaMatrix[8];
    else
    {
      fCTemp1=fStoichiometricConc[1]*
            exp(fBetaMatrix[8]/fStoichiometricConc[1]);
      fCTemp2=1.E-3*fStoichiometricConc[1];
      if (fCTemp1<fCTemp2)  fStoichiometricConc[1]=fCTemp2;
      else  fStoichiometricConc[1]=fCTemp1;
    }
    if(iteration>15) {
       printf("\nKick you out after %d iteration!!\n", iteration);
       exit(0);
    }
  } // while(cFLAG)
}
```

```
#include "header.h"
/*********************************************************************/
/* Function: fIonicStrength.cpp                                      */
/* Purpose: Calculation of Ionic Strength of solution.               */
/* Input: struct species_Rank species[9] ->, float fConcMolality[8]) */
/* Output: dh_data -> alfa under a specific temperature.             */
/*********************************************************************/
float fIonicStrength(struct species_Rank species[9],
                 float fConcMolality[8])
{
  int i;
  float fSI;

  fSI=0.0;
  for(i=0; i<8; i++)
  {
    fSI+=0.5*(fConcMolality[i]*(species[i].value*species[i].value));
  }
     //printf("\nThe ionic strength of the compost solution: %f\n",
fSI);
  return(fSI);
}
#define SQR(X) ((X)*(X))

#include <math.h>
#include <stdio.h>

void iniflash(float fCm[2], float fSMol[3], float fConcMolality[8],
        float fHnry[3], float fStoichiometricConc[],
        float fEquConst[5], float ppCO2)
{
  int i,  Ntry;
  float ptot=fHnry[2];  //  pH2O=fHnry[2]  ppH2O=fHnry[2];
  float fStoichoimetricWater=55.55;      //
  float temp0, temp1, Q, error0, error1;
  // float xy[3];  similar to fMolFrac[] in fVaporComp().

  float fMolarVol[3], fPHI[3], fMolFrac[3];

  ptot*=55.55;
  fCm[0]=1.;   // Guessing! CM(IVAP), in error in FLASH of TIDES. 0.0.
  fConcMolality[0]=100.;
  fConcMolality[1]=100.;

  fConcMolality[2]=ppCO2/fHnry[1]; /*  /fGama[2];*/

  for(i=0; i<3; i++)
  {
    if(i<2)
    {
      fMolFrac[i]=0.;        // xy[i] in FLASH() of TIDEs.
    }
    else
    {
      fMolFrac[i]=1.;
    }
  }    // End of for(i=0; i<3; i++).
  fSMol[0]=fStoichiometricConc[0];
  fSMol[2]=fStoichoimetricWater;

  fCm[1]=fSMol[2]-fHnry[2]*fCm[0]/ptot;
    // printf("\nCM(IVAP) in TIDES is %f", fCm[0]);
    // printf("\nCM(IH2OL) in TIDES is %f", fCm[1]);

  fConcMolality[6]=1.E-8;
  fConcMolality[7]=fEquConst[4]/fConcMolality[6];
  fConcMolality[3]=fConcMolality[2]*fEquConst[1]/fConcMolality[6];
  fConcMolality[4]=fConcMolality[3]*fEquConst[2]/fConcMolality[6];
  fSMol[1]=fConcMolality[2]+fConcMolality[3]+fConcMolality[4];

  Ntry=0;
  while (Ntry<35)
  {
    Ntry++;
    temp0=fConcMolality[0];
    temp1=fConcMolality[1];
    Q=fEquConst[0];
    Q+=fEquConst[1]*fEquConst[0]*fSMol[1]*fHnry[1]/
       (fEquConst[4]*fCm[0]*ptot) +.018*fCm[1]*
       (1.+fEquConst[1]*fEquConst[0]*fConcMolality[0]/
         (fEquConst[4]*fConcMolality[1]));
    Q/=(1.+ fEquConst[4]/(fEquConst[0]*fConcMolality[0]));
    fConcMolality[1]=2.*fSMol[0]/ ( .018*fCm[1]+ pow(( SQR(
.018*fCm[1])
       +(4.*fSMol[0]/Q)* ( .018*fCm[1]+fCm[0]*fHnry[0]/ptot ) ),0.5));

    fConcMolality[0]=SQR(fConcMolality[1])/Q;
    error1=fabs(fConcMolality[1]-temp1)/fConcMolality[1];
    error0=fabs(fConcMolality[0]-temp0)/fConcMolality[0];
    if ((error1<1.E-3)||(error0<1.E-3))  break;
  }  // End of While(Ntry<35).
  fConcMolality[5]=fEquConst[3]*fConcMolality[0]*fConcMolality[3];
  fStoichiometricConc[1]=fConcMolality[2]+fConcMolality[3]
                     +fConcMolality[4]+fConcMolality[5];
}


#include <stdio.h>
#include <stdlib.h>
/*********************************************************************/
/* Function: dhdata.cpp                                              */
/* Purpose: Calculation of Debye-Huckel parameter Ar, according to   */
/*          alfa=Ar/2.303, value of Ar from TIDES 1988.              */
/* Input: kelvin -> Absolute temperature T;                          */
/* Output: dh_data -> alfa under a specific temperature.             */
/*********************************************************************/

float dhdata(float kelvin)
{
   float dh_data;
   float rkelvin;
   float c1,c2,c3;
   c1=3.7323;
   c2=-1354.21;
   c3=176349.0;

   if(kelvin>=373.15)
   {
     printf("Temperature is larger than 100C, invalid from dhdata:\n");
     exit(0);
   }
   rkelvin=1./kelvin;
   dh_data=c1+c2*rkelvin+c3*rkelvin*rkelvin;
      // dh_data is the alfa, which equals to 2.303*Ar in table (1961).
   return(dh_data);
}

/*********************************************************************/
/* Function: fAssignBeta()  (Second version)                         */
/* Purpose: Calculation of interaction parameters between:           */
/*         molecule-molecule, molecule-ion, ion-ion, etc.            */
/* Reference: 1.Computer program TIDES;                              */
/* Input: kelvin -> Absolute temperature T.                          */
/* Output: fBeta[][],fBetax[][] -> Bi,j(0) and Bi,j(1).              */
/*********************************************************************/
#include <stdlib.h>
#include <stdio.h>

void fAssignBeta(float fBeta[9][9], float fBetax[9][9], float kelvin)
{
  int i,j;

  for(i=0; i<9; i++)
  {
    for(j=0; j<9; j++)
    {
      fBeta[i][j]=0.;
      fBetax[i][j]=0.;
    }
  }
  //NH3 Beta parameters.
  fBeta[0][0]=-0.03980694+17.0142/kelvin;
  fBeta[0][1]=-0.000125*kelvin+0.03162;
  fBeta[0][2]=2.2782-0.0135*kelvin+0.20114E-4*(kelvin*kelvin);

  fBeta[0][3]= -0.73713+0.444511E-2*kelvin-0.64706E-5*(kelvin*kelvin);

  fBeta[0][4]=0.3238-0.0008779*kelvin;  //0.06;
  fBeta[0][5]=0.08;         //0.0 TIDES Code.
  fBeta[0][6]=0.015;
  fBeta[0][7]=0.227-4.998E-4*kelvin+8.84E-7*(kelvin*kelvin);

  //NH4+ Beta parameters.
  fBeta[1][2]= -0.03347+.0001134*kelvin;
      //0.037-2.38E-4*kelvin+3.83E-7*(kelvin*kelvin); //0.0.
  fBeta[1][3]=0.000375*kelvin-0.1049;
                 //.13, 1975.  .
  fBeta[1][4]=0.0002495*kelvin-0.0881;   //-0.24, 1975.
  fBeta[1][5]=-0.00125*kelvin+0.41625;  //0.21;  //0.050, 1975.  Code.
  fBeta[1][7]=0.060;  //0.03, 1975.  0.06 Code.
  //CO2 Beta parameter.
  fBeta[2][2]=-0.09008357+25.38527/kelvin;
  fBeta[2][3]=0.0;
  fBeta[2][4]=0.0;
  fBeta[2][5]=17.54-0.089537*kelvin+0.11278E-3*(kelvin*kelvin);
  fBeta[2][6]=0.033;
  fBeta[2][7]=0.26-9.072E-4*kelvin+1.618E-6*(kelvin*kelvin);

    //HCO3- beta parameters.
  fBeta[3][6]=0.071;
  //CO3-- beta.
  fBeta[4][6]=0.086;
  //NH2COO- beta.
  fBeta[5][6]=0.198;
  //H+ Beta.
  fBeta[6][7]=0.208;

  //Betax parameters.
  fBetax[1][3]=0.5;  //0.018+3.06*fBeta[1][3].
  // fBetax[1][4]=
  fBetax[1][5]=0.4;
  //fBeta[1][7]=?

  fBetax[3][6]=0.018+3.06*fBeta[3][6];
  //fBetax[4][6]=0.018+3.06*fBeta[][];
  fBetax[5][6]=0.018+3.06*fBeta[5][6];
  //fBetax[6][7]=0.018+3.06*fBeta[][];

  for(i=1; i<9; i++)
  {
    for(j=0; j<i; j++)
    {
      fBeta[i][j]=fBeta[j][i];
      fBetax[i][j]=fBetax[j][i];
    }
  }
}


#include <string.h>
#include "header.h"
void rank(struct species_Rank species[9])
{
   //Initialize value and name.
  strcpy(species[0].name, "NH3");
  strcpy(species[1].name, "NH4+");
  strcpy(species[2].name, "CO2");
  strcpy(species[3].name, "HCO3");
  strcpy(species[4].name, "CO3--");
  strcpy(species[5].name, "NH2COO-");
  strcpy(species[6].name, "H+");
  strcpy(species[7].name, "OH- ");
  strcpy(species[8].name, "H2O");

  species[0].value=0.;
  species[1].value=1.;
  species[2].value=0.;
  species[3].value=-1.;
  species[4].value=-2.;
  species[5].value=-1.;
  species[6].value=1.;
  species[7].value=-1.;
  species[8].value=0.;
     /* printf("\n %s %f\n", species[5].name, species[5].value); */
}


#include <math.h>
#include <stdio.h>
#include "header.h"
#include "main.h"

/*****************************************************************/
/* Function: Activity.cpp (Second version)                        */
/* Purpose: Calculation of activity coeff. and activity of water.  */
/* Reference: Edward, 1978.                                        */
/* Input: kelvin -> Absolute temperature T;                        */
/*         fBeta,fBetax -> interaction para from AssignBate().     */
/*       fConcMolality[] -> Molecular concentration as molality.   */
/* Output: fGama[] -> activity coefficients, fGama[9] is water.    */
/*****************************************************************/

void fActivityCoeff(float fGama[9], float fBeta[9][9], float
fBetax[9][9],
       float fConcMolality[8], struct species_Rank species[9],
       float fAlfa, float fI)
{
  int   i,j,k;
  float  fZfloat;
  float  fISqrt;     /* fI-Ionic strength, fISqrt-square root of I */
  float temp1, temp2, temp3, temp4;
  float wtemp1, wtemp2, fTotalConc;

  fISqrt=sqrt(fI);
  /* calculate activity coefficients fGama(i), i=0 to 7. */

  temp1=-(fAlfa/3.)*(fISqrt/(1.+1.2*fISqrt)+2.*log(1.+1.2*fISqrt)/1.2);
  temp2=0.5*(1.-(1.+2.*fISqrt)*exp(-2.*fISqrt))/fI;
  temp3=.25*(1.-(1.+2.*fISqrt+2.*fI)*exp(-2.*fISqrt))/(fI*fI);
  for(i=0; i<8; i++)
  {
    fZfloat=species[i].value*species[i].value;
    fGama[i]=fZfloat*temp1;
    for(k=0; k<8; k++)
    {
      fGama[i]+=2.*(fBeta[i][k]+fBetax[i][k]*temp2)*fConcMolality[k];
      for(j=0; j<8; j++) {
        temp4=-
fZfloat*fConcMolality[k]*fConcMolality[j]*fBetax[k][j]*temp3;
        fGama[i]+=temp4;
      }
    }
    fGama[i]=exp(fGama[i]);
  }

  /* Calculate activity of water using equation from 1978. */
  wtemp1=2.*(fAlfa/3.)*fI*fISqrt/(1.+1.2*fISqrt);
  fTotalConc=0.;
  wtemp2=0.;
  for(i=0; i<8; i++)
  {
    fTotalConc-=fConcMolality[i];
    for(j=0; j<8; j++)
    {
      wtemp2-=fConcMolality[i]*fConcMolality[j]
                      *(fBeta[i][j]+fBetax[i][j]*exp(-2.*fISqrt));
    }
  }
  wtemp2+=fTotalConc;
  fGama[8]=exp((wtemp1+wtemp2)*0.018015);  /* Mw=0.018015 */
}


#include <math.h>
#include <stdio.h>
#include "header.h"
#include "main.h"

/**********************************************************************/
/* Function: ActivityDerivative.cpp                                   */
/* Purpose: Calculation of the derivatives of activity coefficients   */
/*   by an approximate method. They are only calculated when the      */
/*   error in fConcMolality is greater than 1.E-3. FLAG=TRUE.         */
/* Input: kelvin -> Absolute temperature T; fGama[]; species[];       */
/*        fBeta,fBetax -> interaction para from AssignBate().         */
/*        fConcMolality[] -> Molecular concentration as molality.     */
/* Output: fDGama[][] -> Derivatives of activity coefficients.        */
/**********************************************************************/

void fActivityDerivative(float fGama[9],float fBeta[9][9],
               float fBetax[9][9], float fConcMolality[8],
               struct species_Rank species[9], float fDGama[8][8],
               int iteration, float fAlfa, float fI)
{
  int   i,k,j,l,LStart;
  float  eps=0.01;
  float  fIModi, fISqrt;
                        /*fI-Ionic strength, fISqrt-square root(I)*/
  float temp1, temp2, temp3, fZfloat;
  float fModiConcMol[8];

  for(i=0; i<8; i++)
  {
    fModiConcMol[i]=fConcMolality[i];
  }

  LStart=0;
   if (iteration > 0) LStart=1; // Skip NH3 not calculate.
  for(l=LStart; l<8; l++)
  {
    if(l==2) continue;   // Skip CO2 not calculated.
    fModiConcMol[l]+=eps;
    fIModi=fI+.5*species[l].value*species[l].value*eps;
    fISqrt=sqrt(fIModi);

    temp1=-
(fAlfa/3.)*(fISqrt/(1.+1.2*fISqrt)+2.*log(1.+1.2*fISqrt)/1.2);
    temp2=0.5*(1.-(1.+2.*fISqrt)*exp(-2.*fISqrt))/fIModi;
    temp3=.25*(1.-(1.+2.*fISqrt+2.*fIModi)*exp(-
2.*fISqrt))/(fIModi*fIModi);

    for(i=1; i<8; i++)
    {
      fZfloat=species[i].value*species[i].value;
      fDGama[i][l]=fZfloat*temp1;
      for(k=0; k<8; k++)
      {

fDGama[i][l]+=2.*(fBeta[i][k]+fBetax[i][k]*temp2)*fModiConcMol[k];
        for(j=0; j<8; j++)
          fDGama[i][l]-=fZfloat*fModiConcMol[k]*fModiConcMol[j]
                                *fBetax[k][j]*temp3;
      }
      fDGama[i][l]=(fDGama[i][l]-log(fGama[i]))/eps;
      fDGama[l][i]=fDGama[i][l];
    }  //End of for(i=1; i<8; i++)

  }    //End of for(l=LStart; l<8; l++)
}


/********************************************************************/
/* Function: ewequ.cpp                                              */
/* Purpose: Calculation of dissociation equilibrium constants.      */
/* Reference: 1.Computer program TIDES;                             */
/*                                                                  */
/* Input: kelvin -> Absolute temperature T.                         */
/* Output: fEquConst[] -> equilibrium constants saved in an array.  */
/*          have units of molality, or moles of solute/kg water.    */
/********************************************************************/
#include <math.h>

void ewequ1(float fEquConst[5], float kelvin)
{
   int i;
    //Fixed sequence!  0-NH3 dissociation  1-CO2 dissociation
    //2-HCO3      3-NH2COO        4-H2O
   float kconst1[5][4]={{-5914.082, -15.06399, -0.01100801, 97.97152},
                 {-7726.010, -14.50613, -0.0279842, 102.2755},
                 {-9137.258, -18.11192, -0.02245619, 116.7371},
                 { 604.11640, -4.017263, 0.00503095, 20.15214},
                 {-13445.90, -22.47730, 0.0, 140.932}};
    /* from TIDES (1988), function EWEQU */
   for(i=0; i<5; i++)
   {
     fEquConst[i]=exp(kconst1[i][0]/kelvin+log(kelvin)*kconst1[i][1]
            +kconst1[i][2]*kelvin+kconst1[i][3]);
   }
 //  fEquConst[0]*=6.;  Attempt to follow effect of organic matter on
Ka,
 //   but not work properly.
}


#include <stdio.h>
#include <math.h>
#include  "header.h"

/*********************************************************************/
/* Function: setupABmatrix.cpp                                       */
/* Purpose: Evaluation of arrays before fitting into LUDCOMPSITION().*/
/* Input: kelvin -> Absolute temperature T; fGama[]; species[];      */
/*      fConcMolality[] -> Molecular concentration as molality;      */
/*      fDGama[][], fStoichoimetricConc[], fEquConst[].              */
/* Note: fAlfaMatrix & fBetaMatrix were expanded to 9 from 8.        */
/* Output: fAlfaMatrix[][], fBetaMatrix[].                           */
/*********************************************************************/

void setupABmatrix(float fAlfaMatrix[9][9], float fBetaMatrix[9],
        float fGama[9], float fConcMolality[8],
        float fStoichoimetricConc[2], float fEquConst[5], float ratepH,
        struct species_Rank species[9], float fDGama[8][8],
        float fHnry[], float ppCO2)
{
    int i,j;

    for(i=0; i<9; i++)
    {
      for(j=0; j<9; j++)
      {
        fAlfaMatrix[i][j]=0.;
        fBetaMatrix[i]=0.;
      }
    }
     // NH3+H2O <-> NH4+ +OH-
    fAlfaMatrix[0][0]=-1./ (fConcMolality[0]);
    fAlfaMatrix[0][1]= 1./ (fConcMolality[1]);
    fAlfaMatrix[0][7]= 1./ (fConcMolality[7]);

    for(j=0; j<8; j++)
    {
      fAlfaMatrix[0][j]+=fDGama[1][j]+fDGama[7][j]-
fDGama[0][j]+.018015;
    }  /* Mw=0.018015 is derivative of log(fGama[9]).  */

fBetaMatrix[0]=log(fEquConst[0])+log(fConcMolality[0]/fConcMolality[7]
       /fConcMolality[1])+log(fGama[0]*fGama[8]/(fGama[1]*fGama[7]));

      /* NH3 material balances.  */
    fAlfaMatrix[1][0]=1.;
    fAlfaMatrix[1][1]=1.;
    fAlfaMatrix[1][5]=1.;
    fBetaMatrix[1]=fStoichoimetricConc[0]-fConcMolality[0]-
        fConcMolality[1]-fConcMolality[5];

      // CO2+H2O <-> HCO3- + H+
    fAlfaMatrix[2][2]=-1./ (fConcMolality[2]);
    fAlfaMatrix[2][3]= 1./ (fConcMolality[3]);
    fAlfaMatrix[2][6]= 1./ (fConcMolality[6]);
    for (j=0; j<8; j++)
    {
      fAlfaMatrix[2][j]+=fDGama[3][j]+fDGama[6][j]-
fDGama[2][j]+.018015;
    }

fBetaMatrix[2]=log(fEquConst[1]/ratepH)+log(fConcMolality[2]/fConcMolal
ity[3]
        /fConcMolality[6])+log(fGama[2]*fGama[8]/(fGama[3]*fGama[6]));

      // HCO3- + H2O <-> CO3-- + H+
    fAlfaMatrix[3][3]=-1./ (fConcMolality[3]);
    fAlfaMatrix[3][4]= 1./ (fConcMolality[4]);
    fAlfaMatrix[3][6]= 1./ (fConcMolality[6]);
    for (j=0; j<8; j++)
    {
      fAlfaMatrix[3][j]+=fDGama[4][j]+fDGama[6][j]-fDGama[3][j];
    }

fBetaMatrix[3]=log(fEquConst[2]/ratepH)+log(fConcMolality[3]/fConcMolal
ity[4]
        /fConcMolality[6])+log(fGama[3]/(fGama[4]*fGama[6]));

    /* CO2 material balances.  */
    fAlfaMatrix[4][2]=1.;
    fAlfaMatrix[4][3]=1.;
    fAlfaMatrix[4][4]=1.;
    fAlfaMatrix[4][5]=1.;
    fAlfaMatrix[4][8]=-1.;
    fBetaMatrix[4]=fStoichoimetricConc[1]-fConcMolality[2]-
       fConcMolality[3]-fConcMolality[4]-fConcMolality[5];

      // NH3+ HCO3- <-> NH2COO- + H2O
    fAlfaMatrix[5][0]=-1./ (fConcMolality[0]);
    fAlfaMatrix[5][3]= 1./ (fConcMolality[3]);
    fAlfaMatrix[5][5]= 1./ (fConcMolality[5]);
    for(j=0; j<8; j++)
    {
      fAlfaMatrix[5][j]+=fDGama[5][j]-fDGama[0][j]-fDGama[3][j]-
.018015;
    }

fBetaMatrix[5]=log(fEquConst[3])+log(fConcMolality[0]*(fConcMolality[3]
        /fConcMolality[5]))+log(fGama[0]*fGama[3]/(fGama[5]*fGama[8]));

      // H2O <-> H+ + OH-
    fAlfaMatrix[6][6]= 1./ (fConcMolality[6]);
    fAlfaMatrix[6][7]= 1./ (fConcMolality[7]);
    for(j=0; j<8; j++)
    {
      fAlfaMatrix[6][j]+=fDGama[6][j]+fDGama[7][j]+.018015;
    }
    fBetaMatrix[6]=log(fEquConst[4]/ratepH)-log(fConcMolality[6]
        *fConcMolality[7])-log(fGama[6]*fGama[7]/fGama[8]);
             /* Correction on "-" operator on Jan.21,1998. */

       /* Electroneutrolity: m1+(ratepH)*m6=m3+2*m4+m5+m7  */
    if (i!=6){
      for(i=0; i<8; i++)
      {
      fAlfaMatrix[7][i]=species[i].value;     /* 0,1,0,-1,-2,-1,1,-1 */
            /* Different from TIDES.   */
      fBetaMatrix[7]-=(float)(species[i].value)*fConcMolality[i];
      }
    }
    else {
      fAlfaMatrix[7][6]=ratepH;
      fBetaMatrix[7]-=ratepH*fConcMolality[6];
    }

      // CO2(aq) <-> CO2(GAS)
    fAlfaMatrix[8][2]=1./fConcMolality[2];
    for(j=0; j<8; ++j)
    {
      fAlfaMatrix[8][j]+=fDGama[2][j];
    }
    fBetaMatrix[8]=-log(fConcMolality[2])-log(fGama[2])
                 -log(fHnry[1]/ppCO2);  // *.84798 took off.

}

/********************************************************************/
/* Function: fHnry1.cpp                                             */
/* Purpose: Calculation of Henry's constants for gases of NH3, CO2.*/
/*          and H2O.                                                */
/* Reference: 1.Computer program TIDES;                             */
/*                                                                  */
/* Input: kelvin -> Absolute temperature T.                         */
/* Output: fHnry[3] -> Henry's constants, units: kg-atm/moles.      */
/********************************************************************/

#include <math.h>
#include <stdio.h>
void fHnry1(float fHnry[3], float kelvin)
{
   int i;
   float hconst1[3][4]={{-7579.948, -13.58857, 0.008596972, 96.21868},
                        {-17060.71, -68.31596, 0.06598907, 430.1788},
                        {-7362.6981, -9.0, .00695208, 70.4346943}};
                           //0-NH3   1-CO2  3-H2O.
   for(i=0; i<3; i++){
     fHnry[i]=exp(hconst1[i][0]/kelvin+log(kelvin)*hconst1[i][1]
                +hconst1[i][2]*kelvin+hconst1[i][3]);
     // printf("\nHenry_c1 is (from TIDES)(kg-atm/mol):%f", fHnry[i]);
   }
}
```

```
#include <stdio.h>
#include <math.h>
#include <stdlib.h>
/*====================================================================*/
/* Function: ludcomposition()                                         */
/* Purpose: Solve non-singular simultan. linear equations like Ax=B   */
/*        Using method of Doolittle LU decomposition. In this case,   */
/*            a is A, b is B                                          */
/* Reference: "Handbook of Calculation Method Using Fortran 77",      */
/*            Chinese edition.                                        */
/* Input : int n -> indices number of array 'a'                       */
/*       float a[][] -> floating-point array, after calculation,      */
/*                     a triangular array will be saved in array 'a'  */
/*       float b[]-> floating point array, being both input & output */
/* Output:  The result is saved in array 'b'                          */
/*====================================================================*/

void ludcomposition(int n, float a[9][9], float b[9])
{
  int i,j,k;
  int ii,ll;
  int imax;
  float aamax,sum,dum,vv[9],indx[9];

  /*--------------------------------------------------------*/
  /* LU decomposition combined with pivot element selecting */
  /*--------------------------------------------------------*/

  for(i=0;i<n;i++){
    aamax=0.;
    for(j=0;j<n;j++){
      if(fabs(a[i][j])>aamax) aamax=fabs(a[i][j]);
    }
    if(aamax==0.){
      printf("Singular matrix!!\n");
      exit(1);
    }
    vv[i]=1./aamax;
  }
  for(j=0;j<n;j++){
    if(j>0){
      for(i=0;i<=j-1;i++){
        sum=a[i][j];
        if(i>0){
          for(k=0;k<i;k++){
            sum-=a[i][k]*a[k][j];
          }
          a[i][j]=sum;
        }
      }
    }
    aamax=0.;
    for(i=j;i<n;i++){
      sum=a[i][j];
      if(j>0){
        for(k=0;k<j;k++){
          sum-=a[i][k]*a[k][j];
        }
        a[i][j]=sum;
      }
      dum=vv[i]*fabs(sum);
      if(dum>=aamax){
        imax=i;
        aamax=dum;
      }
    }
    if(j!=imax){
      for(k=0;k<n;k++){
        dum=a[imax][k];
        a[imax][k]=a[j][k];
        a[j][k]=dum;
      }
      vv[imax]=vv[j];
    }
    indx[j]=imax;

    if(j != (n-1)){
      if(a[j][j]==0.) a[j][j]=1e-20;
      dum=1./a[j][j];
      for(i=j+1;i<n;i++){
        a[i][j]*=dum;
      }
    }
  }
  if(a[n-1][n-1]==0.) a[n-1][n-1]=1e-20;

  /*---------------------------------------------*/
  /*            Calculate results                */
  /*---------------------------------------------*/
ii=-1;
  for(i=0;i<n;i++){
    ll=indx[i];
    sum=b[ll];
    b[ll]=b[i];
    if(ii!=-1){
      for(j=ii;j<i;j++){
        sum-=a[i][j]*b[j];
      }
    }
    else if(sum!=0.) ii=i;
    b[i]=sum;
  }
  for(i=n-1;i>=0;i--){
    sum=b[i];
    if(i<(n-1)){
      for(j=i+1;j<n;j++){
        sum-=a[i][j]*b[j];
      }
    }
    b[i]=sum/a[i][i];
  }
}

#include <string.h>
```

```
#include <stdio.h>
#include <stdlib.h>
#include <math.h>
#include <dos.h>
#include "header.h"
#include "main.h"
#define GASCONST 0.082
/*==============================================================*/
/* Function: multpH()                                           */
/* Purpose: Calculation of NH3ppm, NH3conc, ionic strength,     */
/*          based on adjusted pH.                               */
/* Input :  fConcMolality[2] -> H+ conc.                        */
/* Output:  NH3ppm, NH3conc -> NH3 conc.in air, pH ->           */
/*          NH3conc has unit of kgN/m3 da.                      */
/*==============================================================*/

void multpH(float &NH3conc, float &NH3ppm, float &pH,
     float Hactivity, float &HactCoeff, float temperature,
     float fStoichiometricConc[])
{       /* fGama[] is to store outputs from fActivityCoef(). */
  float fGama[3];
  float fBeta[3][3];
  float fConcMolality[3];
  float kelvin, fRT;
  float fEquConst[5], fHnry[3];
  float PPNH3, PPCO2;
  struct species_Rank species[3]; //Defines an array of structure
variables.
            //Can also be defined as "species_Rank  species[]".
  float  fI, NH3molL;  //

       // units: moles/kg H2O.
  fConcMolality[2]=Hactivity/HactCoeff;      // H+ concentration
  fConcMolality[0]=0.1;
  fConcMolality[1]=0.01;

  kelvin=273.15+temperature;
  fRT=GASCONST*kelvin;
  ewequl(fEquConst, kelvin);
  fHnry1(fHnry,  kelvin);
  rankpH(species);
  fAssignBetapH(fBeta,  kelvin);
  CalcMolecularSpeciesConc2(fGama, fBeta, kelvin, fConcMolality,
      fI, fEquConst, fStoichiometricConc, species, fHnry);

  HactCoeff=fGama[2];
    printf("  HactCoeff=%f\n", HactCoeff);
  pH=-log10(fConcMolality[2]*fGama[2]);
    printf("pH= %f\n", pH);

  PPNH3=fHnry[0]*fGama[0]*fConcMolality[0];

  NH3molL=0.5*PPNH3/fRT;        // mol/liter of air  // .5* 50%
  NH3ppm=NH3molL*22.4E6;   //  ppm.
  NH3conc=NH3molL*14.;     // gN/litre da. or kgN/m3 da.
}
```

```
/*********************************************************************/
/* Function: CalcMolecularSpeciesConc2.cpp                            */
/* Purpose: Calculation of molecular conc of 8 species,               */
/*          when total conc.(Stoichiometric) of C unknown.            */
/* Reference: 1.Computer program TIDES;                               */
/* Input: fBeta -> interaction para from AssignBate().                */
/*        kelvin -> Absolute temperature T.                           */
/*        fConcMolality[] -> from fInitialEstimates.                  */
/*        fStoichiometricConc[0] -> N conc. in solution.              */
/*        fEquConst[] -> from ewequl.                                 */
/*        ppCO2 -> CO2 partial pressure from Stella.                  */
/* Output: fConcMolality[] -> calculation of eight species conc.      */
/*       pH -> log10(aH), fI -> ionic strength of solution            */
/*********************************************************************/

void CalcMolecularSpeciesConc2(float fGama[3], float fBeta[3][3],
     float kelvin, float fConcMolality[3],
     float &fI, float fEquConst[5], float fStoichiometricConc[2],
     struct species_Rank species[3], float fHnry[])
{
  int i, j, iteration=0, dFLAG=TRUE, cFLAG=TRUE;
  float fCTemp1, fCTemp2;
  float fAlfaMatrix[2][2], fBetaMatrix[2];

  float fAlfa;

  fAlfa=dhdata(kelvin);

  while(cFLAG)
  {

    fI=0.5*(fConcMolality[1]+fConcMolality[2]);
    fActivityCoeffpH(fGama, fBeta, fConcMolality,
               species, fAlfa, fI);
      /*  The following step is important for speeding up.  */
/*    if(dFLAG)
    {
      fActivityDerivative(fGama, fBeta, fBetax, fConcMolality,
            species, fDGama, iteration, fAlfa, fI);
      dFLAG=FALSE;
    }       */
    iteration++;
    setupABmatrixpH(fAlfaMatrix, fBetaMatrix, fGama, fConcMolality,
       fStoichiometricConc, fEquConst, species, fHnry);

    ludcompositionpH(2, fAlfaMatrix, fBetaMatrix);
    cFLAG = FALSE;

    for(i=0; i<2; i++)
    {
    if (fBetaMatrix[i]>=0.)  fConcMolality[i]+=fBetaMatrix[i];
       else
       {
        fCTemp1=fConcMolality[i]*exp(fBetaMatrix[i]/fConcMolality[i]);
        fCTemp2=1.E-3*fConcMolality[i];
        if (fCTemp1<fCTemp2)  fConcMolality[i]=fCTemp2;
        else  fConcMolality[i]=fCTemp1;
       }

        /*---------------------*/
        /*  Convergence Check  */
        /*---------------------*/

      if ( fabs(fBetaMatrix[i]) > 5.E-3*(fConcMolality[i]) )
       cFLAG = TRUE;
      } // End of for(i=0; i<8; i++)

    if(iteration>10) {
       printf("\nIn MiltipH.cpp, kick you out after %d iteration!!\n",
iteration);
       exit(0);
    }
  } // while(cFLAG)

  for(i=0; i<3; ++i)
  {
   // printf("\n coef[%d] is %f ", i, fGama[i]);
  //  printf("   molality[%d] %17.14f", i, fConcMolality[i]);
  }

}


#include <stdio.h>
#include <math.h>
#include <stdlib.h>

/*====================================================================*/
/* Function: ludcompositionpH()                                       */
/* Purpose: Solve non-singular simultan. linear equations like Ax=B   */
/*         Using method of Doolittle LU decomposition. In this case, */
/*            a is A, b is B                                          */
/* Reference: "Handbook of Calculation Method Using Fortran 77",      */
/*            Chinese edition.                                        */
/* Input : int n -> indices number of array 'a'                       */
/*       float a[][] -> floating-point array, after calculation,      */
/*                    a triangular array will be saved in array 'a'   */
/*       float b[]-> floating point array, being both input & output */
/* Output:  The result is saved in array 'b'                          */
/*====================================================================*/

void ludcompositionpH(int n, float a[2][2], float b[2])
{
  int i,j,k;
  int ii,ll;
  int imax;
  float aamax,sum,dum,vv[2],indx[2];

  /*--------------------------------------------------------*/
  /* LU decomposition combined with pivot element selecting */
  /*--------------------------------------------------------*/

  for(i=0;i<n;i++){
    aamax=0.;
  for(j=0;j<n;j++){
    if(fabs(a[i][j])>aamax) aamax=fabs(a[i][j]);
  }
  if(aamax==0.){
    printf("Singular matrix!!\n");
    exit(1);
  }
  vv[i]=1./aamax;
}

for(j=0;j<n;j++){
  if(j>0){
    for(i=0;i<=j-1;i++){
      sum=a[i][j];
      if(i>0){
        for(k=0;k<i;k++){
          sum-=a[i][k]*a[k][j];
        }
        a[i][j]=sum;
      }
    }
  }
  aamax=0.;
  for(i=j;i<n;i++){
    sum=a[i][j];
    if(j>0){
      for(k=0;k<j;k++){
        sum-=a[i][k]*a[k][j];
      }
      a[i][j]=sum;
    }
    dum=vv[i]*fabs(sum);
    if(dum>=aamax){
      imax=i;
      aamax=dum;
    }
  }

  if(j!=imax){
    for(k=0;k<n;k++){
      dum=a[imax][k];
      a[imax][k]=a[j][k];
      a[j][k]=dum;
    }
    vv[imax]=vv[j];
  }
  indx[j]=imax;

  if(j != (n-1)){
    if(a[j][j]==0.) a[j][j]=1e-20;
    dum=1./a[j][j];
    for(i=j+1;i<n;i++){
      a[i][j]*=dum;
    }
  }
}
if(a[n-1][n-1]==0.) a[n-1][n-1]=1e-20;
```

```
  /*----------------------------------------------*/
  /*            Calculate results                 */
  /*----------------------------------------------*/

  ii=-1;
  for(i=0;i<n;i++){
    ll=indx[i];
    sum=b[ll];
    b[ll]=b[i];
    if(ii!=-1){
      for(j=ii;j<i;j++){
        sum-=a[i][j]*b[j];
      }
    }
    else if(sum!=0.) ii=i;
    b[i]=sum;
  }
  for(i=n-1;i>=0;i--){
    sum=b[i];
    if(i<(n-1)){
      for(j=i+1;j<n;j++){
        sum-=a[i][j]*b[j];
      }
    }
    b[i]=sum/a[i][i];
  }
}
```

```
#include <string.h>
#include "header.h"

void rankpH(struct species_Rank species[3])
{
   //Initialize value and name.
  strcpy(species[0].name, "NH3");
  strcpy(species[1].name, "NH4+");
  strcpy(species[2].name, "H+");

  species[0].value=0.;
  species[1].value=1.;
  species[2].value=1.;

     /* printf("\n %s %f\n", species[5].name, species[5].value); */
}
```

```
#include <stdio.h>
#include <math.h>
#include  "header.h"
/*********************************************************************/
/* Function: setupABmatrixpH.cpp                                     */
/* Purpose: Evaluation of arrays before fitting into LUDCOMPSITION().*/
/* Input: kelvin -> Absolute temperature T; fGama[]; species[];      */
/*      fConcMolality[] -> Molecular concentration as molality;      */
/*      fDGama[][], fStoichoimetricConc[], fEquConst[].              */
/* Note: fAlfaMatrix & fBetaMatrix were expanded to 9 from 8.          */
/* Output: fAlfaMatrix[][], fBetaMatrix[].                             */
/* Date:       Jan. 21, 1998                                           */
/***********************************************************************/
void setupABmatrixpH(float fAlfaMatrix[2][2], float fBetaMatrix[2],
        float fGama[3], float fConcMolality[3],
        float fStoichoimetricConc[2], float fEquConst[5],
        struct species_Rank species[3],  float fHnry[])
        // float fDGama[8][8],    was cut for simplifying purpose
{
    int i,j;

    for(i=0; i<2; i++)
    {
      for(j=0; j<2; j++)
      {
        fAlfaMatrix[i][j]=0.;
      fBetaMatrix[i]=0.;
      }
    }
     // NH3+H2O <-> NH4+ +OH-
    fAlfaMatrix[0][0]=-1./ (fConcMolality[0]);
    fAlfaMatrix[0][1]= 1./ (fConcMolality[1]);

 /*   for(j=0; j<3; j++)
    {
      fAlfaMatrix[0][j]+=fDGama[1][j]+fDGama[7][j]-
fDGama[0][j]+.018015;
    }  */      /* Mw=0.018015 is derivative of log(fGama[9]).  */
    fBetaMatrix[0]=log(fEquConst[0]/fEquConst[4])
      +log(fConcMolality[0]*fConcMolality[2]/fConcMolality[1])
       +log(fGama[0]*fGama[2]/fGama[1]);

      /* NH3 material balances.  */
    fAlfaMatrix[1][0]=1.;
    fAlfaMatrix[1][1]=1.;
    fBetaMatrix[1]=fStoichoimetricConc[0]-fConcMolality[0]-
        fConcMolality[1];
}

#include <stdio.h>
#include <math.h>
#include <stdlib.h>
/*===================================================================*/
/* Function: ludcompositionpH()                                      */
/* Purpose: Solve non-singular simultan. linear equations like Ax=B  */
/*         Using method of Doolittle LU decomposition. In this case, */
/*            a is A, b is B                                         */
/* Reference: "Handbook of Calculation Method Using Fortran 77",     */
/*            Chinese edition.                                       */
/* Input : int n -> indices number of array 'a'                      */
/*       float a[][] -> floating-point array, after calculation,     */
/*                     a triangular array will be saved in array 'a' */
/*       float b[]-> floating point array, being both input & output */
/* Output:  The result is saved in array 'b'                         */
/*===================================================================*/
```

```
void ludcompositionpH(int n, float a[2][2], float b[2])
{
  int i,j,k;
  int ii,ll;
  int imax;
  float aamax,sum,dum,vv[2],indx[2];

  /*--------------------------------------------------------*/
  /* LU decomposition combined with pivot element selecting */
  /*--------------------------------------------------------*/
  for(i=0;i<n;i++){
    aamax=0.;
    for(j=0;j<n;j++){
      if(fabs(a[i][j])>aamax) aamax=fabs(a[i][j]);
    }
    if(aamax==0.){
      printf("Singular matrix!!\n");
      exit(1);
    }
    vv[i]=1./aamax;
  }
  for(j=0;j<n;j++){
    if(j>0){
      for(i=0;i<=j-1;i++){
        sum=a[i][j];
        if(i>0){
          for(k=0;k<i;k++){
            sum-=a[i][k]*a[k][j];
          }
          a[i][j]=sum;
        }
      }
    }
    aamax=0.;
    for(i=j;i<n;i++){
      sum=a[i][j];
      if(j>0){
        for(k=0;k<j;k++){
          sum-=a[i][k]*a[k][j];
        }
        a[i][j]=sum;
      }
      dum=vv[i]*fabs(sum);
      if(dum>=aamax){
        imax=i;
        aamax=dum;
      }
    }

    if(j!=imax){
      for(k=0;k<n;k++){
        dum=a[imax][k];
        a[imax][k]=a[j][k];
        a[j][k]=dum;
      }
      vv[imax]=vv[j];
    }
    indx[j]=imax;

    if(j != (n-1)){
      if(a[j][j]==0.) a[j][j]=1e-20;
      dum=1./a[j][j];
      for(i=j+1;i<n;i++){
        a[i][j]*=dum;
      }
    }
  }
  if(a[n-1][n-1]==0.) a[n-1][n-1]=1e-20;

  /*----------------------------------------------*/
  /*            Calculate result                  */
  /*----------------------------------------------*/
  ii=-1;
  for(i=0;i<n;i++){
    ll=indx[i];
    sum=b[ll];
    b[ll]=b[i];
    if(ii!=-1){
      for(j=ii;j<i;j++){
        sum-=a[i][j]*b[j];
      }
    }
    else if(sum!=0.) ii=i;
    b[i]=sum;
  }
  for(i=n-1;i>=0;i--){
    sum=b[i];
    if(i<(n-1)){
      for(j=i+1;j<n;j++){
        sum-=a[i][j]*b[j];
      }
    }
    b[i]=sum/a[i][i];
  }
}

/*********************************************************************/
/* Function: fAssignBetapH()  (Second version, pH version)           */
/* Purpose: Calculation of interaction parameters between:           */
/*          NH3, NH4+, H+, etc.                                      */
/* Reference: 1.Computer program TIDES;                              */
/* Input: kelvin -> Absolute temperature T.                          */
/* Output: fBeta[][] -> Bi,j(0).                                     */
/*********************************************************************/
#include <stdlib.h>
#include <stdio.h>

void fAssignBetapH(float fBeta[3][3], float kelvin)
{
  int i,j;

  for(i=0; i<3; i++)
  {
    for(j=0; j<3; j++)
    {
      fBeta[i][j]=0.;

    }
  }
  //NH3 Beta parameters.
  fBeta[0][0]=-0.03980694+17.0142/kelvin; // -0.026+12.29/kelvin;
  fBeta[0][1]=-0.000125*kelvin+0.03162; // 0.0.
  fBeta[0][2]=0.015;       //  NH3- H+ (2.)

  //H+ Beta.
//  fBeta[6][7]=0.208;

  for(i=1; i<3; i++)
  {
    for(j=0; j<i; j++)
    {
      fBeta[i][j]=fBeta[j][i];

    }
  }
}

#include <math.h>
#include <stdio.h>
#include "header.h"
#include "main.h"

/***********************************************************************/
/* Function: ActivitypH.cpp (Second version)                           */
/* Purpose: Calculation of activity coeff. and activity of ater.       */
/* Reference: Edward, 1978.                                            */
/* Input: kelvin -> Absolute temperature T;                            */
/*        fBeta,fBetax -> interaction para from AssignBate().          */
/*      fConcMolality[] -> Molecular concentration as molality.        */
/* Output: fGama[] -> activity coefficients, fGama[9] is water.        */
/***********************************************************************/

void fActivityCoeffpH(float fGama[3], float fBeta[3][3],
       float fConcMolality[3], struct species_Rank species[3],
       float fAlfa, float fI)
{
  int   i,j,k;
  float  fZfloat;
  float  fISqrt;     /* fI-Ionic strength, fISqrt-square root of I */
  float templ;

  fISqrt=sqrt(fI);
  /* calculate activity coefficients fGama(i), i=0 to 7. */

  templ=-(fAlfa/3.)*(fISqrt/(1.+1.2*fISqrt)+2.*log(1.+1.2*fISqrt)/1.2);
  for(i=0; i<3; i++)
  {
    fZfloat=species[i].value*species[i].value;
    fGama[i]=fZfloat*templ;
    for(k=0; k<3; k++)
    {
      fGama[i]+=2.*fBeta[i][k]*fConcMolality[k];
    }
    fGama[i]=exp(fGama[i]);
  }
  /* Calculate activity of water using equation from 1978. */
}


#include "header.h"

/*******************************************************************/
/* Function: fIonicStrengthph.cpp                                  */
/* Purpose: Calculation of Ionic Strength of solution.             */
/* Input: struct species_Rank species[9] ->float fConcMolality[8]) */
/* Output: dh_data -> alfa under a specific temperature.           */
/*******************************************************************/

float fIonicStrengthpH(float fConcMolality[3])
{
  int i;
  float fSI;

  fSI=0.5*(fConcMolality[1]+fConcMolality[2]);
     //printf("\nThe ionic strength of the compost solution: %f\n",
fSI);
  return(fSI);
}


/*******************************************************************/
/* Function: fAssignBetapH()  (Second version, pH version)         */
/* Purpose: Calculation of interaction parameters between:         */
/*         NH3, NH4+, H+, etc.                                     */
/* Reference: 1.Computer program TIDES;                            */
/* Input: kelvin -> Absolute temperature T.                        */
/* Output: fBeta[][] -> Bi,j(0).                                   */
/*******************************************************************/
#include <stdlib.h>
#include <stdio.h>

void fAssignBetapH(float fBeta[3][3], float kelvin)
{
  int i,j;

  for(i=0; i<3; i++)
  {
    for(j=0; j<3; j++)
    {
      fBeta[i][j]=0.;

    }
  }
  //NH3 Beta parameters.
  fBeta[0][0]=-0.03980694+17.0142/kelvin; // -0.026+12.29/kelvin;
  fBeta[0][1]=-0.000125*kelvin+0.03162; // 0.0.
  fBeta[0][2]=0.015;       //  NH3- H+ (2.)
  //H+ Beta.
//  fBeta[6][7]=0.208;

  for(i=1; i<3; i++)
  {
    for(j=0; j<i; j++)
    {
      fBeta[i][j]=fBeta[j][i];

    }
  }
}

#include "header.h"
/*********************************************************************/
/* Function: fIonicStrengthph.cpp                                    */
/* Purpose: Calculation of Ionic Strength of solution.               */
/* Input: struct species_Rank species[9] ->float fConcMolality[8])  */
/* Output: dh_data -> alfa under a specific temperature.             */
/*********************************************************************/

float fIonicStrengthpH(float fConcMolality[3])
{
  int i;
  float fSI;

  fSI=0.5*(fConcMolality[1]+fConcMolality[2]);
    //printf("\nThe ionic strength of the compost solution: %f\n",
fSI);
  return(fSI);
}
```